UNIVERSITAT DE BARCELONA

LIF as a metabolic messenger: study of glucose sensing by NSCLC and LIF-mediated nutrient stress responses

Miguel Hernández Madrigal

Aquesta tesi doctoral està subjecta a la llicència ***Reconeixement 4.0. Espanya de Creative Commons***.

Esta tesis doctoral está sujeta a la licencia ***Reconocimiento 4.0. España de Creative Commons***.

This doctoral thesis is licensed under the ***Creative Commons Attribution 4.0. Spain License***.

UNIVERSITAT DE BARCELONA

FACULTAT DE FARMÀCIA I CIÈNCIES DE L'ALIMENTACIÓ
(responsable de la tesi doctoral)

LIF as a metabolic messenger: study of glucose sensing by NSCLC and LIF-mediated nutrient stress responses

MIGUEL HERNÁNDEZ MADRIGAL - 2022

UNIVERSITAT DE BARCELONA

FACULTAT DE FARMÀCIA I CIÈNCIES DE L'ALIMENTACIÓ
Tesi realitzada a l'IDIBELL

PROGRAMA DE DOCTORAT DE BIOMEDICINA

LIF as a metabolic messenger: study of glucose sensing by NSCLC and LIF-mediated nutrient stress responses

Memòria presentada per Miguel Hernández Madrigal per optar al títol de doctor per la Universitat de Barcelona

Directora: Cristina Muñoz Pinedo

MUÑOZ PINEDO CRISTINA - 44220520F

Firmado digitalmente por MUÑOZ PINEDO CRISTINA - 44220520F
Fecha: 2022.04.06 11:20:27 +02'00'

Autor: Miguel Hernández Madrigal

HERNANDEZ MADRIGAL MIGUEL - 48696533J

Firmado digitalmente por HERNANDEZ MADRIGAL MIGUEL - 48696533J
Nombre de reconocimiento (DN): c=ES, serialNumber=IDCES-48696533J, givenName=MIGUEL, sn=HERNANDEZ MADRIGAL, cn=HERNANDEZ MADRIGAL MIGUEL - 48696533J
Fecha: 2022.04.06 09:31:32 +02'00'

Tutor: Antonio Gentilella

Firmado por Antonio Gentilella el día 05/04/2022 con un certificado emitido por la Fábrica Nacional de

MIGUEL HERNÁNDEZ MADRIGAL - 2022

Agradecimientos

Todo este trabajo, así como todo el viaje que me ha traído hasta aquí no habría sido posible sin muchas personas que me han acompañado, ayudado y a veces hasta empujado, en el mejor de los sentidos.

En primer lugar, quiero dar las gracias a todos vosotros con los que he compartido las alegrías y miserias de la vida en el laboratorio los últimos años. Gracias, Cristina, toda tu ayuda y tus consejos dentro y fuera del laboratorio. Gracias por generar un espacio de trabajo tan positivo, y por darme el espacio para desarrollar mis propias hipótesis y por el reto intelectual de nuestras discusiones. No es fácil encontrar supervisores que traten a sus trabajadores como iguales, que discutan ciencia de tú a tú a pesar del abismo en cuanto a experiencia que nos separa, y que a pesar del estado crítico del mundo académico consigan hacer todos los malabares burocráticos que hoy en día son necesarios sin dejar que esa presión nos llegue a aplastar a los de debajo. Y cómo hablar de gestión sin darte las gracias, Joaquim. No solo has hecho posible que todo esto siga adelante, sino que has sido un amigo desde el primer día y me has puesto los pies en la tierra más de cien veces, recordándome con muchas risas y cachondeo que al final del día esto es un trabajo, y que, si un día todo sale mal, ya habrá otra oportunidad de fastidiarlo otra vez mañana. Y si hablamos de amigos desde el primer día, no puede faltar Francesca. Nunca había encontrado una amiga en una persona más radicalmente distinta a mí. Y, sin embargo, a base de pasarlo mal juntos, de retarnos y hasta pelearnos, hemos acabado siendo mutuamente necesarios ¡y hasta nos lo hemos pasado bien! No sé si habría aguantado todo esto sin ti. Gracias por tus piques, por la motivación y por cubrirme siempre las espaldas. Y como no hay dos sin tres, llegó Fedra a completar el grupo. Gracias por ser la voz de la razón en este gallinero, por mantenernos cuerdos, por tirar para adelante con todo siempre, y por estar siempre velando por las malas cabezas de todos nosotros. Tu paciencia infinita y toda esa empatía son un ejemplo enorme.

También quiero dar las gracias a todos mis demás compañeros: Paola, Vero, Nil, Felipe, Silvia, Lidia, Mabel, Isha, Laura, Eli, Mireia, Sara H., Gaby, Sara O, Pau, Judit, Helena, Pilar, a todas las ONAs… y muchos más que no caben aquí.

Gracias por todos los buenos ratos, los cafés y bizcochos en la oficina, la ayuda con los experimentos, por compartir lo bueno y lo malo y más que nada por todo el apoyo emocional durante todo lo que hemos aguantado juntos. Y a toda esa gente maravillosa que vertebra el IDIBELL y que soportar las preguntas de oleada tras oleada de novatos que les rompen las máquinas y se lo ensucian todo. Gracias Vane, Joan, Saioa, Vaquero, Lola, Jose, Antonia, Javi y tantos otros.

Pero claro, este viaje que me ha traído aquí no empezó hace solo cuatro años, sino hace mucho, mucho más. Y por eso tengo que dar a las gracias a mi familia. Gracias, abuelo, que ya no estás, por enseñarme el orgullo en lo que hacemos con la mente y el trabajo, y gracias abuela por enseñarme a no preocuparme tanto si alguna vez se me escapa un tachón y tengo que apañar el cuadro. Juli, gracias por darme ejemplo, incluso siendo la pequeña, con tu habilidad para esperar lo mejor de la gente y tu actitud positiva, con tu seguir adelante sin dejar que un mal día se contagie al resto de la semana ni al día de los demás. Papá, mamá, gracias por criar a una persona inquisitiva y curiosa, por enseñarme la resiliencia para seguir adelante y terminar lo que empiezo, y el valor de echar una mano a los demás sin esperar nada a cambio. Y, sobre todo, por vuestro apoyo incondicional y por la tranquilidad que trae el saber que siempre puedo contar con vosotros pase lo que pase y para todo.

Y, por último, pero nunca menos importante, gracias a ti, Eva. Gracias por creer en mí siempre mucho más que yo, por convencerme de que puedo hacer más de lo que te haya demostrado nunca antes, y por hacerme ver que cuando no puedo, no pasa nada. Gracias por todo tu aliento, por ayudarme a confiar en mí mismo, por tanta tanta ayuda. Gracias por tu consuelo cuando las cosas me superan. Gracias por apoyarme en los malos tiempos y por celebrar los buenos conmigo. Gracias por compartir este camino, desde aquellos días cuando no sabía ni a qué dedicarme hasta este último capítulo del viaje académico. Gracias por las risas contagiosas, y por hacer que sin importar en qué rincón del mundo estemos, esté en casa. Cada vez que te he visto dar un paso fuera de lo que parecían tus límites, cada obstáculo que has superado y cada palo que has aguantado me ha dado fuerzas donde no las había para seguir. Nada de esto habría sido posible sin ti.

Table of Contents

1. Summary

Tumours grow in a self-imposed hypoglycaemic microenvironment due to their exacerbated metabolic needs. To thrive in these harsh conditions, malignant cells must adapt their own metabolic routes and hijack the host nutrient supply infrastructure through extracellular signalling.

This study aimed at characterising the secretory response of tumoral cells in response to glucose deprivation, both the molecular signalling leading to this response and the consequences of this response for the tumour. In particular, this study focused on a cytokine never before linked to glucose deprivation: LIF.

Through use of *in silico, in vitro*, and *in vivo* approaches we made two novel findings: firstly, we determined that LIF induction happens through non-canonical N-glycosylation dependent signalling, in the context of glucose deprivation. Furthermore, we have determined that the signalling mechanism leading to LIF production encompasses a complex combination of transcriptional and post-transcriptional signals that involve PERK but none of its canonical transcription factors. Secondly, we discovered a novel pro-tumorigenic role for this cytokine as an angiogenic.

Our findings addressed the gap in literature regarding the mechanism for LIF production in tumours, providing insight relevant to future development of therapeutic approaches. And most importantly, we provide an integrative view of not only how glucose deprivation leads to production of LIF, but also how this cytokine could lead to the resolution of the local hypoglycaemia via angiogenesis.

Resumen

Los tumores imponen un microambiente de constante hipoglicemia debido a su rápida proliferación y al exacerbado consumo de metabolitos que esto conlleva. Para prosperar en estas circunstancias, las células cancerosas alteran su metabolismo y sus rutas de señalización de forma que puedan abusar de la infraestructura de aporte de nutrientes del organismo.

El objetivo de este estudio es caracterizar la respuesta secretora del tumor en respuesta a la falta de glucosa, tanto al nivel de la señalización molecular que integra esta respuesta como al nivel de las consecuencias externas que estas señales tienen para el tumor. En particular, este estudio se centra en una citoquina que nunca antes se había relacionado con la falta de glucosa: LIF (por sus siglas en inglés: Factor Inhibidor de la Leucemia).

A través del uso de técnicas *in silico*, *in vitro* e *in vivo* hemos alcanzado dos descubrimientos. En primer lugar, hemos determinado que la producción de LIF está inducida a través de una ruta no-canónica de detección de la falta de glucosa basada en la falta de N-glicosilación. Además, hemos determinado que el mecanismo que sigue a este fallo en la glicosilación incluye una compleja combinación de señales transcripcionales y postranscripcionales dependientes de PERK, pero no de los factores de transcripción tradicionalmente asociados a esta quinasa. En segundo lugar, hemos descubierto un nuevo rol pro-tumorigénico de esta citoquina como factor pro-angiogénico.

Nuestros hallazgos cubren un vacío en la literatura en lo relativo al mecanismo que causa la producción de LIF por parte del tumor, lo cual podría servir de base para nuevos enfoques terapéuticas. Además, hemos desarrollado una visión unificada que explica cómo la falta de glucosa resulta en la producción de esta citoquina, y cómo LIF a su vez puede actuar para resolver la hipoglicemia local restaurando el riego sanguíneo mediante la angiogénesis.

2. Introduction

2.1 Glucose and Cancer

Glucose is one of the most fundamental molecules for eukaryotic cells. It is needed for energy production, as a building block for nucleotide production, to maintain redox homeostasis and to modify proteins and help them achieve their function. In 1956, German scientist Otto Warburg observed that cancer cells have an exacerbated need of glucose due to their preference of glycolysis as a means to produce ATP over TCA cycle and oxidative respiration (Warburg, 1956), which was then coined as the Warburg effect.

Since this seminal discovery, the complex metabolic re-wiring in malignancies has been subject to major study. So much so that this knowledge is already being applied for diagnostics (PET scans) and therapeutics (2-DG, metformin, kinase inhibitors). Moreover, there is extensive evidence suggesting that tumours can affect not only their metabolism or that of their immediate microenvironment but could even cause metabolic alterations at the systemic level (Ye *et al*., 2018; Esper & Harb, 2005).

2.2 The molecular fates of glucose

Within the cell, glucose is a means to many ends. From energy and building-blocks to redox homeostasis and signalling, glucose is crucial for many biological processes (Diagram 1), and perhaps even more so in cancer cells. One of the main characteristics of cancer cells, which has often been hypothesised to be the cause of their metabolic peculiarities, is their dramatic proliferation rate. In non-malignant cells, sustained proliferation is achieved through an upregulation of glycolysis via several signalling

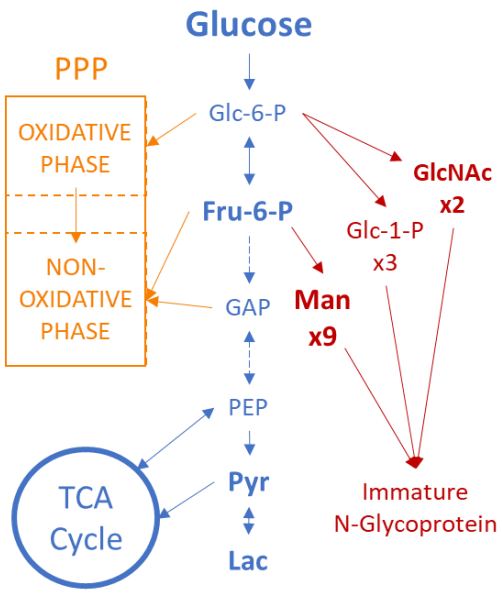

Diagram 1. Glucose metabolic fates*. A diagrammatic representation of the molecular fates of glucose grouped by colour on PPP (orange), glycolysis and TCA (blue), and N-glycosylation (Red).*

pathways such as RAS-PI3K-Akt pathway (Fritz and Fajas, 2010; Iurlaro *et al*., 2014). Rapidly proliferating cancer cells often harbour mutations on the RAS pathway that allows them to maintain highly glycolytic activity. Through glycolysis, eukaryotic cells generate pyruvate, which in turn can be used to fuel amino acid production and can also enter the mitochondria for ATP and fatty acid production via TCA cycle and the fatty acid synthesis pathway (Nelson & Cox, 2017). This mechanism allows cancer cells to maintain basic energetic homeostasis via ATP production from glycolysis while also generating building-blocks to sustain rapid proliferation (Chandel, 2015).

One of the consequences of this anabolic metabolism is a largely increased reactive oxygen species (ROS) production. This, together with an increase in NADPH consumption for fatty acid synthesis, creates a dependence on cancer cells on maintaining high pentose phosphate pathway (PPP) activity in order to maintain redox homeostasis (Patra & Hay, 2014). Moreover, the rapid proliferation of cancer cells also increases the demand for pentose biosynthesis via the PPP in order to generate new nucleic acids (Muñoz-Pinedo *et al*., 2012).

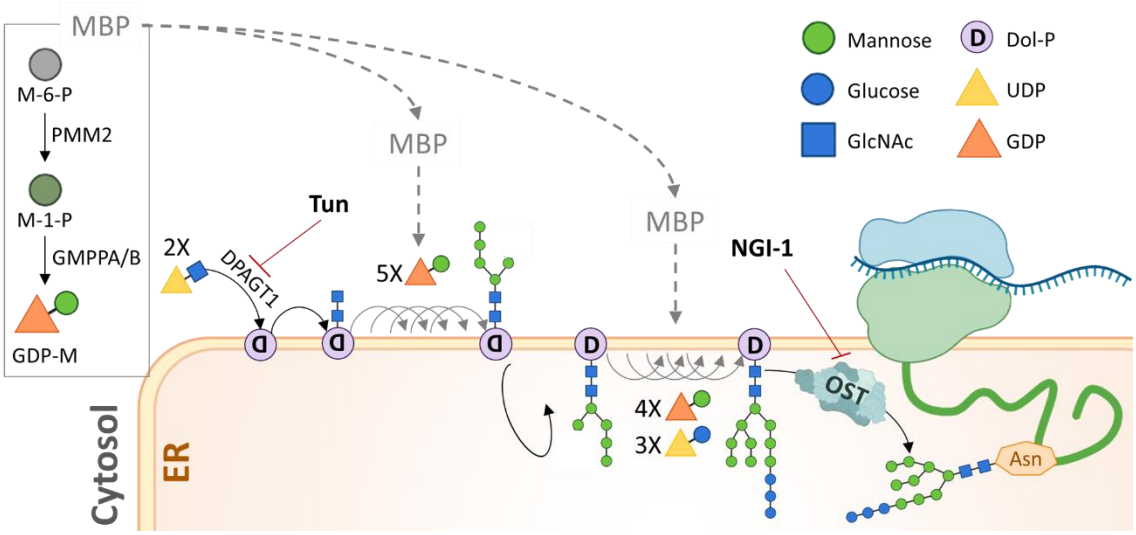

Diagram 2. The complex process of N-glycosylation. *Summary of the early stages of N-glycosylation, including the mannose biosynthetic pathway (MBP), and up to glycan en bloc addition to nascent protein by OST complex. Two inhibitors of N-glycosylation are also represented: tunicamycin (Tun) and NGI-1.*

Last but not least, eukaryotic cells also have another major use for glucose: protein tagging. Many proteins require post-translational modifications in order to perform their normal functions, and one of the most frequent type of modifications is glycosylation, the addition of monosaccharides to proteins. There are several types of glycosylation based on the target residue and the type of glycan

attached. However, the most common and most resource demanding type is N-glycosylation. N-glycan assembly is a tightly regulated process that begins within the endoplasmic reticulum (ER) membrane (Diagram 2). Briefly, glucose is first converted to UDP-glucose and GDP-Mannose or used for UDP-N-acetylglucosamine (GlcNAc) production via the hexosamine biosynthesis pathway. This allows these fundamental monosaccharides to bind to dolichol in the ER membrane and be incorporated in the growing glycan that is eventually attached to the corresponding asparagine (Asn) residue in nascent proteins translated by ER associated ribosomes. This process is often referred to as early N-glycosylation and occurs within the ER. Once attached subsequent modifications can occur on this glycan tree to confer the protein with different binding specificities, which is called late N-glycosylation and occurs mainly in the Golgi apparatus. However, the core 2-GlcNac, 9-Man, 3-Glc glycan must always be synthesised regardless of the subsequent trimming (Bieberich, 2014).

Most types of solid tumours have an intense need for glucose, but NSCLC in particular is highly associated to metabolic alterations including but not limited to high glycolytic activity coupled with high TCA cycle output, thus consuming both glucose and imported lactate (Hensley *et al*., 2016). This indicates a high dependency on glucose and glucose metabolism, making NSCLC an idoneous model for studying cancer responses to glucose restriction.

2.3 Glucose sensing in the tumour cell

As Gerard Evan eloquently put it ‘the things that make tumours are hijacked programs that are part of normal cellular development, repair and regeneration.’ (Evan, 2008), and tumoral responses to hypoglycaemia are no exception. In normal physiological conditions hypoglycaemia can happen during ischemic episodes or due to traumatic injuries that temporarily alter blood supply to some tissues. At the cellular level, healthy cells that find themselves in hypoglycaemic conditions have an increase in AMP/ATP ratios and thus activate AMPK signalling which, in combination with mTOR, works to decrease cell proliferation and energy consumption to maintain ATP levels (Iurlaro *et al*., 2014) until blood flow resumes. Tumour cells hijack this pathway via loss of the LKB1 gene, which

effectively disables canonical AMPK signalling and allows tumours to continue proliferating under glucose deprivation (Galan-Cobo *et al*., 2019). As a consequence, these tumours experience exacerbated oxidative stress. Again, in healthy cells oxidative stress is countered by KEAP1/NRF2 signalling, and thus we often see LKB1 deficient tumours concurrently harbour mutations in the KEAP1 gene that permanently activate this anti-oxidant response to better survive their own exacerbated metabolism (Galan-Cobo *et al*., 2019).

Another mechanism for cellular sensing of glucose levels happens at the transcriptional levels, by carbohydrate response element-binding protein (ChREBP). This transcription factor translocates to the nucleus only in the presence of glucose to transcribe a great range of effector proteins (Yamashita *et al.,* 2001). It has been proposed that xylulose-5-phosphate, an intermediate of the PPP, activates a specific phosphatase which in turn dephosphorylates ChREBP to allow its nuclear translocation (Kabashima *et al*., 2003). Importantly, a recent study has detected increased ChREBP activity in colon cancer, which enables an increased anabolic metabolism and consequent proliferation and malignancy (Lei *et al*., 2020).

2.4 Extracellular responses to hypoglycaemia I: Angiogenesis

Continuing with the same analogy of tumours hijacking normal mechanisms, several physiological pathways can be activated upon oxygen and glucose deprivation to help restore blood flow to injured areas. The fact that both hypoxia (Forsythe *et al*., 1996) and glucose deprivation (Dantz *et* al., 2002; Satake *et al*., 1998) induce expression of pro-angiogenic factors such as the VEGF family has been known since the late nineties. Moreover, studies have shown that VEGF produced in response to hypoglycaemia not only promotes angiogenesis in hypoglycaemic tissues, but also stimulates glucose uptake by endothelial cells (Sone *et al*., 2000). And yet, numerous clinical trials aiming to capitalise on the VEGF family's pro-angiogenic effects on ischemia (Isner 1995; Carmeliet, 2005; Ferrara and Kerbel, 2005), or aiming to inhibit VEGF signalling in tumours (Holash *et al*., 2002; Hurwitz *et al*., 2004; Sandler *et al*., 2006; Miller *et al*., 2007), have demonstrated the issue of angiogenesis upon nutrient deprivation is more

complex than initially thought. Importantly, these therapies have been found to negatively impact non-tumoral microvasculature (Kamba *et al*., 2006; Yang *et al*., 2013), promote tumour metastasis (Páez-Ribes *et al*., 2009) and impede delivery of chemotherapeutic agents to the tumour (Van der Veldt *et al*., 2012). Due to these issues, the effect of anti-VEGF therapies in cancer patient survival has been modest (Ribatti, 2016) and the search for tumour specific angiogenic signalling continues.

Perhaps paradoxically, many parallels between placental development and cancer initiation have been highlighted (Ferretti *et al* 2007). It has been suggested that tumours also hijack signalling mechanisms that are exclusively active during early development in placental trophoblasts (Holtan *et al*., 2009) and angiogenic mechanisms are no exception (Shojaei & Ferrara, 2008). Most endothelial cells become quiescent during postnatal life, and yet tumour-associated endothelial cells express molecules such as the placental growth factor (PlGF) to overcome this quiescence (Seaman *et al*., 2007). The solution to the development of tumour specific anti-angiogenic therapies might lie on targeting these hijacked placental angiogenic signalling mechanisms.

2.5 Extracellular responses to hypoglycaemia II: Cytokines that mediate cachexia

Regarding the issue of how cells and tissues respond to hypoglycaemia to resolve this situation, generating an increase in the vascular input to the tissue is only the first part of the solution. When the hypoglycaemic stress is sustained, cells are capable of producing extracellular signals in an attempt to increase glucose availability in the bloodstream (Fearon *et al*., 2012; Gourdin & Dubois, 2013). Unfortunately, these mechanisms may also be hijacked by tumours leading to one of the most characterised systemic metabolic reprogramming phenomena: cachexia. This is the process through which tumour derived and host derived factors elicit a dramatic decrease in energy and anabolite levels of the host (Esper & Harb, 2005; Argilés *et al*., 1997). The physiological hallmarks of cachexia as first described by Argilés *et al.* (1997) are weight loss, anorexia, asthenia and anaemia which in most cases led to heart failure and death (McBride *et al.,* 1990). Subsequent characterisation of this syndrome led to the

determination of the molecular hallmarks behind these physiological symptoms, which include glucose intolerance, increased hepatic gluconeogenesis, decreased skeletal muscle glucose uptake, increased lipolysis, increased systemic protein turnover, increased acute phase protein synthesis and increased skeletal muscle breakdown (Esper & Harb, 2005). A broad range of studies have delved on the molecular factors driving these molecular alterations leading to the identification of several tumour derived cytokines. Some of the most prominent are those of the gp130 family: Interleukin-6 (IL-6) (Pettersen *et al*., 2017; Carson & Baltgalvis, 2010), Leukemia Inhibitory Factor (LIF) (Arora *et al*., 2018; Beretta *et al*., 2002; Mori *et al*., 1991), Ciliary Neurotrophic Factor (CNTF) (Henderson *et al*., 1994; Lambert *et al*., 2001), Interleukin-11 (IL-11) (Barton & Murphy, 2001) and Oncostatin-M (OSM) (Barton & Murphy, 2001; Stephens & Elks, 2017). Interestingly, these cytokines have a plethora of different effects in different tissue and metabolic contexts, however their effects on metabolism are only beginning to be uncovered.

IL-6 has been described to have a major role in cachexia by acting upon myoblasts to drive autophagy, leading to myotubule depletion and general body weight loss (Pettersen *et al*., 2017), but without a direct link with lipolysis. In line with this, IL-6 has also been reported to induce gluconeogenesis and glucose release from the liver (Febbraio *et al*., 2004; Stouthard *et al*., 1995) which has also been linked to cachexia (Esper & Harb, 2005; Argilés *et al*., 1997).

Similarly, *in vivo* studies on tumour bearing mice, which suffered increased lipolysis and loss of body weight, detected OSM as the earliest cytokine to be detected in the spleen (day 1) without metastasis to the spleen and prior to cachexia onset (Barton & Murphy, 2001). Indicating a role for tumour associated immune cells driving the metabolic reprogramming necessary for cachexia. Moreover, IL-6 was found in the spleen at day 3 after tumour injection, followed by IL-11 at day 6. However, when treated with neutralizing antibody directed against OSM, onset of cachexia was delayed but not prevented, suggesting that OSM participates but is not the main driver of cachexia development. Furthermore, treatment with recombinant IL-11 accelerated the onset of cachexia symptoms (Barton & Murphy, 2001), but had no effects on glucose homeostasis.

LIF does not fall behind in the rank of cachexia-inducing tumour-derived factors; Beretta *et al*. (2002) reported a dramatic decrease in Leptin levels as well as in body weight and food intake on rats treated with a single intracerebroventricular injection of a recombinant adeno-associated viral vector encoding LIF. Furthermore, chronic effects of LIF (modelled by two injections of rAAV-LIF 48 hours apart) led to a remarkable decrease in circulating insulin levels. Additionally, research by Iseki *et al*., (1995) also hinted at LIF having a central role in cachexia by showing that SEKI cells, a widely used cachexia inducing cell lineage, dramatically increased LIF levels in culture media (700pg/mL) and even more dramatically (1700pg/mL) in plasma of tumour bearing mice, prior to onset of cachexia.

Lastly, CNTF, a neurocytokine found to signal almost exclusively in the arcuate nucleus of the hypothalamus (the centre for energy balance regulation by the CNS), has been reported to regulate appetite both in leptin deficient obese mice (Gloaguen *et al*., 1997) and in healthy mice (Stefater *et al*., 2012), which had a strong anorectogenic effect leading to weight loss. In leptin deficient obese mice, this led to an amelioration of the insulin resistance phenotype, yet whether it was a direct consequence of CNTF or a consequence of the amelioration of the obesity was not determined. Moreover, Stefater *et al*. (2012) showed that leptin responsive neurons from CNTFR deficient mice could respond to exogenous CNTF administration, suggesting a cross talk between CNTF and leptin pathways.

Interestingly, DeChiara *et al*. (1995) demonstrated that whilst a knockout mutation on the CNTF receptor gene was lethal, knocking out CNTF itself was not, thus suggesting the existence of a redundant ligand. This was found to be Neuropoietin (NP), another gp130 cytokine responsible for inhibition of insulin signalling at the systemic level through hypothalamic signalling (White *et al*., 2007). Of relevance to this particular project, is the observation that both CNTF and NP signal through CNTF-Rα, which then recruits the LIF-Rα-gp130 heterodimer in order to transduce the signal (Davis *et al*., 1993; Ernst & Jenkins, 2004). Therefore, all CNTF & NP responsive cells are also susceptible to LIF signalling.

Recently, Püschel *et al*. (2020) reported the expression of a wide range of cytokines by NSCLC cells when subject to glucose deprivation, which served as the foundation for this study in establishing a mechanistic link between glucose deprivation and the production of some of the cytokines discussed above.

2.6 LIF, the tumour's Swiss-army knife

LIF was first described as a gp130-dependent secreted glycoprotein, signalling through signal transducer and activator of transcription (STAT) 1 & 3. It has been found to participate in a wide variety of processes making it one of the most pleiotropic cytokines from the IL6 family. An ever-growing body of evidence linked LIF to systemic and local glucose metabolism (Beretta *et al*. 2002; Brandt *et al*., 2015; Broholm *et al*., 2008; Broholm *et al*., 2012; Florholmen *et al*., 2004; Florholmen *et al*., 2006; Iseki *et al*., 1995; Mori *et al*. 1989). Moreover, many recent studies attribute LIF a pro-tumorigenic role in pancreatic (Shi *et al*., 2019; Wang *et al*., 2019), glioblastoma (Pascual-García *et al.*, 2019), oral-squamous (Ohata *et al*., 2017), breast (Albrengues *et al*., 2014), and lung (Chen *et al.*, 2010) carcinomas.

Beyond being a pro-tumorigenic cytokine with the ability to reprogramme glucose metabolism, LIF has been shown to be of crucial importance in the early stages of pregnancy (Salleh & Giribabu, 2014). Briefly, LIF was crucial for recruitment and regulation of immune cells that regulate angiogenesis and immunotolerance during embryo implantation (Schofield & Kimber, 2005; Hanna *et al*., 2006), as well as for trophoblast expression of pro-invasive and pro-angiogenic factors (Poehlmann *et al*., 2005; Suman *et al*., 2013) and spiral artery formation (Winship *et al*., 2015). LIF could thus be single-handedly helping the embryo achieve two functions considered to be molecular hallmarks of cancer: avoiding immune destruction and inducing angiogenesis (Hanahan & Weinberg, 2011).

Moreover, an extremely recent study provided direct evidence of LIF having a pro-angiogenic role both *in vitro* by promoting proliferation of bovine choroidal endothelial cells (BCEs) and *in vivo* by increasing retinal micro-vessel density upon intra-ocular injection (Li *et al*., 2022). This, in conjunction with another novel study showing that tumour angiogenesis is mediated by STAT3-YAP/TAZ

signalling (Shen *et al*., 2021), point towards a potential role for LIF as a key tumour angiogenic factor and a promising therapeutic target.

2.7 A gap in the literature: LIF regulation

Throughout this introduction the pro-tumorigenic nature of LIF and its functions in normal and tumoral tissues have been outlined. As previously stated, there is an abundance of literature establishing the pro-tumorigenic effects of LIF in a wide variety of malignancies (Albrengues *et al*., 2014; Chen *et al.*, 2010; Ohata *et al*., 2017; Pascual-García *et al.*, 2019; Shi *et al*., 2019; Wang *et al*., 2019). However, the issue of how LIF is regulated and what triggers its production in tumours is largely unexplored. To this date, very few studies have attempted to shed some light on this issue, and in both cases the focus was on tumour-promoting mutations rather than on cell signalling.

Upon the discovery that p53 KO mice had lower expression of LIF in the uterus leading to reproductive issues (Hu *et al*., 2007), Baxter and Milner (2010) decided to investigate the role of p53 as a transcription factor for LIF in medulloblastoma. They confirmed p53 binding to the first intron of LIF, and p53 KO in HCT116 (colo-rectal carcinoma) and D283-MED (medulloblastoma) cells decreased, but didn't abolish, LIF release. Moreover, they showed that DAOY cells (medulloblastoma) which lacked functional p53, maintained high expression levels of LIF, suggesting that, although p53 might transcribe LIF, it is not its main regulator (Baxter and Milner, 2010).

More recently, a second study by Wang *et al*. (2019) delved on the origin of LIF in pancreatic ductal adenocarcinoma (PDAC). And they found that both cells subject to knock-down of KRAS and cells lacking KRAS had lower LIF expression than those with active KRAS. Furthermore, they observed that a mouse PDAC model with inducible KRAS only expressed LIF upon KRAS induction. However, many cancer cell lines which have been previously shown to express LIF do not harbour mutations in KRAS, for example the aforementioned DAOY and D283-MED medulloblastoma cells (as reported in the COSMIC catalogue 'cancer.sanger.ac.uk' - Tate *et al*., 2019).

This last part of the introduction has covered the pro-tumorigenic role of LIF and its value as a therapeutic target. There is a widespread concern on elucidating its actions and about neutralizing it, but the signalling mechanism leading to LIF production remains a large gap in the literature. Knowing how it is induced would be invaluable for development of better targeted therapies. The present study shows a novel mechanism for LIF production that is well conserved across cancer types in a mutation independent manner. Moreover, our research has also led to the identification of a novel role for LIF as a tumour angiogenic factor.

3. Aims

The present study initially aimed to investigate the mechanisms leading to LIF release in the context of cancer. This first aim was further subdivided in two parts: (1) establishing the molecular basis of the glucose sensing triggering this response, and (2) establishing the actionable cell signalling cascade leading to LIF production.

The seminal finding that LIF was remarkably induced upon glucose deprivation elicited an additional aim of (3) understanding its potential role in promoting cancer cell survival in a hypoglycaemic microenvironment.

4. Methods

4.1 Cell Culture

A549 (non-small cell lung cancer, NSCLC) cells, a range of lung cancer cell lines (H1299, H2126, H460 and H520), LLC1 (murine Lewis lung carcinoma) cells, HEK293T cells, and HeLa cervical cancer cells were cultured in pyruvate-free high-glucose DMEM (25mM) (Gibco, Life Technologies) supplemented with 10% FBS (Life Technologies) and additional L-glutamine (2mM) (Life Technologies) and incubated at 37°C and 5% CO_2. SW900 (squamous cell lung cancer) cells and a range of rhabdomyosarcoma cells (RD, Rh4, Rh28, Rms13) were cultured in pyruvate-free high-glucose (25mM) RPMI (Life Technologies) supplemented with 10% FBS and additional L-glutamine (2mM) and incubated at 37°C and 5% CO_2. HUVEC (Human Umbilical Vascular Endothelial Cells) were cultured in EGM-2 (Lonza) supplemented with EGM-2 SingleQuots supplements (Lonza) (2% FBS, 0.04% Hydrocortisone, 0.4% hFGF-B, 0.1% VEGF, 0.1% R3-IGF-1, 0.1% Ascorbic Acid, 0.1% hEGF, 0.1% GA-1000, 0.1% Heparin) at 37ºC and 5% CO_2. HBEC (Human Bronchial Epithelial Cells) were cultured in Airway Epithelial Cell Basal Medium (ATCC) supplemented with Airway Epithelial Cell Supplement (500 mg/mL HAS, 0.6mM linoleic acid, 0.6 mg/mL lecithin, 6mM L-Glutamine, 0.4% Extract P, 1mM epinephrine, 5mg/mL transferrin, 10nM T3, 5mg/mL hydrocortisone, 5ng/mL EGF, 5mg/mL Insulin).

4.2 Cell Treatments

For glucose deprivation treatment, cells were washed twice with FBS-free, pyruvate-free, glucose-free DMEM (or glucose-free RPMI for BTE, SW900 and Rhabdomyosarcoma cell lines) and then treated with this medium supplemented with 10% dialyzed FBS (dFBS) and 2mM L-glutamine, while the control cells were supplemented with 25mM fresh glucose (Sigma).

Nutrient re-addition experiments were conducted in the same manner with the re-addition of the corresponding concentration of nutrients to media prepared as previously described. For drug experiments, the compounds were freshly added at the moment of the treatment in media prepared as previously described. For RNA polymerase I & II blockade experiments, Actinomycin D (ActD)

(MedChemExpress) was used at 80nM 1 hour prior to glucose deprivation treatment and was also present at 80nM in the treatment media. For mRNA half-life determination, cells were subject to glucose deprivation for 3 hours prior to treatment with 80nM ActD. For hypoxia experiments, cells were seeded and allowed to attach prior to addition of the corresponding treatment media. Plates were then introduced in an H35 Hypoxystation (Don Withley Scientific) set to 0.1% O_2 conditions and incubated for 24 hours.

4.3 Matrigel Tube Formation Assay

For the tube formation assays, $4x10^4$ HUVECs were seeded on Matrigel (Beckton Dickinson) in 96-well plates, in EGM-2 media (supplement free) containing recombinant human LIF or in conditioned media with anti-LIF neutralizing antibody or the corresponding IgG isotype control. Conditioned media was produced by collecting supernatants of A549 cells after 24 hours under glucose deprivation, centrifuging it on 3K MWCO protein concentrators (Thermo Fisher, Life Sciences) and resuspending the concentrated protein fraction in supplement free EGM-2 media up to the original volume of media. HUVECs were then incubated for 16h at 37ºC and 5% CO_2 and pictures were captured at 2.5X magnification.

4.4 Transwell Migration Assay

For the transwell migration assays, $5x10^4$ HUVECs were seeded on top of Boyden chambers in 24-well plates, in EGM-2 supplemented media. Boyden chambers were inserted in wells containing EGM-2 supplemented media with recombinant human LIF or conditioned media with anti-LIF neutralizing antibody or the corresponding IgG isotype control. HUVECs were allowed to migrate for 24h prior to fixation and staining of the Boyden chamber membranes with crystal violet solution (1xPBS (Biowest), 1% Formaldehyde (Sigma), 1% Methanol (Millipore), 0.05% crystal violet (Sigma)) and capture images by microscopy at 4x magnification.

Similarly, $2.5x10^4$ A549 cells were seeded on top of Boyden chambers in 24-well plates, in complete DMEM. Boyden chambers were inserted in wells containing DMEM with recombinant human LIF or conditioned media with anti-LIF neutralizing antibody or the corresponding IgG isotype control. A549 cells were allowed to migrate for 24h prior to fixation and staining of the Boyden chamber membranes with crystal violet solution (1xPBS (Biowest), 1% Formaldehyde (Sigma), 1% Methanol (Millipore), 0.05% crystal violet (Sigma)) and captured images by microscopy at 4x magnification.

4.5 Transfection

Both small interference RNA (siRNA) and SmartPool siRNA transfection was performed through reverse transfection. A transfection mixture was prepared by pre-incubating at room temperature the oligonucleotide to be transfected, for a final dose of 100nM for siRNAs and 1ug for plasmids with 0.1% Dharmafect1 (Dharmacon, GE) in 200µL supplement free high-glucose DMEM for 25 minutes (min). Cells were then seeded in complete DMEM containing the transfection mixture and incubated for 24h, prior to administration of treatment media as previously described. Plasmid transfection was performed following the same protocol but substituting Dharmafect with Lipofectamine 2000 (Invitrogen).

4.6 ELISA

Culture Supernatants were collected, centrifuged at 1000g, transferred to fresh eppendorfs and stored at -80ºC. Alternatively, cell lysates were collected in RIPA buffer, sonicated for 10s, centrifuged at 12000rcf, transferred to fresh eppendorfs and stored at -20ºC. Immunosorbent 96 well plates (Thermo Scientific) were coated with LIF capture antibody (R&D) in PBS (Biowest) and incubated at room temperature overnight. Subsequently manufacturer's instructions for the DuoSet ELISA kit (R&D) were followed. Briefly, plates were washed and blocked for 1h at room temperature on Blocking buffer (R&D). Supernatants or cell lysates were subsequently incubated for 2h at room temperature, prior to washing and incubation with detection antibody solution (R&D) for 2h at room temperature. Lastly, 20 min incubations with Streptavidin-HRP (R&D) and with colour

developing solution (R&D) ensued. The reaction was then halted by addition of STOP solution (R&D) and optical absorbance was measured using a PowerWave XS microplate spectrophotometer (BioTek Instruments) at 450nm for signal and 540nm for background removal. Protein concentrations were calculated by standard curve fitting using GraphPad Prism.

4.7 Western Blotting

Cells were lysed in RIPA buffer (NaCl 150mM, Tris-HCl 30mM, EDTA 5mM, 10% Glycerol, 1% TritonX-100, 0.5% Sodium Deoxycholate, 0.1% SDS) (Thermo Scientific) with protease and phosphatase inhibitors (Roche). Protein samples were then subject to one freeze-thaw cycle prior to centrifugation at 13000 x g and 4ºC for 15 min to remove unbroken cells and lipid components from the protein sample. Total protein concentration in cell lysates was obtained by BCA protein assay (Thermo Scientific) following manufacturer's instructions. Lysates were dissolved in PBS (Biowest) and Laemmli Buffer (63mM Tris-GCL, 10% glycerol, 2% SDS, 0.01% bromophenol blue, 5% 2-mercaptoetahol) to achieve a final amount of protein of thirty micrograms per sample. Samples were then resolved by SDS-PAGE and transferred into nitrocellulose membranes. Protein containing membranes were then blocked in 5% BSA or milk (depending on antibody) in TBS-T, incubated in the corresponding primary antibody against specific target protein, and lastly incubated in the corresponding HRP-conjugated secondary antibody specific for the species of the primary antibody. Membranes were then briefly incubated in ECL reagent (Promega), and luminescence was observed using an Amersham Imager 600 (Life Science).

4.8 Concanavalin A Blotting

In order to detect total glycosylated protein content, the same protein collection and SDS-PAGE resolution protocol was followed. Membranes were then stained with Ponceau Solution (5% Acetic acid, 0.1% Ponceau S (Fisher Scientific)) as a means to control for protein loading, and images were captured using an Amersham Imager 600 (Life Science) followed by thorough washing with TBS-T. Protein containing membranes were then blocked in Concanavalin A blocking

buffer (10mM HEPES, 150mM $NaCl_2$, 0.1mM $CaCl_2$, 0.01mM $MnCl_2$, 0.08% Sodium Azide; Ph 7.5) for 30 min at room temperature. Membranes were then incubated in Concanavalin A solution (3µg/ml Biotin conjugated Concanavalin-A, 10mM HEPES, 150mM $NaCl_2$, 0.1mM $CaCl_2$, 0.01mM $MnCl_2$, 0.08% Sodium Azide) for 1h at room temperature, followed by a 30-minute incubation in Streptavidin-HRP solution (R&D). Membranes were then briefly incubated in ECL reagent (Promega), and luminescence was observed using an Amersham Imager 600 (Life Science). For quantification, overall lane pixel density was obtained using ImageJ software and normalised against protein loading obtained by overall pixel density in ponceau staining images. Final quantifications were expressed as a fold change of the control sample to facilitate comparison across replicates.

4.9 RNA Extraction and Reverse Transcription PCR

Treated cells were collected by trypsinization and centrifuged at 500 x g for 5 min at room temperature. The cell pellet was then processed using the PureLink RNA Mini Kit (Invitrogen, ThermoFisher) following the manufacturer's instructions. Briefly, cells were lysed in lysis buffer (Invitrogen) supplemented with 1% 2-mercaptoethanol, disaggregated using sterile 25GA syringes and introduced in the microcentrifuge purification columns. A series of centrifuges and washes followed. Final elution of the purified RNA samples was done in 30µL DEPC treated dH_2O. Nucleic acid concentration and purity was measured using a NanoDrop® ND-1000 UV-Vis spectrophotometer (Thermo Scientific).

Subsequently, 1µg RNA was retrotranscribed using the High-Capacity cDNA Reverse Transcription Kit (Applied Biosystems, Invitrogen) following the manufacturer's instructions. Briefly, a mastermix containing 2µL RT buffer, 0.8µL dNTPs (100mM), 2µL RT Random primers, 1µL MultiScribe™ Reverse Transcriptase and 4.2µL H_2O was prepared and 10µL were added to each RNA sample in DNAse-free PCR-compatible tubes and cycled on an Applied Biosystems 2720 Thermal Cycler following RT kit manufacturer's settings.

4.10 PCR and DNA Electroporation

For conventional PCR, a mastermix containing 2.5µL NH_4 reaction buffer (Bioline), 1.5µL of 50mM $MgCl_2$, 1µL of 25mM dNTPs, 0.5µL of Biotaq DNA polymerase (Bioline) and 7µL of H_2O was prepared per sample and 12.5µL aliquots were placed in PCR tubes. Then, 2.5µL of 10µM primer pair specific for the gene of interest were added. Lastly, 10µL cDNA obtained by reverse transcription of RNA were added to each tube and cycled on an Applied Biosystems 2720 Thermal Cycler with the following settings: 5min 94ºC, 35X cycles of 15sec 94ºC, 30sec 61ºC and 60sec 72ºC; and lastly 7 min 72ºC.

Samples were then allowed to cool down and separated by electrophoresis on 2% agarose gels dyed with ethidium bromide and imaged.

4.11 Quantitative Real Time PCR (qPCR)

For qPCR preparation triplicate reactions were set up containing 10ng cDNA, 1 µM primer mixture (forward and reverse mixture) and PowerUp SYBER Green Master mix (Applied Biosystems, Invitrogen) in a final volume of 10µL. Samples were loaded in LightCycler® 480 Multiwell Plate 384 (Roche) and cycled in a LightCycler® 480 (Roche). Annealing temperatures were adjusted according to primer specifications. Primer dimer false positives were excluded by Melting temperature analysis. Relative quantitation of gene expression was calculated through the ΔΔCt method described by Livak and Schmittgen (2001). A preliminary NormFinder experiment was run as described by Andersen *et al.* (2004) to identify the most stable housekeeping gene available under glucose deprivation conditions. Subsequently L32 was selected as a housekeeping control for quantification.

4.12 CRISPR-Cas9 LIF Knock-Out (KO)

Plasmids for lentiviral packaging (pCM2.G & psPAX2 - Addgene) were transformed into competent HB101 *E. coli* by heatshock as per manufacturer's instructions for plasmid amplification. Plasmids for LIF CRISPR-Cas9 KO and Scramble gRNA lentiviral control (VectorBuilder) were transformed into

competent JB109 *E. coli*. Bacteria were then seeded in LB Agar plates with Ampicilin (100µg/mL) and incubated at 37ºC overnight. A single colony was picked and allowed to grow on LB overnight under agitation at 37ºC. Subsequently plasmid DNA purification was performed using a PureLink™ HiPure Plasmid Midiprep Kit (Invitrogen) following manufacturer's instructions. Purity and concentration of the resulting DNA was measured using a NanoDrop® ND-1000 UV-Vis spectrophotometer (Thermo Scientific).

Lentivirus production was performed in HEK293T cells. Briefly, HEK293T cells were seeded and allowed to grow to confluence. 2h before transfection fresh media was added. Packaging plasmids (10ug DNA) and CRISPR-Cas9 plasmid (20ug DNA) were simultaneously co-transfected using lipofectamine2000 (Invitrogen) as per manufacturer's instructions. 24h later media was refreshed, and 24h later the supernatant was collected and concentrated using Amicon® Ultra-15 Centrifugal Filters of 100K MWCO (Merck Millipore).

LLC1 cells were seeded at 5x 104 cells/mL in 12 well-plates and allowed to attach overnight. Media was then replaced with media containing 8µ/mL polybrene 2h prior to infection. Lastly, lentiviral concentrates were resuspended in complete media at a 100X concentration of the original HEK293T supernatant volume and administered to LLC1 cells. 48h later infection media was discarded and cells were transferred to p100 plates in complete media with puromycin (3µg/mL). A non-infected control was used to determine puromycin efficacy. Once the cells in the non-infected plate were completely dead, infected LLC1 cells were amplified and LIF release was measured by ELISA in presence and absence of glucose to confirm effectiveness of the KO.

4.13 Animal Model (*In vivo*)

This protocol was performed with C57BL/6 mice, which were purchased from Charles River Laboratories. Lung tumours were generated by tail-vein injection of LLC1 cells (5 x10^5). Two cohorts of 10 animals each were generated based on the type of cells injected: LIF CRISPR-Cas9 KO LLC1 (LIF-KO) and Scramble gRNA lentiviral control LLC1 (Scram). Animals were fed and watered ad libitum and maintained under controlled temperature (22° C), humidity (50%) and a

light/dark cycle (12 h/12 h). The animal procedures were approved by the Ethics Review Committee for Animal Experimentation from IDIBELL (protocols 11084 and FUE-2020-01637415) and designed according to European guidelines (Directive 2010/63/EU).

The animals were monitored regularly since day-of-injection (d0) until day of sacrifice (d28). Mice were sacrificed on d28 due to the decease of one of the mice in the scramble group on d26. Of the remaining 19 animals, only 12 developed orthotopic lung lesions (6 on each cohort). The rest developed lesions in the tail instead or didn't develop any lesions.

Lungs were collected, weighted, imaged, and preserved in 4% PFA for 48h. They were then paraffin embedded and microtome sectioned in 5µm thick coronal sections. Three equally spaced sections, approximately 100 µm apart, were collected and subject to immunohistochemical staining.

4.14 Immunohistochemical staining (IHC)

Tissue sections were deparaffinated and rehydrated by 1h preincubation at 45ºC followed by serial immersions in xylol and ethanol using the Autostainer XL ST5010 (Leica). Rehydrated tissue was then blocked in 5% goat serum for 1h prior to overnight incubation in humidified chamber at 4ºC with primary antibodies against Ki67 (ThermoFisher Scientific) and CD31 (Abcam) at 1:100 and 1:50 dilutions respectively. Subsequently, samples were washed five times in PBS and incubated for 2h at room temperature in humidified chamber with secondary antibodies Alexa-Fluor 488 conjugated anti-rat (Cell Signaling) and Alexa-Fluor 546 conjugated anti-rabbit (Invitrogen). Lastly, samples were washed five times in PBS prior to staining with 4,6-diamidino-2-phenylindole, dihydrochloride (DAPI) (Invitrogen) and coverslip mounting with ProLong™ Gold Antifade mounting medium (ThermoFisher Scientific). One additional sample without primary antibody was produced to evaluate non-specific secondary antibody binding.

4.15 Tissue imaging and analysis

Whole tissue sections were imaged at 10X magnification using a Zeiss AxioObserver Z1 inverted fluorescence microscope and stitched to produce

whole tissue scans. The resulting images were analysed using FiJi (Schindelin *et al*., 2012). Ki67 high tumoral areas were automatically identified and manually adjusted based on tissue morphology. Non-tumor related signal occurring in surrounding tissues (i.e. heart and lymph nodes) was excluded. Within the previously identified Ki67-high tumour regions, non-continuous CD31+ structures were counted using the cell-counter feature in FiJi. This result was used to calculate blood vessel density, expressed as number of CD31+ structures per tumour area (CD31+ Structures/μm^2).

4.16 Flow Cytometry: Propidium Iodide incorporation

Supernatant of cells in culture were collected using plastic Pasteur pipettes and transferred to cytometry tubes. Cells were incubated in trypsin (Gibco) for 5min at room temperature and collected in the same tubes as the supernatants. Tubes were centrifuged for 5 min at 450rcf. Supernatants were discarded and the resulting cell pellet was resuspended in 300µL of a 0.5µg/mL propidium iodide solution in PBS-EDTA (1µM). After a 15 min incubation at room temperature protected from light, cells were sorted using a Galios^{TM} Flow Cytometer (Beckman Coulter), with a 488nm excitation laser and side scatter (SSC), forward scatter (FSC) and PI specific signal through a 620/30 bandpass filter. SSC and FSC were used to determine total cell population, excluding debris and clumps of cells. PI and FSC were used to separate live and dead cell populations.

4.17 Transcription-Factor Binding-Site prediction

The Transcription-Factor Binding-Site (TFBS) prediction tool PROMO (Messeguer *et al*., 2002), hosted by the algorithmic and genetics group (ALGGEN), was used to identify potential TFBS in the promoter of LIF. In order to do this an unbiased approach was taken by assessing the potential binding of all transcription factor matrices in the *Transfac* database v8.3 and filtering by a maximum dissimilarity rate of 5%.

4.18 Correlation between LIF expression and hypoxia / angiogenesis pathways

The activity level of angiogenesis and hypoxia molecular pathways was inferred from different LUAD and LUSC datasets expression profiles using gene set variation analysis (GSVA) method**.** Gene signatures for angiogenesis and hypoxia pathways were obtained from the Hallmarks collection from MSigDB V.7.0. In summary, for each sample and molecular pathway, we obtained a score between [-1, +1], with values near 1 or -1 indicating a relative high or low activity of the pathway in a specific sample, respectively. Moreover, as the number and the nature of the samples in the datasets affect GSVA scores, we performed a k-fold approach across 100 iterations in order to reduce this effect. For this, we randomly split the dataset in five subsets of the same size (k = 5-fold) and calculated the GSVA score in one of the subsets (1/5th of the samples) and in the rest separately (4/5th of the samples). This process was repeated five times, until each of the 5 subsets were used independently once. Therefore, we obtained five different GSVA scores for each sample and pathway. All this process was repeated 100 times, starting each time with a different sample permutation order. Finally, the final GSVA score for each sample and pathway was calculated as the average of the 500 GSVA scores obtained across the 100 iterations.

Once relative activity for angiogenesis and hypoxia molecular pathways was evaluated for each sample in the LUAD and LUSC datasets, spearman correlation coefficients were calculated between normalized LIF mRNA expression values (log_2TPMs) and the GSVA scores calculated for angiogenesis and hypoxia. Once the different correlation measures were calculated independently in each LUAD and LUSC study, we used the Fisher Z transformed correlation as an estimate to calculate a summary correlation estimate for the relation between LIF expression and angiogenesis or hypoxia in LUAD and LUSC, respectively. The overall correlations for LUAD and LUSC were estimated using the metacor function under meta R package V.5.2.0 and by means of a random effects model.

The k-fold approach analysis methodology was developed by collaborator Sara Hijazo and the correlation analysis was performed with her assistance.

4.19 Association of LIF expression with overall survival in LUAD and LUSC samples

KM plot online facility was used to estimate the association between LIF mRNA expression and overall survival (OS) in LUAD and LUSC samples (Gyorffy *et al*,. 2013). Sources for the datasets used in this analysis include Gene Expression Omnibus (GEO), European Genome-Phenome Archive (EGA) and The Cancer Genome Atlas (TCGA). The association between LIF mRNA expression levels and OS rate in LUAD and LUSC groups was assessed using Kaplan-Meier estimator and log-rank non-parametric test.

5. Materials

REAGENT or RESOURCE	SOURCE	IDENTIFIER
Antibodies		
Rabbit monoclonal anti-ATF-4 (D4B8)	Cell Signaling	11815S
Mouse monoclonal anti-Actin, (C4)	Merck Millipore	MAB1501R
Mouse monoclonal anti-β-Tubulin, (TUB 2.1)	Sigma-Aldrich	T4026
Mouse monoclonal anti-CHOP (L63F7)	Cell Signaling	2895S
Rabbit monoclonal anti-PERK (C33E10)	Cell Signaling	3192S
Rabbit polyclonal anti-NRF1	Sigma-Aldrich (Prestige Antibodies®)	HPA029329
Rabbit polyclonal anti-QRICH1	Sigma-Aldrich (Prestige Antibodies®)	HPA037677
Rabbit monoclonal anti-NRF2 (D1Z9C) XP®	Cell Signaling	12721T
Rabbit polyclonal anti-ATF6	R&D systems	MAB71527-100
Rabbit monoclonal anti-Phospho-eIF2α (Ser51) (119A11)	Cell Signaling	3597S
Rabbit monoclonal anti-eIF2α (D7D3) XP®	Cell Signaling	5324S
Rat monoclonal anti-Ki67 (SolA15)	ThermoFisher	14-5698-82
Rabbit polyclonal anti-CD31	Abcam	ab28364
Goat Anti-Mouse IgG–Peroxidase	Sigma-Aldrich	A9917
Goat Anti-Rabbit IgG–Peroxidase	Sigma-Aldrich	A0545
Goat Anti-Rabbit IgG Alexa Fluor 546	Invitrogen	a11010
Goat Anti-Rat IgG Alexa Fluor 488	Cell Signaling	4416S
Bacterial and virus strains		
Escherichia coli (JM109)	Promega	L2005
Escherichia coli (HB101)	Promega	L2015
Chemicals, buffers, media, peptides, and recombinant proteins		
Actinomycin D	MedChem Express	#HY-17559
Crystal Violet	Sigma-Aldrich	#61135
DharmaFECT1	Fisher Scientific	#T-2001-02
Lipofectamine 2000	Invitrogen	#11668-019
Dulbecco's Modified Eagle Medium (DMEM)	ThermoFisher	#41965-062
Dulbecco’s Phosphate Buffered Saline 10X	Biowest	#X0515-500
Dulbecco's Modified Eagle Medium (DMEM)-glucose free	ThermoFisher	#11966-025
Hanks' Balanced Salt Solution (HBSS)	Gibco, ThermoFisher	# 24020-091
MEM Non-Essential Amino Acids Solution (100X)	Gibco, ThermoFisher	#11140050
DMEM, high glucose, no glutamine	Gibco, ThermoFisher	#11960044
Formaldehyde solution	Sigma-Aldrich	#252549
Methanol	Merck-Millipore	#106009
Ponceau S Staining Solution	ThermoFisher	A40000279

Corning® Matrigel® Basement Membrane Matrix, LDEV-free, 10 mL	Corning	#354234
Pierce™ Protein Concentrator PES, 3K MWCO, 5-20 mL	ThermoFisher	#88526
Amicon® Ultra-15 Centrifugal Filters of 100K MWCO	Merck-Millipore	UFC910024
Falcon® Permeable Support for 24-well Plate with 8.0 µm Transparent PET Membrane, Sterile	Corning	#353097
PowerUp SYBR Green Master mix	Applied biosystems	#A25741
RPMI 1640	Life Technologies	#21875034
RPMI 1640 – glucose free	Life Technologies	#11879020
A-769662	Sigma-Aldrich	SML2578-5MG
Compound C	Calbiochem, Merck	#171260
PERK Inhibitor GSK2656157 10 mM	MedChem Express	HY-13820
AMG PERK-44	Tocris, BioTechne	#5517
ERK1/2 inhibitor PD98059	Calbiochem, Merck	513000
IKK inhibitor BAY-117082	Calbiochem, Merck	196870
GCN2 inhibitor A-92	AXON Medchem	2720
Bafilomycin A	Sigma-Aldrich	B1793
Propidium Iodide	Sigma-Aldrich	P4170
4µ8C	Sigma-Aldrich	SML0949-5MG
MKC-8866	Fosun Orinove PharmaTech Inc.	N/A
Metformin hydrochloride	Supelco, Merck	PHR1084
Oligomycin from Streptomyces diastatochromogenes	Sigma-Aldrich	O4876-5MG
PFKFB3 inhibitor, 3PO 25mg	Calbiochem, Merck	#525330
4-Hydroxy-TEMPO	Sigma-Aldrich	#176141-1G
MitoTEMPO	Sigma-Aldrich	SML0737-5MG
Necrostatin-1	Enzo LifeScience	BML-AP309-0020
2-Deoxy-D-glucose	Sigma-Aldrich	D6134-1G
Thapsigargin	Sigma-Aldrich	T9033-.5MG
Tunicamycin from *Streptomyces sp.*	Sigma-Aldrich	T7765-1MG
NGI-1	Sigma-Aldrich	SML1620-5MG
Methyl pyruvate	Sigma-Aldrich	371173
D-(+)-Mannose	Sigma-Aldrich	M6020
D-(+)-Glucose	Sigma-Aldrich	G7021
L-Glutamine (200 mM)	ThermoFisher	#25030024
Sodium L-lactate	Sigma-Aldrich	L7022-5G
N-Acetyl-D-glucosamine	Sigma-Aldrich	A3286-5G
D-(−)-Fructose	Sigma-Aldrich	F0127
D-(+)-Galactose	Sigma-Aldrich	G0750-5G
Concanavalin A from *Canavalia ensiformis* - Biotin	Sigma-Aldrich	C2272-2MG
ISRIB	Sigma-Aldrich	SML0843-5MG

2BACT	Aobius	AOB17667
A-92	Axon Medchem	#2720
LB	Invitrogen	#12795-027
Agar	Pronadisa	#1800
Ampicilin	Sigma-Aldrich	A9393-5G
Puromycin	Sigma-Aldrich	P8833-25MG
DAPI (4,6-diamidino-2-phenylindole, dihydrochloride)	Invitrogen	D1306
ProLong™Gold Antifade Mounting Medium	ThermoFisher	P36930
Critical commercial assays		
DuoSet ELISA Development Systems	R&D systems	#DY008
Human LIF DuoSet ELISA	R&D systems	#DY7734-05
PureLink™ RNA Mini Kit	Invitrogen	#121830128A
Pierce™ BCA Protein Assay Kit	ThermoFisher	#23225
PureLink™ HiPure Plasmid Midiprep Kit	Invitrogen	#K210005
Experimental models: Cell lines		
A549	Maria Molina	ATCC CCL-18
H1299	Montserrat Sanchez Cespedes	ATCC CRL-5803
H2126	Montserrat Sanchez Cespedes	ATCC CCL-256
H460	Vanessa Soto Cerrato	ATCC HTB-177
H520	Vanessa Soto Cerrato	ATCC HTB-182
Lewis Lung Carcinoma / LL/2 (LLC1)	ATCC	ATCC CRL-164
LLC1 LIF CRISPR-Cas9 KO	Self-produced	N/A
LLC1 Scramble gRNA-Cas9	Self-produced	N/A
SW900	Vanessa Soto Cerrato	ATCC HTB-59
Human Bronchial Epithelial Cells (HBEC)	ATCC	ATCC PCS-300-010
Human Umbilical Vascular Endothelial Cells (HUVEC)	Mariona Graupera	N/A
RD	ECACC	ECACC 85111502
Rms13	Òscar Martínez Tirado	N/A
Rh4	Òscar Martínez Tirado	N/A
Rh28	Òscar Martínez Tirado	N/A
HeLa	Douglas Green	ATCC CCL-2
HEK293T	Ramón Alemany	CRL-3216™
Experimental models: Organisms		
C57BL/6		
siRNA Oligonucleotides		
siRNA targeting sequence: ATF4 #1 GCCUAGGUCUCUUAGAUGA (Sigma-Aldrich)	Ohoka *et al*., EMBO J 2005	N/A

siRNA targeting sequence: ATF4 #2 CCAGAUCAUUCCUUUAGUUUA [dT][dT] (Sigma-Aldrich)	Gargalovic *et al*., PNAS 2006	N/A
siGENOME siRNA Non-Targeting siRNA Pool #1	Horizon Discovery	D-001206-13-20
siGENOME EIF2AK3 (Human)-PERK siRNA SMARTPool	Horizon Discovery	M-004883-03-0005
siRNA targeting sequence: ATF6 #1 GGCAGGACUACGAAGUGAUGATT (Sigma-Aldrich)	Eric Chevet	N/A
siRNA targeting sequence: ATF6 #2 GAACAGGAUUCCAGGAGAAUU (Sigma-Aldrich)	Sullivan *et al*., Dev Cell 2020	N/A
siRNA targeting sequence: CHOP #1 AAGAACCAGCAGAGGUCACAA (Sigma-Aldrich)	Yamaguchi and Wang, J Biol Chem, 2004	N/A
siRNA targeting sequence: CHOP #2 GGUCCUGUCCUCAGAUGAA (Sigma-Aldrich)	Sullivan *et al*., Dev Cell 2020	N/A
siRNA targeting sequence: NRF-2 GAGAAAGAAUUGCCUGUAAUU [dT][dT] (Sigma-Aldrich)	Singh *et al*., AJRCMB 2006	N/A
siRNA targeting sequence: siXBP1 #1 (3) GAAUUCCUCUAUUUGUUCA (Sigma-Aldrich)	Custom	N/A
siRNA targeting sequence: siXBP1 #2 (4) Seq (Sigma-Aldrich)	MISSION esiRNA	EHU069131
siRNA targeting sequence: STT3 A GCGAUUGUCCUAUGAGAAG (Sigma-Aldrich)	Yasuda *et al*., FASEB J 2015	N/A
siRNA targeting sequence: STT3 B GCUCUAUAUGCAAUCAGUG (Sigma-Aldrich)	Yasuda *et al*., FASEB J 2015	N/A
siRNA targeting sequence: QRICH1 CCAAGUACUUCCUAUUGAA [dT][dT] (Sigma-Aldrich)	Sigma pre-designed	SASI_Hs01_00125414
siRNA Non-Targetting (NT) sequence: UAAGGCUAUGAGAGAUAC [dt][dt] (Sigma-Aldrich)	Elgendy *et al*., Mol Cell 2011	N/A
qPCR primers		
AGR2. Fw: GGTGACCAACTCATCTGGACTC; Rv: TGACTGTGTGGGCACTCATCCA	OriGene qSTAR primer	HP209366
LIF. Fw: CCCATCACCCCTGTCAACG; Rv: GGGCCACATAGCTTGTCCA	Rajput *et al*., Mol Cancer Ther 2013	N/A
LIF-D. Fw: CATCTGAGGTTTCCTCCAAGG; Rv: GAGGTTGTTGTGACATGGGT	Self-designed	N/A
LIF-M. Fw: GAAGCGTGTGGTCTGCG; Rv: GAGGTTGTTGTGACATGGGT	Self-designed	N/A
LIF-T. Fw: TGTCACCTTTCACTTTCCTTCC; Rv: GAGGTTGTTGTGACATGGGT	Self-designed	N/A
L-32. Fw: AACGTCAAGGAGCTGGAAG; Rv: GGGTTGGTGACTCTGATGG	Iurlaro *et al*., Mol Cell Biol 2017	N/A
XBP1s. Fw: TTACGAGAGAAAACTCATGGCC; Rv: GGGTCCAAGTTGTCCAGAATGC	Iurlaro *et al*., Mol Cell Biol 2017	N/A

Recombinant DNA		
Scramble gRNA lentiviral control vector pLV[CRISPR]-hCas9/Puro-U6>Scramble _gRNA1	Vectorbuilder	VB180522-1197
pLV[CRISPR]-hCas9:T2A:Puro U6>mLif[gRNA#2203]	Vectorbuilder	VB900048-2266
pcDNA3.1	M. Buschbeck's lab	N/A
pDM2.G	AddGene	#12259
psPAX2	AddGene	#12260

6. Results I: The mechanisms leading to LIF release

6.1 Glucose deprivation induces LIF release

The preliminary finding behind this PhD thesis comes from a cytokine array of supernatants from A549 lung adenocarcinoma cells under glucose deprivation. One of the seemingly upregulated cytokines was LIF.

Thus, we first sought to validate this finding through studying LIF release in a variety of cell lines and not only under complete glucose deprivation but also under glucose restriction. We found that LIF production upon lack of glucose is a widespread phenomenon across most lung cancer subtypes, independent of the mutational background (Fig 1A). Moreover, LIF release upon glucose deprivation was also observed in cervical cancer cells (HeLa) and at least one rhabdomyosarcoma cell line (RD) (Fig 1B).

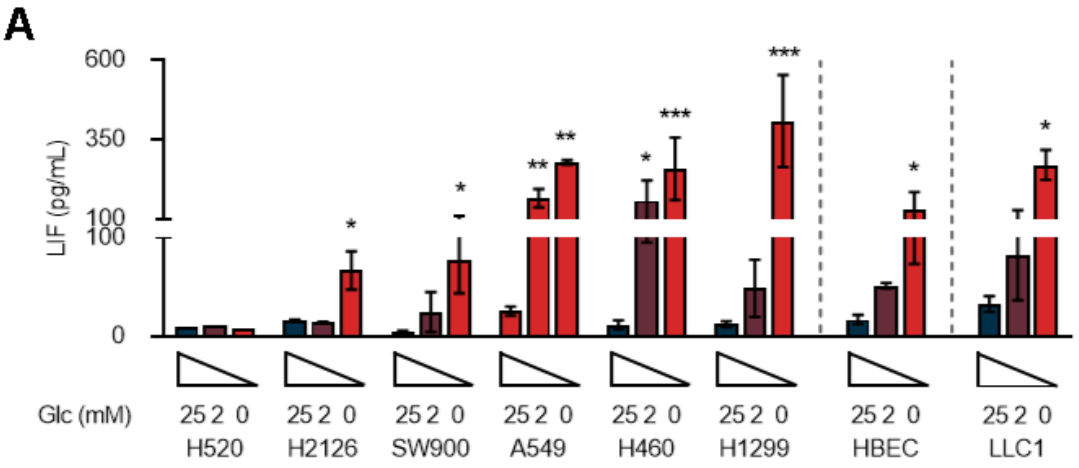

Cell Line	H520	H2126	SW900	A549	H460	H1299	HBEC	LLC1
Histology	LUSC	NSCLC	NSCLC	LUAD	LCC	NSCLC	Non-Malign	Murine LC
KRAS	WT	WT	Mut (35 G>T)	Mut (34 G>A)	Mut (183 A>T)	WT	-	Mut (34 G>T)
NRAS	WT	WT	WT	WT	WT	Mut (181 C>A)	-	Mut (183 A>C)
LKB1	WT	WT	WT	Mut (109 C>T)	Mut (109 C>T)	WT	-	WT
p53	Mut (438 G>A)	Mut (184 G>T)	Mut (499 C>T)	WT	WT	Del	-	Mut (334 R>T)
KEAP1	WT	WT	WT	Mut (997 G>T)	Mut (706 G>C)	WT	-	WT

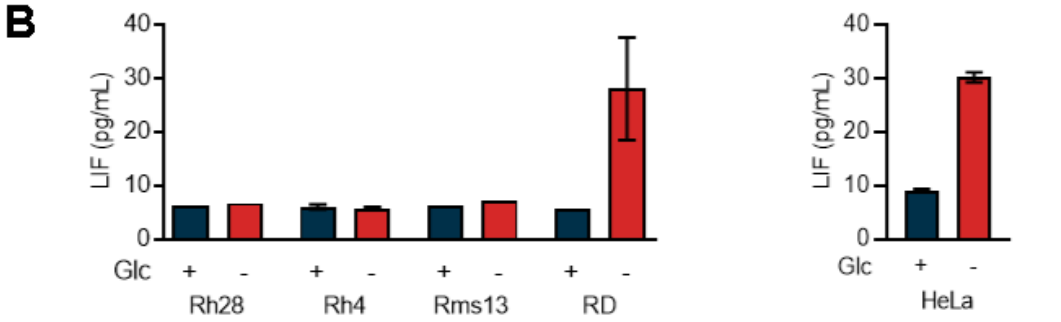

Cell Line	Histology	KRAS/NRAS	PAX3 fusion	p53
RD	Embryonal	Nras (Q61H)	No	TP53
Rh28	Alveolar	WT	Yes	WT
Rh4		WT	Yes	TP53
Rms13		WT	Yes	TP53

Cell Line	Histology	KRAS/NRAS	LKB1/KEAP1	p53
HeLa	CSCC	WT	WT	WT

Fig 1. LIF is secreted upon glucose stress by a broad range of malignant and non-malignant cells. (A) LIF protein measured by ELISA in supernatants from lung derived cell lines with diverse mutational backgrounds after 24h incubation in DMEM with decreasing concentrations of glucose (Glc) (n=3). Including non-malign Human Bronchial Epithelial Cells (HBEC) and Lewis Lung Carcinoma (LLC1) murine cells. (B) LIF protein measured by ELISA in supernatants from rhabdomyosarcoma and cervical cancer (HeLa) cell lines with diverse mutational backgrounds after 24h incubation in DMEM with decreasing concentrations of glucose (Glc) (n=1-4). Graphs represent the mean and SEM; *-**** indicate significant differences obtained by paired t-test ($p<0.05$-0.0001).

We found that this phenomenon was specifically driven by glucose deprivation, but not by other physiological disturbances that often accompany glucose deprivation in live organisms, such as hypoxia (Fig 2A) or drugs mimicking hypoxia (Fig 2B); complete deprivation of amino-acids (Fig 2C) or glutamine deprivation (Fig 2D). Moreover, supplementation with non-essential amino-acids also had no effects on LIF release (Fig 2E), Lastly, we established that oxidative stress did not induce LIF release (Fig 2F).

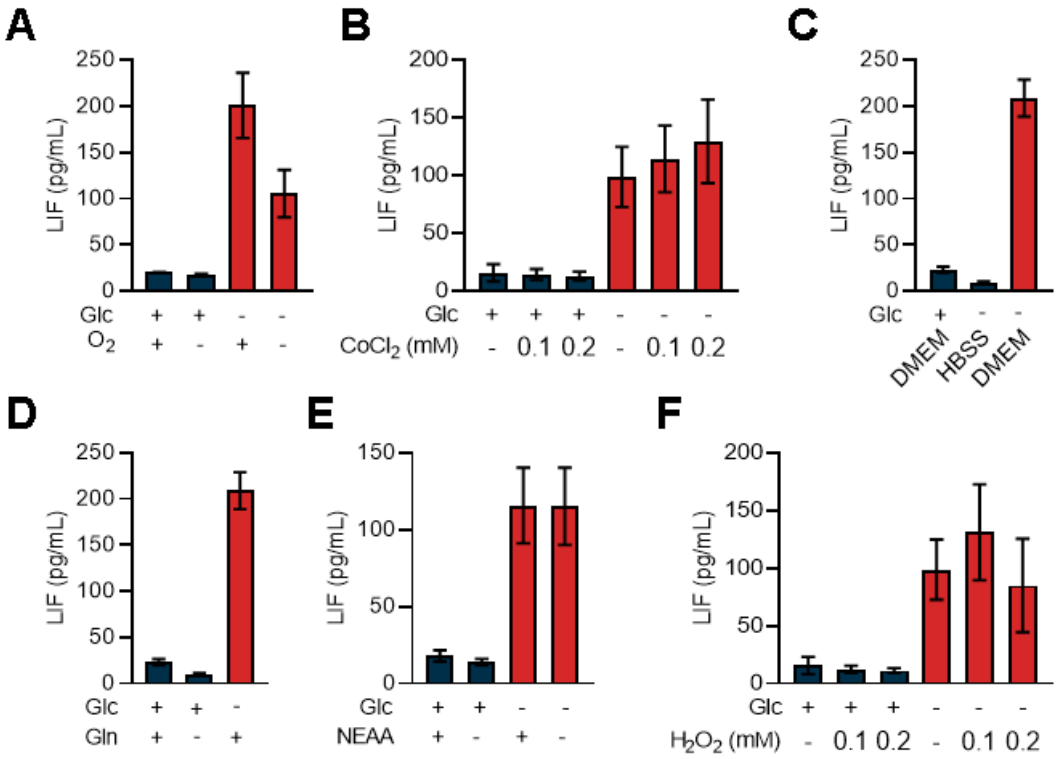

Fig 2. LIF secretion is a glucose-specific response. (A) LIF protein measured by ELISA in supernatants of A549 cells incubated under hypoxic conditions (0.1% O_2) and glucose deprivation over 24h (n=2) or (B) under chemical pseudo-hypoxia induced by $CoCl_2$ and glucose deprivation (n=3). (C)* LIF protein measured by ELISA in supernatants of A549 cells incubated under complete amino-acid deprivation by incubation in HBSS (n=4), (D) under glutamine deprivation (n=4), (E) in glucose deprivation with supplementation of non-essential amino-acids (NEAA) (n=3), or (F) under severe oxidative stress induced by H_2O_2 (n=3). Graphs represent the mean and SEM. *Supernatants for the ELISA in panel C were produced by J. Redondo for a different experiment and repurposed here.

6.2 LIF response is predominantly secretory

LIF is a pleiotropic cytokine, and as such it has been described to have both intracellular and extracellular functions. In order to determine whether LIF production upon glucose deprivation functions as an extra-cellular stress signal or as part of an intracellular adaptation programme, we studied the isoforms of LIF produced by A549 cells. We found that upon glucose deprivation, only the secreted isoforms of LIF are expressed, whereas the intracellular isoform of LIF was not present (Fig 3A-B). Furthermore, we found that LIF was virtually absent from the supernatant of A549 cells under normal conditions and was immediately secreted as cells were placed in glucose deprived conditions, with significant differences observed as early as 3h (Fig 3C). Lastly, we compared LIF abundance in the lysate and supernatant of A549 cells under different degrees of hypoglycaemia and observed that intracellular levels of LIF were insignificant in all cases (Fig 3D), further evidencing that the LIF response upon glucose deprivation is predominantly secretory.

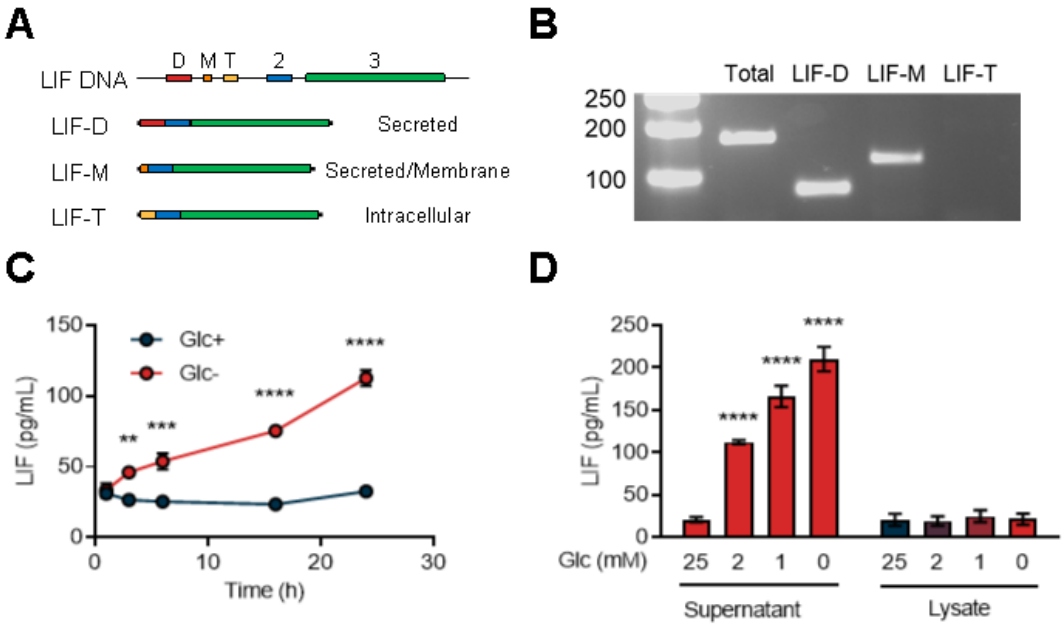

Fig 3. Most LIF produced under glucose deprivation is secreted. (A) Diagrammatic representation of LIF isoforms based on their exons. (B) PCR of primers specific for total LIF and each individual LIF isoform from mRNA of A549 cells incubated under glucose deprivation for 6h. (C) LIF secretion kinetic from A549 cells incubated with 25 mM (Glc+) or 0 mM glucose (Glc-) (n=4). (C) LIF protein measured by ELISA in supernatants and lysates of A549 cells after 16h incubation in DMEM with decreasing concentrations of glucose (n=3). Graphs represent the mean and SEM; *-**** indicate significant differences obtained by One-way ANOVA (C) or paired t-test (D) ($p<0.05$-0.0001).

It is of relevance to mention that quantification of LIF in the intracellular fraction was only possible via ELISA. A series of tests using different commercially available antibodies were run, including production of concentrated lysates by increasing plate surface and decreasing lysis buffer volume, and concentration of supernatant proteins using low MWCO filters or iso-citrate concentration. However, LIF was never successfully blotted by western blot. Among the tests run, we resorted to blotting serial dilutions of recombinant human LIF and found that out of three different commercially available antibodies only one could reliably detect LIF at concentrations in the range of 30pg (Fig 4). If ELISA results from Fig 3D are to be used as a reference, the total amount of LIF in the lysate should be in the range of 1pg LIF for a fully confluent well of a 6-well plate (35mm diameter).

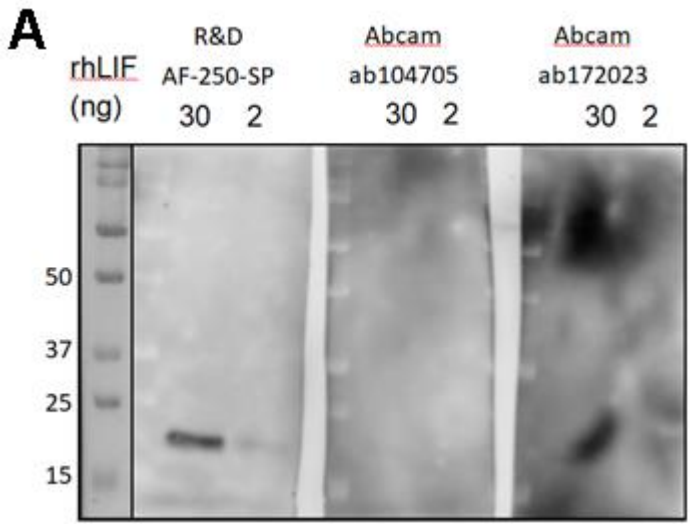

Fig 4. Anti-LIF antibodies are not sensitive enough. (A) Recombinant human LIF protein loaded at 30ng and 2ng final amount, SDS-PAGE separated and blotted with three different primary antibodies. Expected MW: 19.6KDa.

6.3 Defects in N-glycosylation trigger LIF release

Given that LIF was expressed in a wide array of cells as a specific response to glucose deprivation, we aimed to further investigate the specific metabolic trigger downstream of lack of glucose leading to LIF release. As previously discussed, glucose has many metabolic uses in cancer cells, namely: energy and biomolecule production, redox balance, and protein glycosylation (Fig 5A). To approach the issue of which of these metabolic roles was the main trigger leading to LIF release, we subjected A549 cells to glucose deprivation while also supplementing the media with different glucose derived metabolites relevant to each of these functions (Fig 5B).

We observed that mannose supplementation completely inhibited LIF production under glucose deprivation. This could be indicative of the involvement of the N-glycosylation metabolic pathway, since mannose is the main substrate used for core glycan synthesis, at a rate of 9 mannose molecules per N-glycosylated residue of a protein. Importantly, a high concentration of fructose (25mM) also partially inhibited LIF release, but not the lower concentration (5mM). For reference, plasma levels of fructose in non-diabetic patients are in the range of 8.1 ± 1.0 µM (Kawasaki *et al*., 2002). This could be due to the potential conversion of fructose to mannose via the mannose biosynthetic pathway, and the competition of this conversion with other potential uses of fructose for glycolysis and NADP reduction.

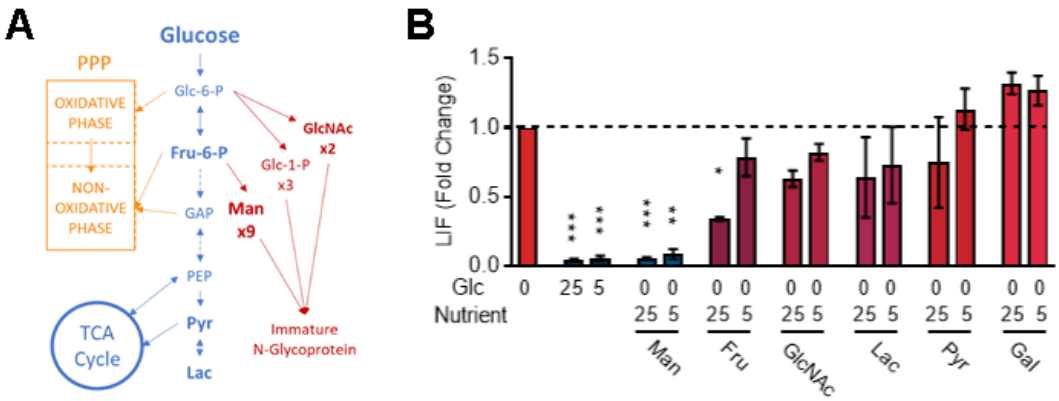

Fig 5. Mannose re-addition prevents LIF release during glucose deprivation. (A) Diagrammatic representation of three main metabolic pathways downstream of glucose; from left to right: pentose phosphate pathway (PPP), glycolysis and TCA, and N-glycosylation. (B) Changes in secreted LIF in supernatants from A549 cells after 48h incubation in glucose deprived conditions with re-addition of several glucose derived metabolites (n=3). Man = Mannose, Fru = Fructose, GlcNac = N-acetylglucosamine, Lac = Lactate, Pyr = Pyruvate, Gal = Galactose. Graphs represent the mean and SEM; *-**** indicate significant differences obtained by One-way ANOVA ($p<0.05$-0.0001).

To further dissect these metabolic pathways, we used chemical inhibitors or intermediates for each of the aforementioned routes. Inhibitors of glycolysis (3PO) and TCA cycle (Oligomycin, OM; and metformin, Metf) did not induce LIF release (Fig 6A-B). Furthermore, inhibitors of some canonical sensors of glycolytic imbalance mTOR (Rapamycin and Torin1) and AMPK (ComC) also failed to inhibit LIF release (Fig 6C-E). Additionally, a positive regulator of AMPK signalling (A769662) did not trigger LIF release (Fig 6E). Together, these results

evidence a lack of involvement of the glycolytic metabolic pathway in triggering LIF release.

Secondly, the pentose phosphate pathway (PPP) and its main role in redox homeostasis was probed using cytosolic and mitochondrial ROS scavengers (tempol and mitotempo) (Fig 6F), as well as NADPH replenisher (N-acetylcysteine, NAC) (Fig 6G). However, these did not decrease LIF production. Lastly, an inhibitor of the PPP was used (DHEA) in presence of glucose, yet it failed to promote LIF release (Fig 6H). This indicates that LIF is not produced in response to impaired redox homeostasis secondary to glucose deprivation.

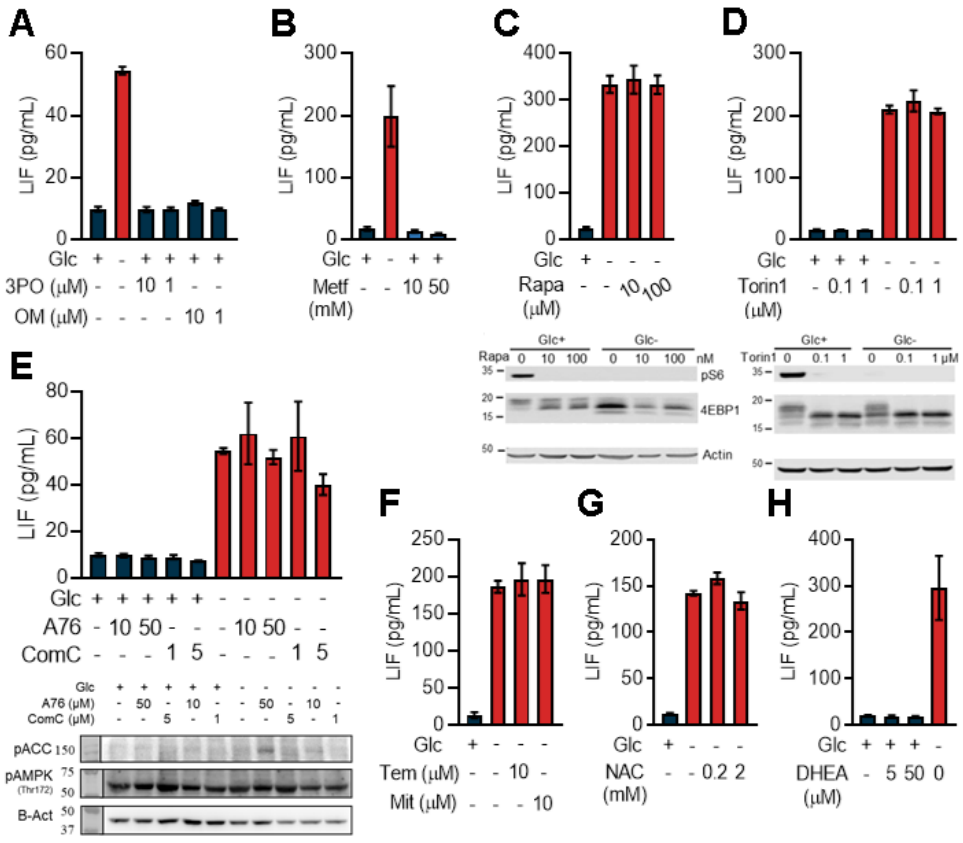

Fig 6. LIF release is not dependent on PPP or glycolytic outputs. (A) LIF secreted by A549 cells after 24h treatment with inhibitors of glycolysis, 3PO (n=3), mitochondrial respiration, oligomycin (OM) (n=3), and (B) mitochondrial complex I inhibitor metformin (Metf) (n=6). (C)*[1] LIF secreted by A549 cells after 24h treatment with inhibitors of mTOR Rapamycin (Rapa) (n=2) and (D)*[2] Torin1 (n=3). (E) LIF secreted by A549 cells after 24h treatment with activator of AMPK, A769662 (A76), and inhibitor of AMPK, Compound C (ComC) (n=3). (F)*[3] Secreted LIF from A549 cells after 24h treatment with scavengers of cytosolic (Tempol) and mitochondrial (Mitotempo) ROS (n=2), (G) with NADPH replenisher N-acetylcysteine (NAC) (n=3), and (H) with the inhibitor of glucose-6-P dehydrogenase, dehydroepiandrosterone (DHEA) (n=2). Graphs represent the mean and SEM. *[1,2]Blots in C-D were produced by F. Püschel and are included in Püschel *et al*. (2020). *[3] Supernatants for panel F were produced by J. Redondo for a different experiment and repurposed here.

Thirdly, we studied the N-glycosylation pathway (Fig 7A). For this purpose, we used three different inhibitors: 2-deoxyglucose (2DG), tunicamycin and NGI-1. 2-DG is a glucose and mannose analogue known to block glycolysis but also, and predominantly under normoxia, to enter the glycosylation route and block branching of the core glycan structure in N-glycosylation (Datema and Schwarz, 1978). The competitive nature of this type of inhibition means it can be compensated by sufficient supplementation with mannose (Kurtoglu *et al*., 2007 and León-Annichiarico *et al*., 2015). Tunicamycin and NGI-1 are direct inhibitors of the two key enzymes of the N-glycosylation route: Dolichyl-Phosphate N-Acetylglucosaminephosphotransferase 1 (DPAGT1) (Yoo *et al.*, 2018) and the oligosaccharyl transferase complex (OST), respectively (Lopez-Sambrooks *et al.*, 2016), and thus their actions cannot be compensated by addition of mannose. All three inhibitors, as well as glucose deprivation, reduced glycosylation as measured by concanavalin A staining (Fig. 7B-C). Moreover, the three of them induced LIF release in presence of glucose, both in A549 (Fig 7D) and LLC1 (Fig 7E) cells. Moreover, re-addition of mannose reduced LIF release upon 2-DG treatment but not upon treatment with tunicamycin or NGI-1 (Fig 7D-E). Lastly, the kinetic of LIF release in response to 2DG and tunicamycin was comparable to that of glucose deprivation (Fig 7F), which is suggestive of a similar mechanism of action.

In summary, we found that the metabolic trigger leading to LIF release in the context of lack of glucose was N-glycosylation, but not defective glycolysis or TCA, nor failed redox homeostasis.

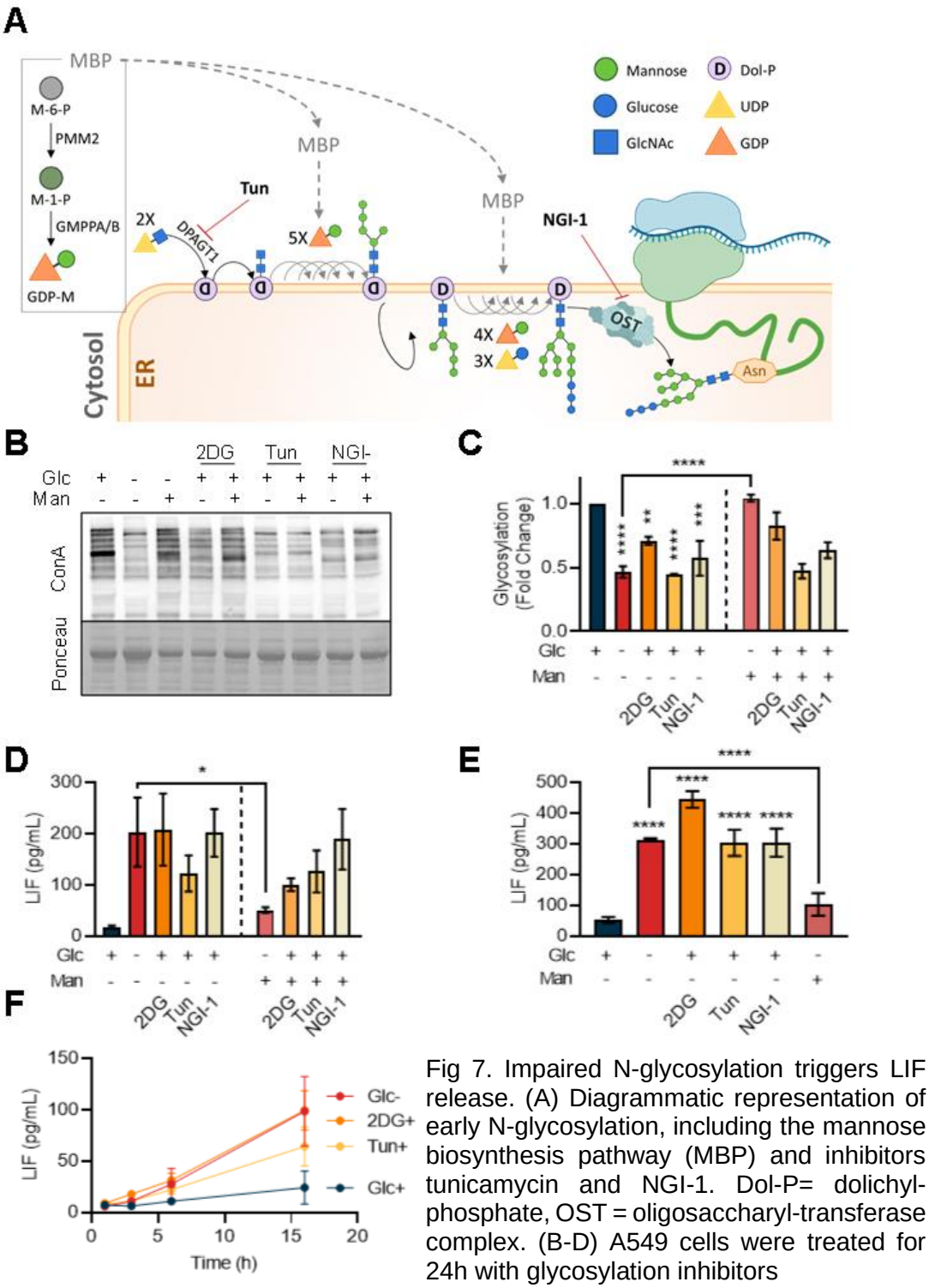

Fig 7. Impaired N-glycosylation triggers LIF release. (A) Diagrammatic representation of early N-glycosylation, including the mannose biosynthesis pathway (MBP) and inhibitors tunicamycin and NGI-1. Dol-P= dolichyl-phosphate, OST = oligosaccharyl-transferase complex. (B-D) A549 cells were treated for 24h with glycosylation inhibitors tunicamycin (Tun), NGI-1 and 2-deoxyglucose (2-DG) or deprived of glucose, in presence and absence of mannose (Man) as a substrate for N-glycosylation (n=3). Quantifications of western blots measuring Concanavalin-A (ConA) binding are shown in C, with one representative blot shown in B (n=3). LIF levels in the supernatant are shown in D. (E) Secreted LIF from supernatants of LLC1 cells treated for 24h with Tun, NGI-1 and 2-DG, deprived of glucose, or deprived of glucose but supplemented with mannose (Man) (n=3). (F) LIF kinetic upon treatment with 2DG, Tun or glucose deprivation (n=3). Graphs represent the mean and SEM; *-**** indicate significant differences obtained by one-way ANOVA ($p<0.05$-0.0001).

6.4 LIF correlates with early N-glycan biosynthesis

To further validate our findings and to test their applicability on more complex systems, we studied *in silico* the correlation between LIF and curated gene signatures for the mannose biosynthesis pathway (MBP), the first step required for mannose incorporation into nascent N-glycans. We performed gene expression correlation analysis in a collection of publicly available LUAD and LUSC human tumour transcriptomic datasets followed by a meta-analysis to collectively evaluate the overall correlation across studies. This meta-analysis uncovered a positive correlation between the *synthesis of GDP-Mannose* gene set variation analysis (GSVA) scores with LIF expression in LUAD (pooled correlation coefficient = 0.12 ±0.040; n=3963) and LUSC (pooled correlation coefficient = 0.19 ±0.055; n=2076). Additionally, we also found a positive correlation between the *diseases of glycosylation* GSVA score and LIF expression in LUAD (pooled correlation coefficient = 0.21 ±0.030; n=3963) and LUSC (pooled correlation coefficient = 0.37 ±0.040; n=2076); and between *asparagine n-linked glycosylation* GSVA score and LIF expression in LUAD (pooled correlation coefficient = 0.13 ±0.030; n=3963) and LUSC (pooled correlation coefficient = 0.16 ±0.045; n=2076).

Thus, we decided to dissect the specific correlation between each individual gene in the early N-glycosylation pathway with LIF, in a representative dataset of LUAD and LUSC (Fig 8A). This revealed that the main genes correlated with LIF expression were PMM2, GMMPA and GMPPB, all core genes of the MBP pathway. Furthermore, gene expression analysis of the individual genes of the early N-glycosylation pathway in publicly available transcriptomic data of an *in vitro* model of breast cancer subject to glucose deprivation for 4h (Gameiro & Struhl, 2018) confirmed that the most transcriptionally upregulated gene of this pathway was indeed GMPPB (Fig 8B). Lastly, this analysis was reproduced in public transcriptomic data from HeLa cells treated with tunicamycin (Fig 8C) and once again, GMPPB was the most upregulated gene in the early N-glycosylation pathway.

This approach further validates our experimental findings suggesting that problems with glycosylation trigger LIF release and highlights the role of GMPPB as a potential marker for impaired glycosylation to be explored in further studies.

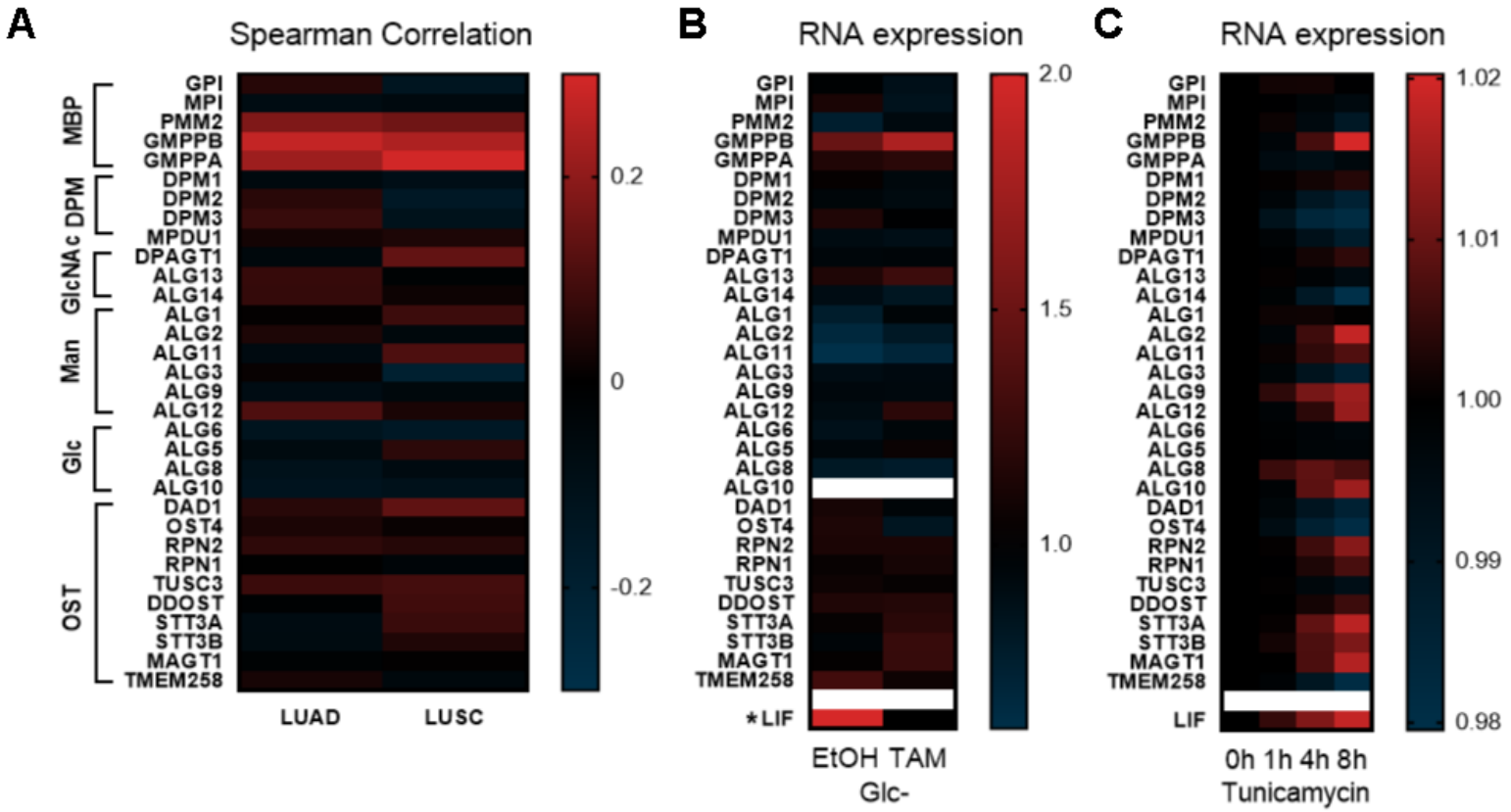

Fig 8. GMPPB correlates with LIF release and is the most upregulated enzyme of the early N-glycosylation pathway upon glucose deprivation. (A) Heatmap displaying the Spearman correlation between LIF and genes of the early N-glycosylation pathway organised according to their role in the N-glycosylation process, in two public TGCA transcriptomic datasets of LUAD (n=191) and LUSC (n=450). *Spearman analysis performed by collaborator Eline Blommaert*. (B) Heatmap of RNA expression of the genes of the early N-glycosylation pathway in a breast epithelial non-transformed (EtOH) and transformed (TAM) model of breast cancer, subject to glucose deprivation for 4h (n=2) (from publicly available data in Gameiro & Struhl (2018)) *LIF expression was 2.6, heatmap threshold was set to 2.0 to improve visualization. (C) Heatmap of RNA expression of the genes of the early N-glycosylation pathway in HeLa cells treated with Tun for 0, 1, 4 and 8h (n=3) (from publicly available data in Rendleman *et al.*, (2018)).

6.5 PERK mediates LIF induction

Given the prior observation that defective glycosylation triggers LIF release, we decided to begin the search for the signalling pathway leading to LIF production at the organelle responsible for glycosylation: the endoplasmic reticulum. The ER stress response, also known as the unfolded protein response (UPR) is engaged by problems with protein folding detected by the chaperone GRP78 and is divided in three major branches directed by three GRP78-interacting sensors (Diagram 3). We dissected these branches by means of knockdown or chemical inhibition of their respective gatekeepers: IRE1, ATF6 and PERK.

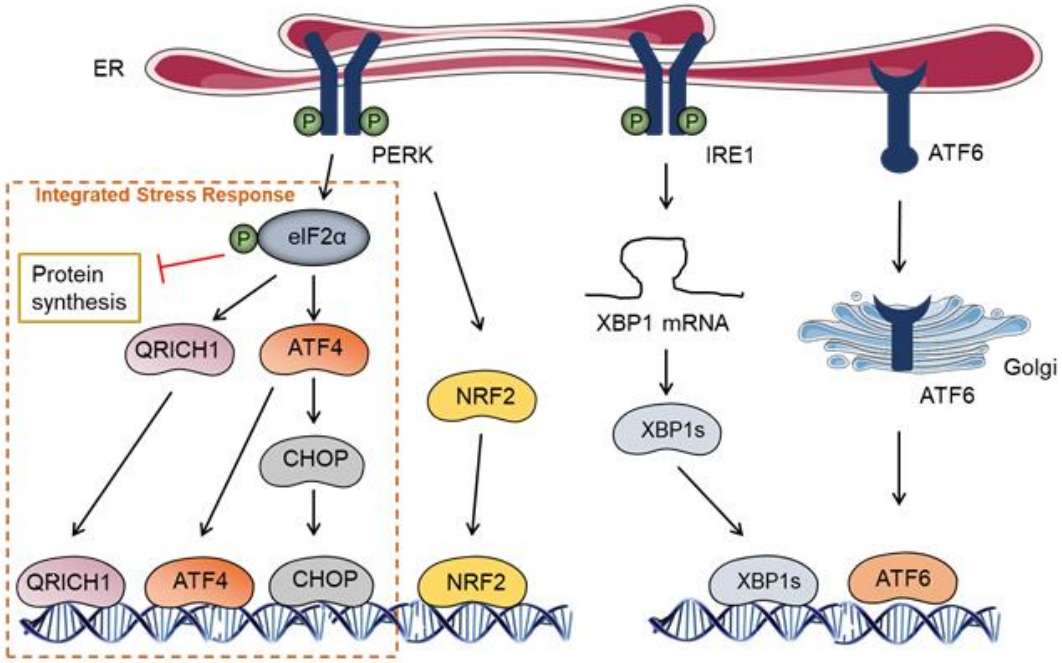

Diagram 3. Representation of the unfolded protein response (UPR) signalling pathway and its main downstream transcription factors. Adapted from Iurlaro & Muñoz-Pinedo (2016).

Firstly, A549 cells were treated with two different IRE1 endoribonuclease inhibitors (4μ8C and MKC-3946) in the presence or absence of glucose. Both inhibitors were effective in preventing the increase of the IRE1 target AGR2 but failed to prevent LIF release (Fig 9A-B). Additionally, two siRNA sequences were used to knockdown XBP1, the main effector downstream of IRE1, and in both cases the levels of secreted LIF were unaltered (Fig 9C-D).

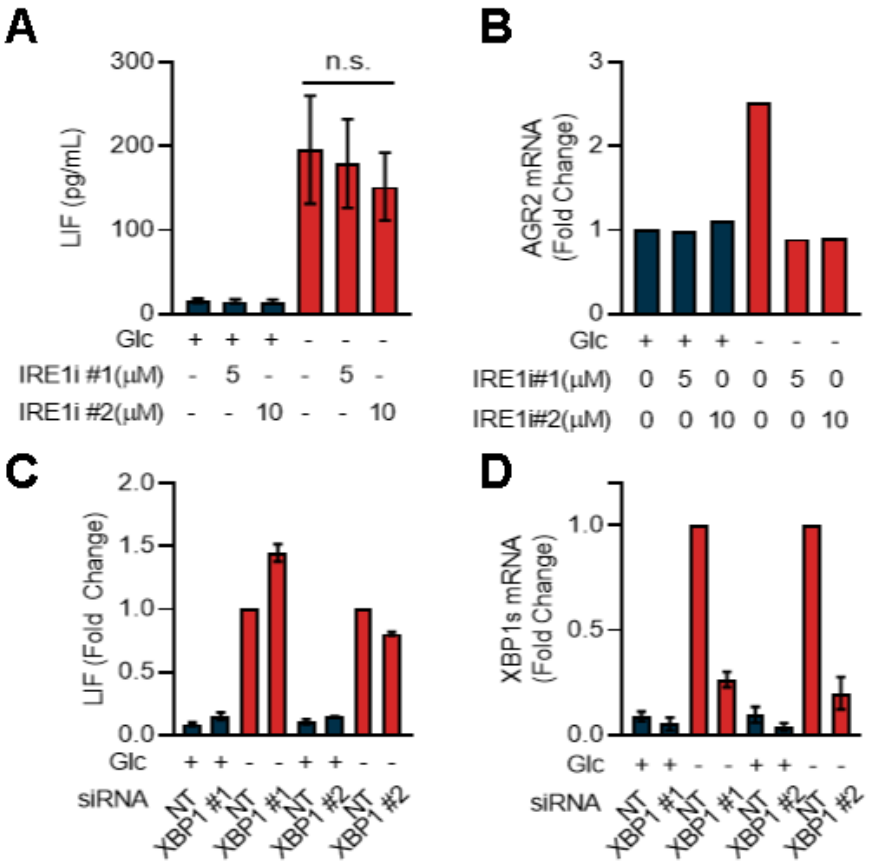

Fig 9. LIF release is not driven by IRE1 signalling in the context of glucose deprivation. (A) Secreted LIF measured by ELISA in supernatants of A549 cells under glucose deprivation (24h) treated with IRE1 inhibitors 4μ8C (IRE1i#1) and MKC-3946 (IRE1i#2) (n=4), and (B) their effect on AGR2 gene expression in the same experiment. (C) Secreted LIF in supernatants of A549 cells subject to XBP1 knockdown (24h) and subsequent glucose deprivation (24h) with two different siRNA oligos (n=3) and (D) their effect on XBP1s mRNA in the same experiment. Graphs represent the mean and SEM.

Secondly, signalling through the ATF6 branch was blocked by knockdown of ATF6 with two different siRNA oligos, but this also failed to prevent LIF secretion in conditions of glucose deprivation (Fig 10A-B).

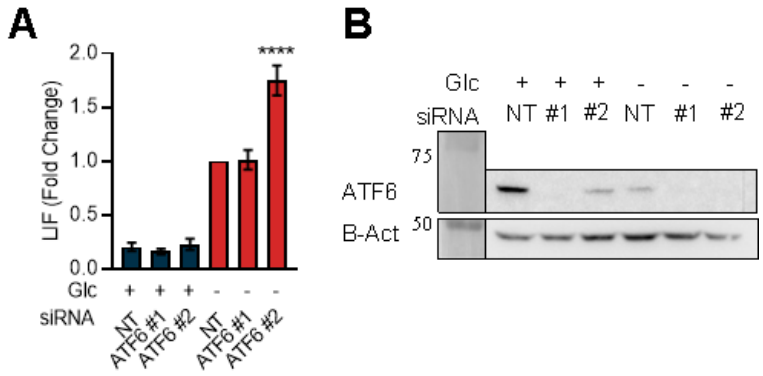

Fig 10. LIF release is not driven by ATF6 signalling in the context of glucose deprivation. (A) Secreted LIF measured by ELISA in supernatants of A549 cells subject to ATF6 knockdown (24h) and subsequent glucose deprivation (24h) with two different siRNA oligos (n=3) and (B) their effect on ATF6 protein in the same experiment. Graphs represent the mean and SEM; *-**** indicate significant differences obtained by paired t-test (p<0.05-0.0001).

Thirdly, the PERK branch of the UPR was blocked by treatment with two different inhibitors: AMG-PERK44 and GSK2656157. Both inhibitors caused a reduction in the levels of the downstream target ATF4 and a dose dependent decrease of LIF secretion induced by glucose deprivation (Fig 11A-B).

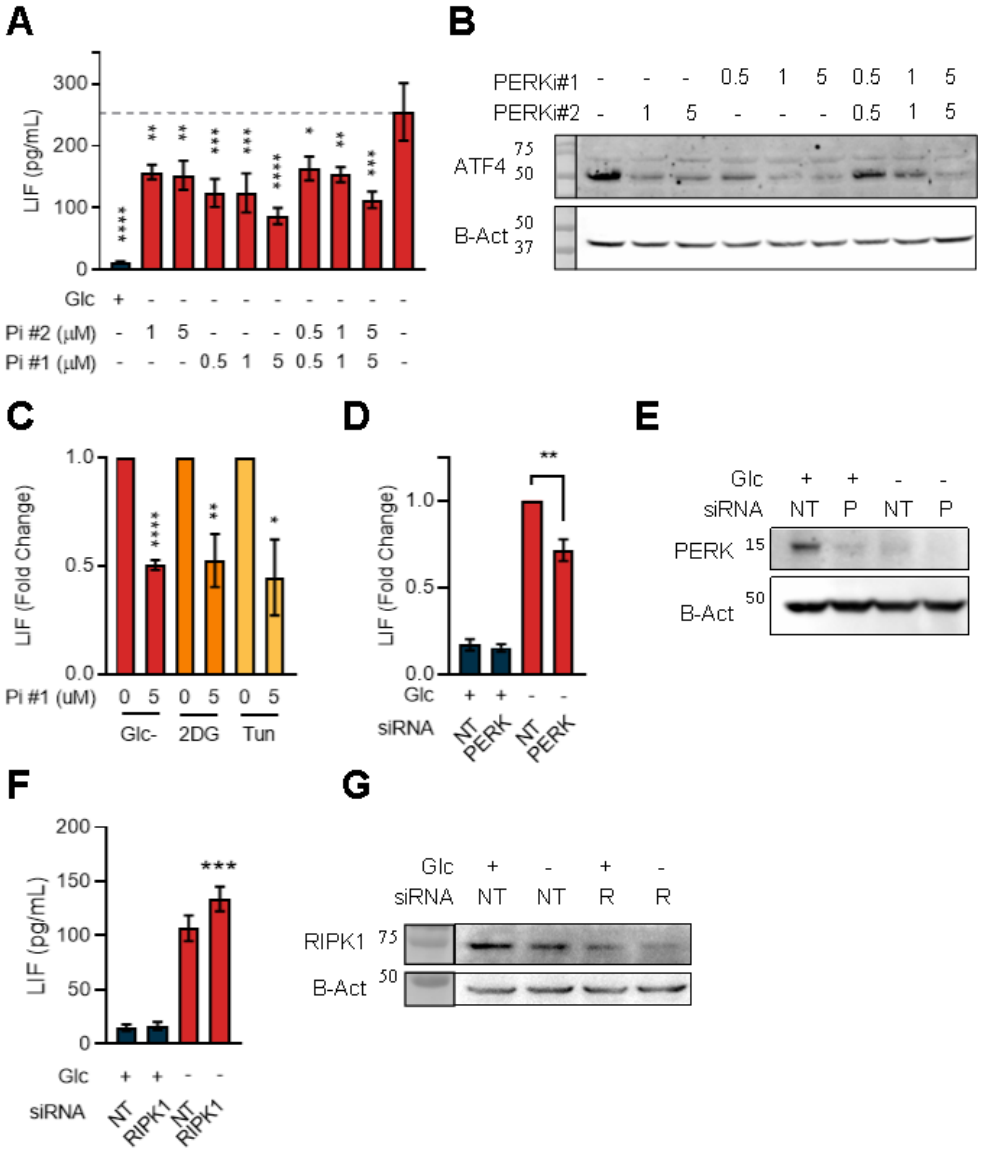

Fig 11. LIF release upon glucose deprivation is mediated by PERK signalling. (A) Secreted LIF measured by ELISA in supernatants of A549 cells under glucose deprivation treated with PERK inhibitors GSK2656157 (Pi#1) and AMG-PERK44 (Pi#2) for 24h (n=3) and (B) their effect on ATF4 protein levels in the same experiment. (C) Secreted LIF measured by ELISA in supernatants of A549 cells under different glycosylation inhibiting conditions treated with PERK inhibitor GSK2656157 (Pi#1) for 24h (n=3). (D) LIF levels in supernatants of A549 cells treated with a pool of siRNAs against PERK (24h) prior to glucose deprivation (24h) (n=3) and (E) their effect in PERK protein levels in the same experiment. (F) Secreted LIF on supernatants of A549 cells subject to RIPK1 knockdown for 24h prior to glucose deprivation for 24h (n=3) and (G)* its effect on RIPK1 protein levels in the same experiment. Graphs represent the mean and SEM; *-**** indicate significant differences obtained by one-way ANOVA (A) and paired t-test (C-F) ($p<0.05$-0.0001). *Blot in panel G was produced by F. Favaro.

Moreover, inhibition of PERK using GSK2656157 reduced LIF secretion induced by glycosylation inhibitors (Fig 11C). A SMARTPool™ combination of four siRNA sequences targeting PERK also induced a significant decrease in the levels of secreted LIF (Fig 11D-E). Given the concerns regarding the GSK PERK inhibitor specificity, the main described off-target of this inhibitor, RIPK1 (Rojas-Rivera *et al.*, 2017) was also knocked down using siRNA and LIF release was measured by ELISA. The levels of LIF secreted under glucose deprivation were unaffected by RIPK1 knockdown (Fig 11F-G).

Additionally, in order to establish the specificity of LIF release as a response to impaired glycosylation and not any inducer of the UPR, another well studied UPR inducer, thapsigargin (Thg), was used in presence of glucose to study LIF release (Fig 12A-B) and no changes in LIF release were detected.

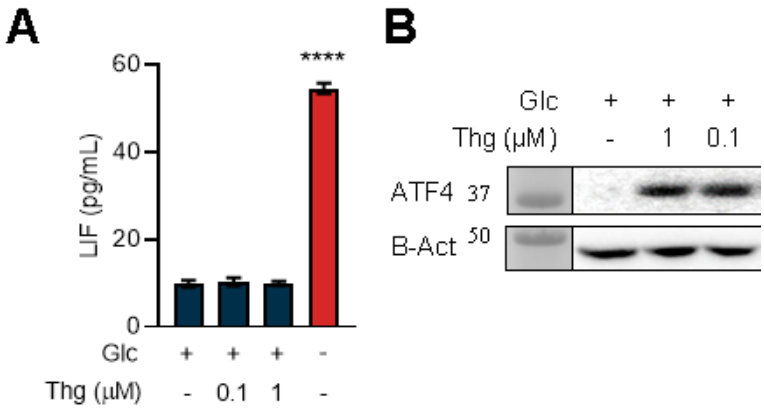

Fig 12. Non-specific activation of PERK does not induce LIF secretion. (A) Secreted LIF measured by ELISA in supernatants of A549 cells treated with ER stress inducer Thapsigargin (Thg) for 24h (n=3) and (B) its effect on ATF4 protein levels in the same experiment. Graph represents the mean and SEM; *-**** indicate significant differences obtained by paired t-test ($p<0.05$-0.0001).

Lastly, we considered the potential involvement of GCN2, another ISR kinase with similar actions as PERK, particularly given that previous research by the Koumenis group (Ye *et al.,* 2010) showed the involvement of GCN2 in responses to glucose deprivation. We used GCN2 inhibitor A-92 to treat A549 under glucose deprivation, alone or in combination with PERK inhibition (Fig 13). Although GCN2 inhibition did not result in any significant decrease in LIF release, the combination of GCN2 and PERK inhibition achieved a near complete block.

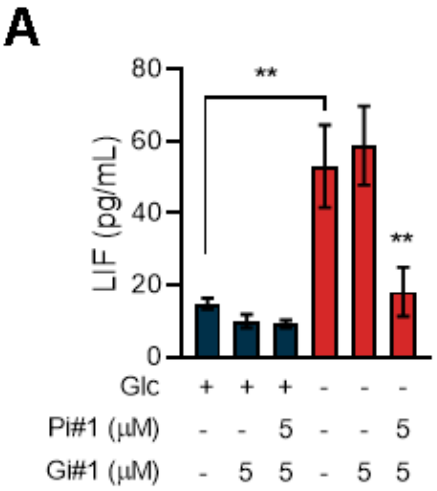

Fig 13. GCN2 inhibition adds to PERK inhibition in preventing LIF release. Secreted LIF measured by ELISA in supernatants of A549 cells under glucose deprivation treated with GCN2 inhibitor A-92 (Gi#1) alone or in combination with Pi#1 (n=3). Graph represents the mean and SEM; *-**** indicate significant differences obtained by paired t-test (p<0.05-0.0001).

Moreover, validation experiments of PERK and GCN2 inhibition in LLC1 cells under glucose deprivation revealed that although PERK participates in LIF regulation, GCN2 also had a significant summative effect (Fig 14). This suggests that the common downstream phosphorylation target of both kinases, eIF2a, could be relevant for regulation of LIF production in the context of defective glycosylation driven by glucose deprivation.

In summary, we provided evidence that LIF induction is mediated by the PERK branch of the UPR in both A549 and LLC1 cells. In addition, we showed that the trigger for LIF release remains glycosylation specific, since non-specific UPR driven by Thg did not induce LIF release. Lastly, we showed that in some cell lines GCN2 participates in this mechanism, suggesting translational regulation by eIF2a phosphorylation.

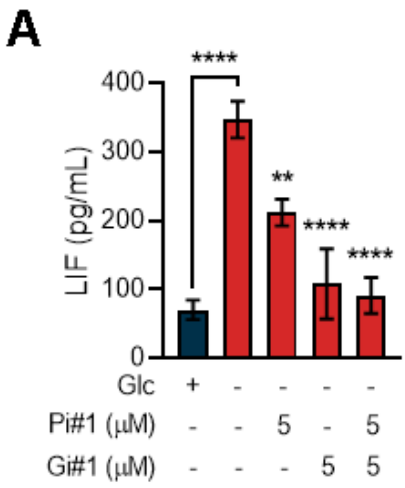

Fig 14. PERK and GCN2 inhibition prevent LIF release upon glucose deprivation in LLC1 cells. (A) Secreted LIF measured by ELISA in supernatants of LLC1 cells under glucose deprivation treated with Pi#1, Gi#1, and a combination of both (n=5). Graph represents the mean and SEM; *-**** indicate significant differences obtained by paired t-test (p<0.05-0.0001).

6.6 LIF production involves transcriptional and translational cues

A preliminary experiment aimed at determining mRNA expression kinetics of LIF upon glucose deprivation in different cell lines provided a surprising result. LIF mRNA was transiently upregulated in A549 cells, whereas it was permanently upregulated in LLC1 cells and not upregulated at all in SW900 cells, when compared with cells incubated in 25mM glucose (Fig 15A-C). And yet, protein kinetics of LIF were almost identical in all three cell lines. This was suggestive of post-transcriptional regulation.

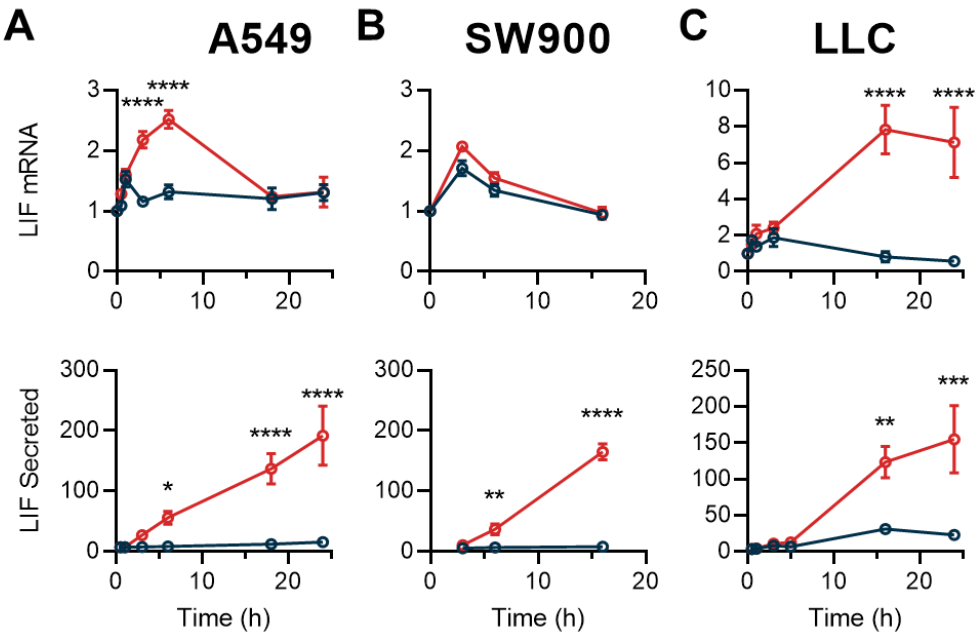

Fig 15. LIF is regulated differently in three lung cancer cell lines under glucose deprivation. (A) LIF mRNA expression (top) and protein secretion (bottom) through a glucose deprivation kinetic from A549 cells, (B) SW900 cells and (C) LLC1 cells (n=3). Graphs represent the mean and SEM; *-**** indicate significant differences obtained by one-way ANOVA ($p<0.05$-0.0001).

For this reason, we studied the half-life of LIF mRNA in presence and absence of glucose by placing A549 cells under glucose deprivation for three hours prior to addition of ActD, an inhibitor of RNA polymerases, and collection of mRNA samples to form a kinetic. LIF mRNA half-life, calculated as described by Chen *et al.,* (2008), remained almost unaltered under glucose deprivation (Fig 16). These differences were not deemed to be sufficient to cause the changes observed at the protein level.

A recently discovered long non-coding antisense RNA complementary to LIF (LIF-AS1) induced by p63 was described to have effects on LIF post-transcriptional regulation (Qian *et al*., 2017). Therefore, we decided to investigate LIF-AS1 expression in the context of glucose deprivation. A kinetic of p63 RNA expression, the proposed regulator of LIF-AS1, showed a dramatic decrease upon glucose deprivation (Fig 17A). LIF-AS1 mRNA kinetic displayed a single peak after 3h under glucose deprivation, however this peak completely disappeared by 6h (Fig 17B). Lastly, silencing of

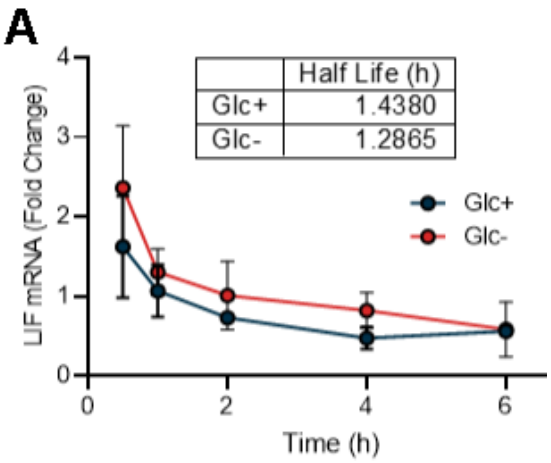

Fig 16. LIF mRNA half-life is not altered upon glucose deprivation. (A) LIF mRNA kinetic starting after 3h of glucose deprivation and upon treatment with ActD. Graph represents the mean and SEM.

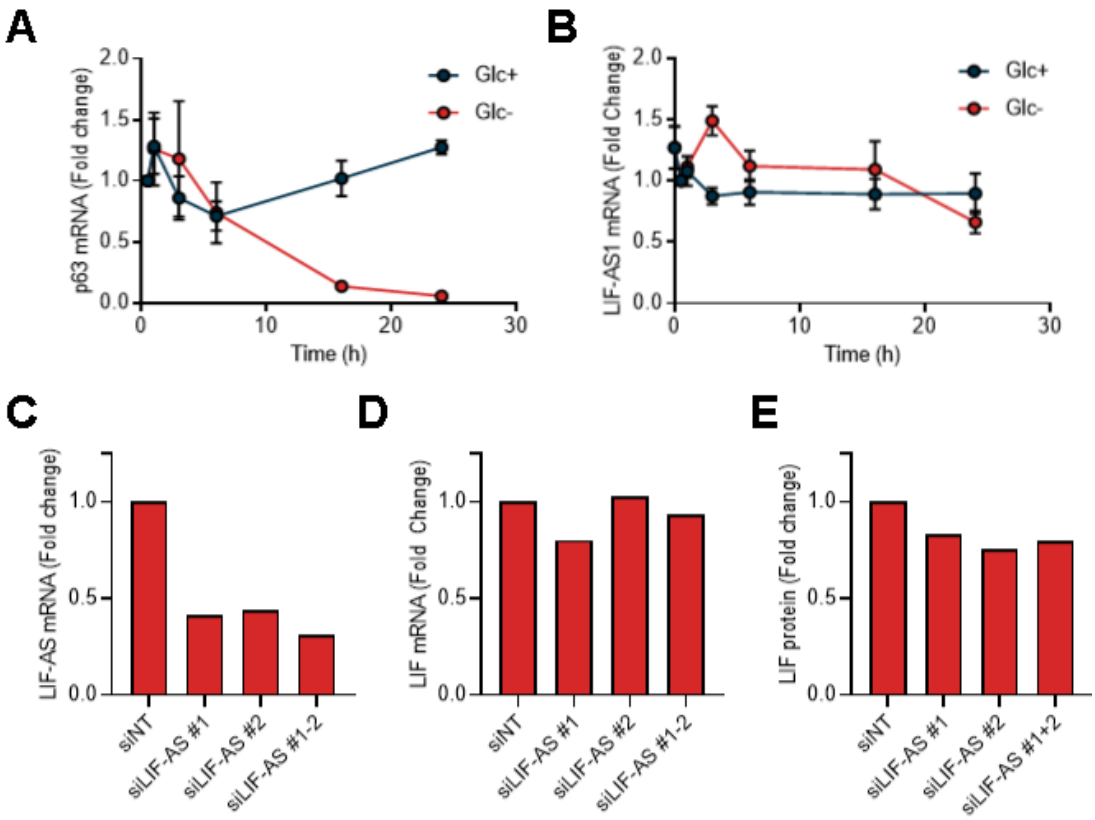

Fig 17. LIF-AS1 does not regulate LIF under glucose deprivation. (A) mRNA kinetic of p63 and (B) LIF-AS1 from A549 cells under glucose deprivation. (C) mRNA expression of LIF-AS1 and (D) LIF, and (E) protein levels of LIF from A549 cells subject to LIF-AS1 siRNA knockdown (24h) followed by glucose deprivation (24h) (n=1). Graphs represent the mean and SEM.

LIF-AS1 in the context of glucose deprivation had very limited effects on LIF both at the mRNA and protein level (Fig 17C-E). In light of this results, we discarded the hypothesis that LIF is regulated post-transcriptionally by LIF-AS1 in the context of glucose deprivation.

We further investigated the potential post-transcriptional regulation of LIF using publicly available ribosome profiling data (Gameiro & Struhl, 2018) and found that LIF translation efficiency was upregulated upon 4h of glucose deprivation in a model of immortalized breast epithelium, both before and after treatment with tamoxifen to induce a phenotype switch towards a cancer-like state (Fig 18). This result further agrees with our hypothesis that LIF is regulated in part post-transcriptionally in the context of glucose deprivation.

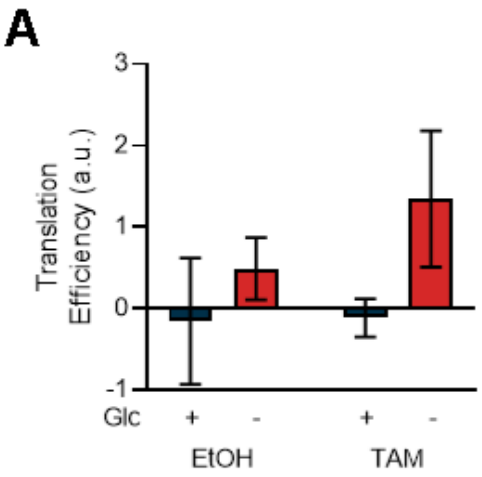

Fig 18. LIF translation efficiency is increase in a breast cancer *in vitro* model upon glucose deprivation. (A) LIF translation efficiency calculated as a function of LIF ribosome protected fragments and LIF RNA expression from public ribosome profiling data (Gameiro & Struhl, 2018) in a breast epithelial non-transformed (EtOH) and transformed (TAM) model of breast cancer, subject to glucose deprivation for 4h (n=2). Graphs represent the mean and SEM.

6.7 Transcriptional input is necessary for LIF production

Given the complexity of the downstream effects of PERK, which include both translational and transcriptional regulation, we sought to determine whether the transcriptional input was necessary in our system. When treated A549 and SW900 cells with 80nM ActD prior to and during glucose deprivation. Both cell types failed to produce any LIF protein under transcription inhibiting conditions (Fig 19A-B). This indicates that although post-transcriptional regulatory mechanisms might be in play, transcription is also necessary.

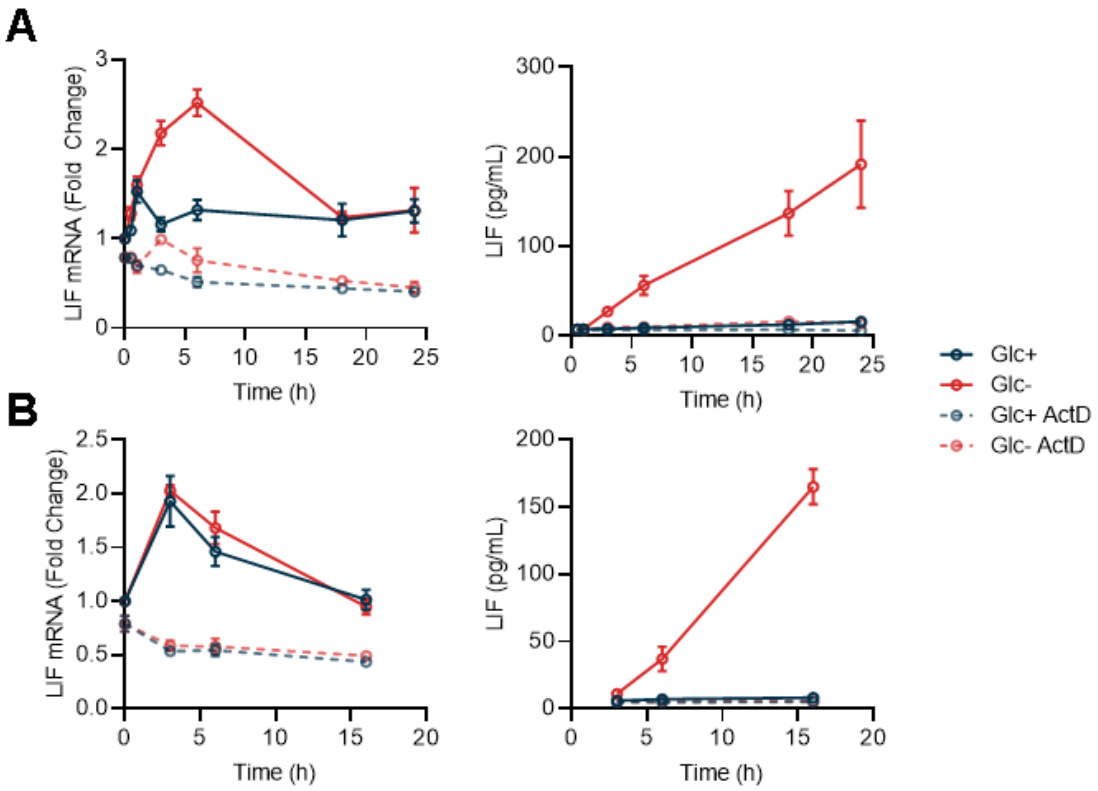

Fig 19. Transcription blockade prevents LIF protein production during glucose deprivation. (A) mRNA and protein kinetic of LIF from A549 cells under glucose deprivation and pre-treated with ActD (-1h). (B) mRNA and protein kinetic of LIF from SW900 cells under glucose deprivation and pre-treated with ActD (-1h). Graphs represent the mean and SEM.

6.8 LIF is not regulated by canonical PERK transcription factors

Following our findings that some degree of transcription is needed for LIF production (Fig 19) and considering that PERK regulates LIF production (Fig 11), we decided to investigate the input from all known transcription factors directly downstream of PERK: ATF4, CHOP, NRF2 and QRICH1.

Knock down of these genes by siRNA followed by glucose deprivation yielded no significant inhibition on LIF release (Fig 20A-D) indicating that LIF is not positively regulated by either of them.

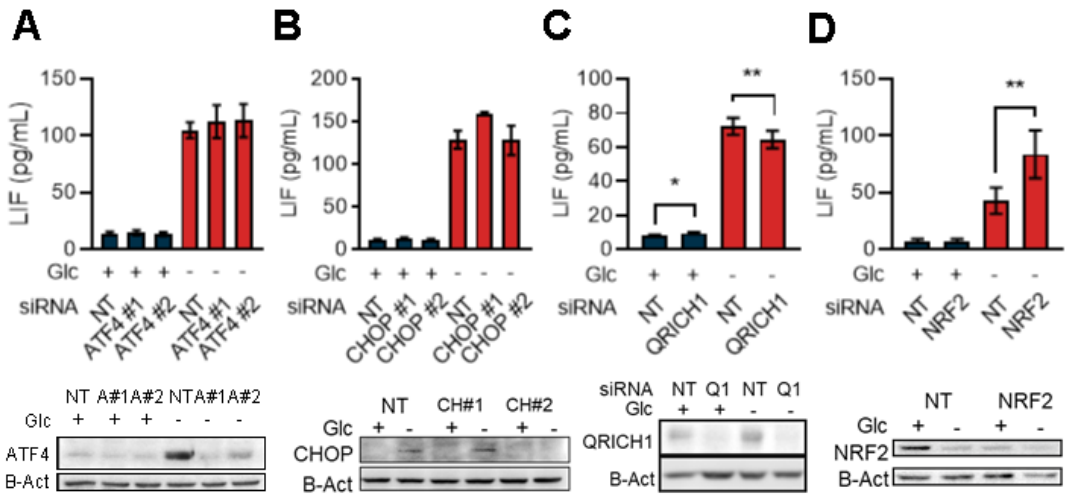

Fig 20. Canonical transcription factors downstream of PERK do not regulate LIF. (A)* Secreted LIF measured by ELISA in supernatant of A549 cells subject to ATF4, (B)* CHOP, (C) QRICH1 and (D) NRF2 knockdown (24h) prior to incubation under glucose deprivation (24h) (n=3). Graphs represent the mean and SEM. *-**** indicate significant differences obtained by paired t-test ($p<0.05$-0.0001). *Blots accompanying Fig 21A-B were produced by F. Favaro.

6.9 MAPK signalling downstream of PERK affects LIF

Since the canonical transcription factors downstream of PERK had been experimentally ruled out, we decided to take an unbiased approach and explore the transcription factor binding sites in the putative promoter of LIF. To do this, the PROMO transcription factor binding site (TFBS) prediction algorithm was used (Messeguer *et al*.,2002), using the TRANSFAC matrices database (v8.3). All transcription factors whose sequence has a dissimilarity rate <5% with sequences within 500 base-pairs upstream of the exon1D of LIF were included

TF-Binding site	# sites		
MAZ [T00490]	13	Pax-5 [T00070]	7
ELF-1 [T01113]	13	p53 [T00671]	7
POU2F2 (Oct-2.1) [T00646]	11	RXR-alpha [T01345]	7
AhR:Arnt [T05394]	10	c-Jun [T00133]	7
RAR-beta [T00721]	10	C/EBPalpha [T00105]	7
c-Fos [T00123]	10	GR [T05076]	7
NF-AT2 [T01945]	10	TFIID [T00820]	7
TBP [T00794]	10	AP-2alphaA [T00035]	6
GCF [T00320]	9	STAT4 [T01577]	6
AP-1 [T00029]	9	XBP-1 [T00902]	6
IRF-1 [T00423]	9	FOXP3 [T04280]	6
NF-AT1 [T00550]	9	GATA-1 [T00306]	6
Elk-1 [T00250]	9	TFII-I [T00824]	6
c-Ets-2 [T00113]	9	IRF-2 [T01491]	6
T3R-beta1 [T00851]	9	ER-alpha [T00261]	5
ENKTF-1 [T00255]	8	GR-alpha [T00337]	5
c-Myb [T00137]	8	GR-beta [T01920]	5
c-Ets-1 [T00112]	7	C/EBPbeta [T00581]	4
		YY1 [T00915]	4

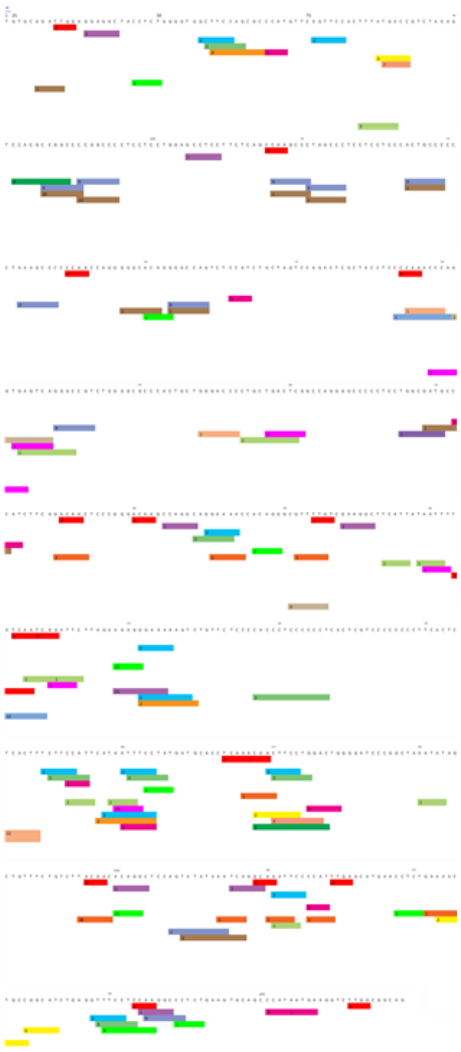

Fig 21. Transcription-factor binding-site prediction on the LIF promoter. PROMO algorithm was used in combination with TRANSFAC matrices (v8.3) to predict putative binding sites for transcription factors to a –500bp sequence upstream of LIF exon1D. Only binding sites with a dissimilarity rate <5% to their putative transcription factor are reported. Transcription factor symbol and the number of binding sites identified are reported on a table on the left. A graphic representation of the binding sites is provided on the right.

(Fig 21). Amongst the putative TF-BS identified, we observed several that are associated with ERK signalling, namely c-Fos (10 sites), AP-1 (9 sites), Elk-1 (9 sites), ETS-1 (7 sites) and -2 (9 sites), c-Jun (7 sites) and FOXP3 (6 sites).

Once again, we performed a meta-analysis of the gene expression correlation analysis on several public curated datasets and found a positive correlation between the *MAPK signalling pathway* GSVA scores and LIF expression in LUAD (pooled correlation coefficient = 0.15 ±0.035; n=3963) and LUSC (pooled correlation coefficient = 0.40 ±0.035; n=2076).

Interestingly, (Shin *et al*., 2015). recently identified a new a mechanism for glucose deprivation responses which includes MAPK / ERK signalling independent from PERK to regulate different cell fates. Moreover, a previous study (Wang *et al*., 2019) hinted at regulation of LIF by MAPK in KRAS mutant cells. Therefore, we decided to treat A549 cells with ERK1/2 inhibitor PD98059 and found that it significantly inhibited LIF release (Fig 22).

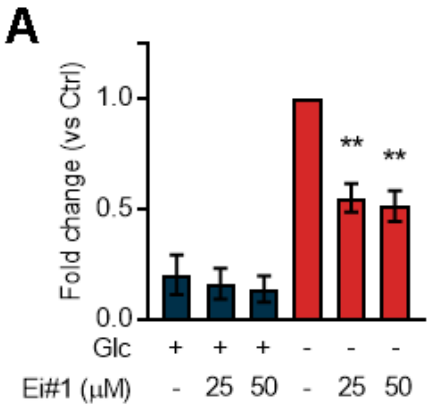

Fig 22. ERK1 & 2 inhibition blocks LIF release under glucose deprivation. (A) Fold change in LIF secretion measured by ELISA in supernatants of A549 cells treated with ERK1/2 inhibitor PD98053 (Ei#1) in presence and absence of glucose (n=5). Graphs represent the mean and SEM; *-**** indicate significant differences obtained by RM one-way ANOVA (p<0.05-0.0001).

Additionally, NF-κB signalling has been shown to be partially affected by PERK (Deng *et al*., 2004), and since this is the master regulator of cytokines, we decided to investigate its effect on LIF. Knock-down of p65 had no effects on the amount of LIF produced upon glucose deprivation (Fig 23A). Chemical inhibition of IKK by BAY 11-7082 induced some non-significant reduction of LIF release at the highest dose (10μM) (Fig 23B), however this could be due to previously reported non-specific inhibition of AP-1, specifically with doses higher than 10μM (Lee *et al*., 2012). This would be in line with the hypothesis that ERK1/2 could participate in the transcriptional regulation of LIF.

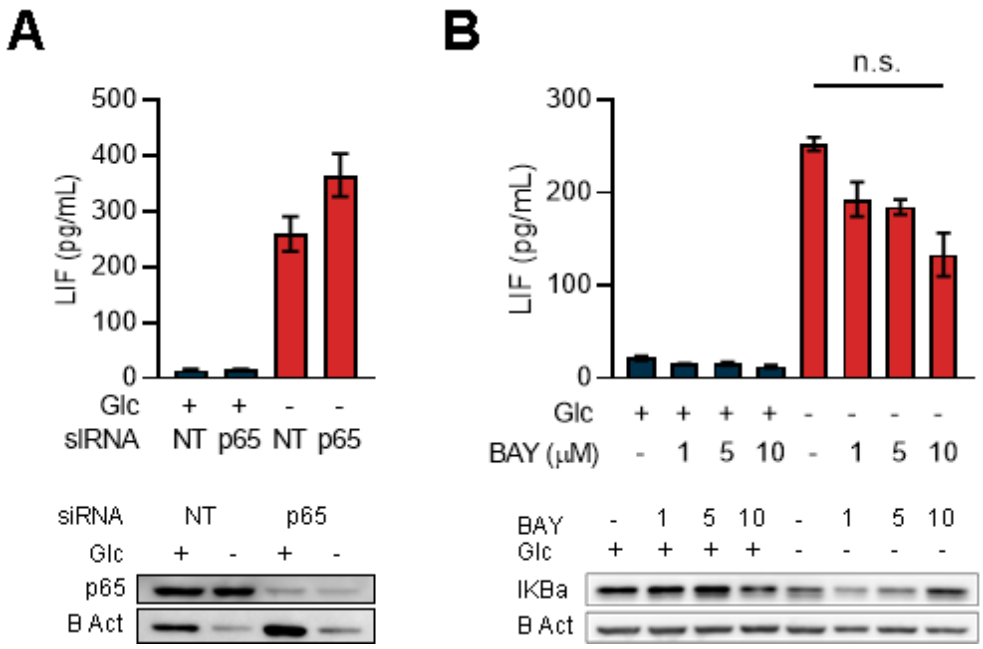

Fig 23. Inhibition of NF-κB signalling does not prevent LIF release under glucose deprivation. (A) Secreted LIF on supernatants of A549 cells subject to p65 knockdown for 24h prior to glucose deprivation for 24h (n=3). (B)Secreted LIF on supernatants of A549 cells treated with IKK inhibitor BAY11-7082 and under glucose deprivation (24h). Graphs represent the mean and SEM; n.s. indicates p-values>0.05 obtained by paired t-test. *Blots accompanying this figure were produced by F. Favaro.

6.10 Results I: Summary

Through this first part of this PhD study we have established that glucose deprivation induces LIF production as a highly specific secretory glucose stress signal in many different cell types, including non-malignant epithelial cells. Moreover, we have shown that the metabolic trigger for LIF production is through defective N-glycosylation, which activate PERK and, in some cases, GCN2 to induce LIF production and secretion through transcriptional and post-transcriptional routes. Lastly, we have shown that ERK1/2 could play a relevant role in signalling downstream of PERK.

7. Results II: The functional role of LIF in cancer

7.1 LIF is a pro-tumorigenic cytokine: *in silico*

To cover the second major aim of this PhD, a two-pronged approach was used to determine the role LIF plays in the context of cancer. Firstly, an *in silico* approach was taken by evaluating the prognostic value of LIF expression in overall survival (OS) of cancer patients from a variety of curated public databases. For this purpose, the online tool KM plot was used (Gyorffy *et al*., 2013). We found that high expression of LIF significantly correlated with decreased OS in LUAD, LUSC, hepatocellular carcinoma, head and neck squamous cell carcinoma, renal clear cell carcinoma and cervical squamous cell carcinoma (Fig 24).

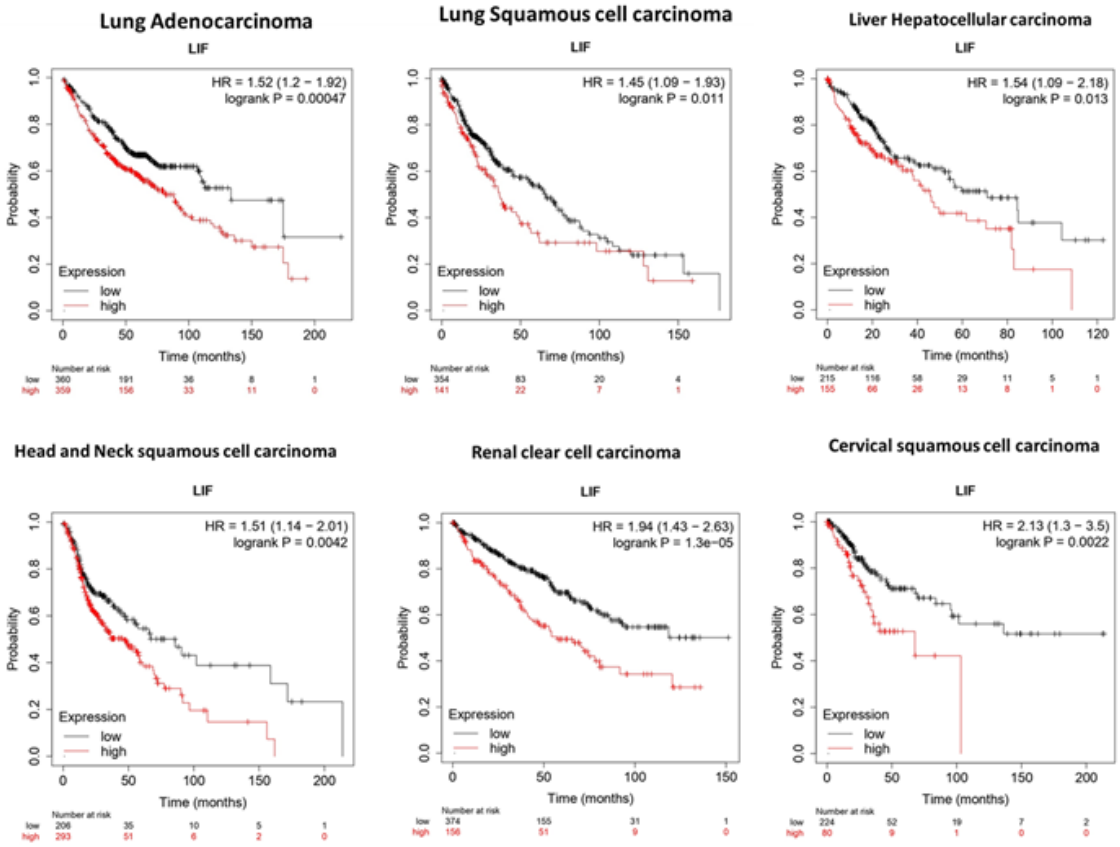

Fig 24. High LIF expression predicts poor prognosis in several cancer types. Kaplan-Meier curves of LIF-Low and LIF-High expression groups in LUAD (n = 719), LUSC (n = 495), liver hepatocellular carcinoma (n = 370), head and neck squamous cell carcinoma (n = 499), renal clear cell carcinoma (n = 530) and cervical squamous cell carcinoma (n = 304) patients generated using the online tool KMplot from validated non-redundant datasets. P values come from log-rank non-parametric tests.

7.2 LIF is a pro-tumorigenic cytokine: *in vitro*

We evaluated the effects of LIF on A549 cells *in vitro* by addition of recombinant human LIF (rhLIF) in conditions of glucose deprivation. We did not observe any changes in cell death or proliferation (Fig 25A-B), however A549 cell migration across a transwell insert towards media containing rhLIF was significantly increased (Fig 25C). This could be indicative of pro-metastatic effects of LIF.

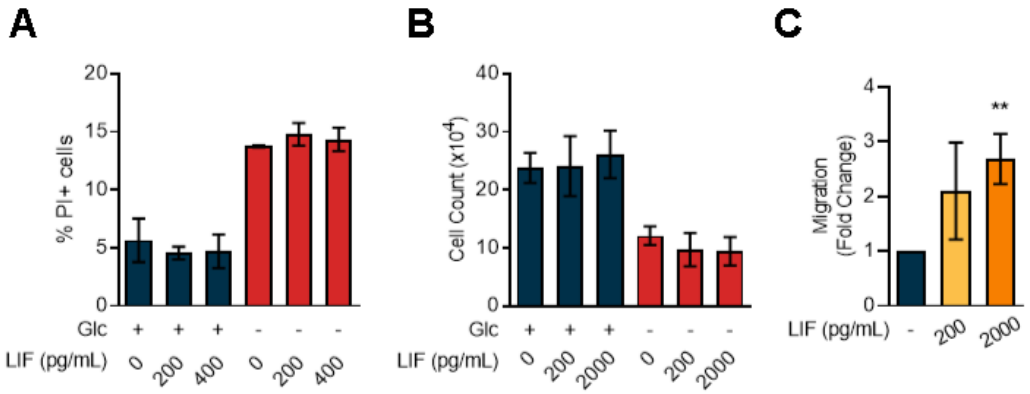

Fig 25. LIF promotes A549 migration. (A) A549 cell death upon treatment with recombinant human LIF and under glucose deprivation, quantified by propidium iodine incorporation flow cytometric assay (n=4). (B) A549 cell proliferation upon treatment with recombinant human LIF and under glucose deprivation quantified by cell counting (n=5). (C) A549 cell migration across a transwell insert towards media supplemented with recombinant human LIF (n=5). Graphs represent the mean and SEM; *-**** indicate significant differences obtained by paired t-test ($p<0.05$-0.0001).

7.3 LIF is a pro-tumorigenic cytokine: *in vivo*

To examine the tumoral role of LIF *in vivo*, an orthotopic model of lung cancer was generated by tail-vein injection of LIF CRISPR-KO LLC1 cells and their LIF WT counterparts generated by infection with scramble gRNA (Fig 26A), in syngeneic C57BL/6 mice. Visible differences in their tumour burden were appreciated upon collection of the lungs (Fig 26B), with higher tumour burden in the scramble cohort. Mice bearing LIF-KO tumours appeared healthier as evidenced by differences in weight increase (Fig 26C) and average food intake (Fig 26D). Increased tumour mass was matched by an increase in lung weight in the scramble cohort (Fig 26E). The average tumour area was higher in LIF WT tumours as measured in three equally spaced tissue sections and determined by Ki67 staining (Fig 26F). However, microscopic analysis revealed that the total number of tumours was higher in the LIF-KO cohort, suggesting that LIF contributed to increased tumour size but not to cell tropism towards the lung or to

tumour implantation. Upon categorization of these lesions according to their size, it was observed that the LIF-KO cohort had more microscopic lesions but fewer macroscopic lesions (Fig 26G). In summary, LIF-KO resulted in decreased overall disease progression evidenced both by symptoms and tumour growth.

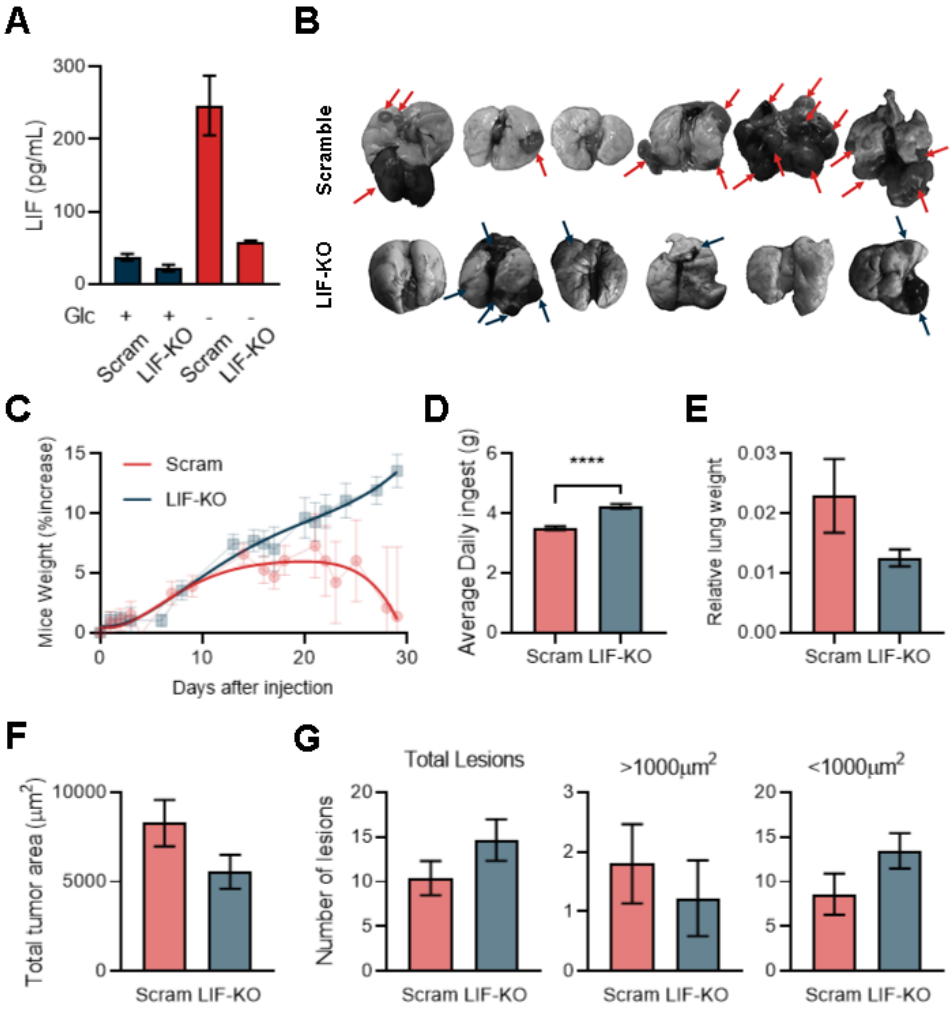

Fig 26. LIF is pro-tumorigenic in an orthotopic lung cancer murine model*. (A) Secreted LIF from LIF CRISPR-Cas9 KO (LIF-KO) LLC1 cells and their scramble gDNA transduced counterparts (Scram) upon glucose deprivation (24h) (n=3). (B) Photography of tumour bearing mouse lungs from the Scram and LIF-KO LLC1 injected mouse cohorts; coloured arrows indicate visible lesions. (C) Mice weight increase of LLC1 tumour bearing mice represented as a percentage of their weight at d0 pre-injection of LLC1 cells. Solid coloured lines represent a polynomial curve fit model to aid interpretation of the results. (D) Average daily ingest of LLC1 tumour bearing mice measured from d0 pre-injection to day of sacrifice. (E) Lung weight of LLC1 tumour bearing mice measured at day of sacrifice relative to mice weight at d0 pre-injection. (F) Tumour area in three non-consecutive equally spaced lung tissue sections from LLC1 tumour bearing mice from LIF-KO LLC1 injected mice and Scramble vector LLC1 injected mice cohorts. (G) Tumour size distribution across the LIF-KO LLC1 injected and Scramble vector LLC1 injected cohorts. Average lesions per section of tissue (n=6) were split based on their size in two categories and the number of lesions pertaining to each category was represented. From left to right: Total lesions, lesions >1000µm^2, lesions <1000µm^2. Graphs represent the mean and SEM; *-**** indicates significant differences ($p< 0.05$ - 0.0001) obtained by unpaired t-test. *Animal procedures were done by F. Luciano and F. Jiménez.

7.4 LIF and angiogenesis: *in silico*

Given the finding that LIF is induced in response to decreased glucose, we re-evaluated its potential expression and role in the context of solid tumors, as glucose concentration is frequently lower than the concentration in extracellular fluid of normal tissues (Sullivan *et al.*, 2019). As a surrogate of tumors with poor irrigation that may also experience low glucose levels, we examined the possible correlation of LIF expression with the Cancer Hallmark 'hypoxia'. Data from multiple datasets were pooled in a meta-analysis, and we and observed a positive correlation of *hypoxia* GSVA scores with LIF expression in LUAD (pooled correlation coefficient = 0.30 ±0.040; n=3963) and LUSC (pooled correlation coefficient = 0.39 ±0.050; n=2076) (representative datasets Fig. 27A). This is an indication that LIF is indeed induced in poorly irrigated areas such as the core of solid tumours.

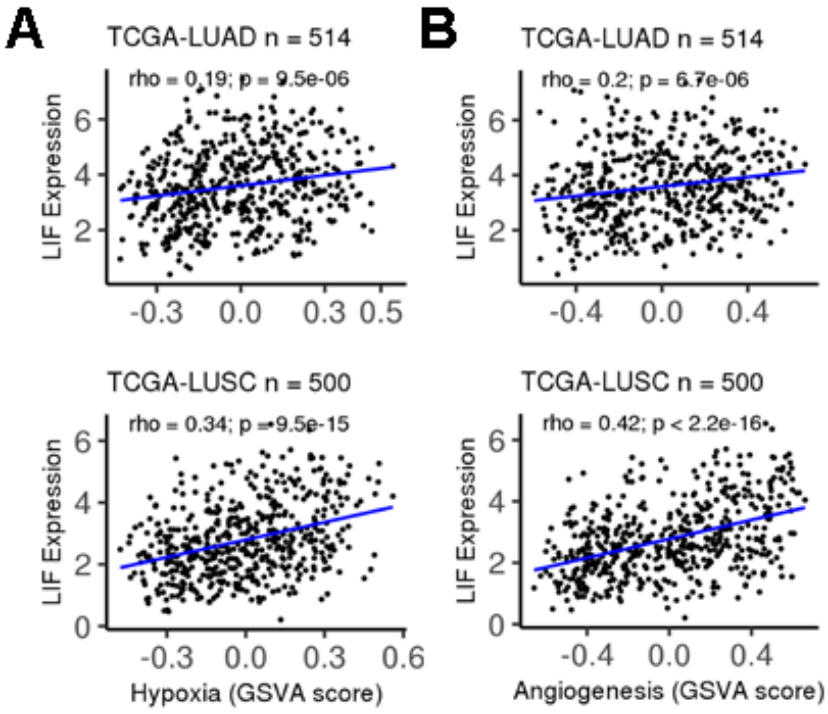

Figure 27. LIF expression positively correlates with *hypoxia* and *angiogenesis*. (A) LIF expression values (log2(TPM)) in TCGA-LUAD (n = 514) and TCGA-LUSC (n = 500) datasets were plotted against hypoxia and (B) angiogenesis GSVA scores. Spearman correlation coefficients (rho) and p values are given for the correlations. *Data analysis was performed by S. Hijazo.

Next, we hypothesised that one of the pro-tumorigenic functions fulfilled by LIF as a glucose stress signal could be to recruit endothelial cells and build a vascular network to re-supply the tumour with nutrients. Thus, we replicated the previous meta-analysis comparing *angiogenesis* GSVA scores with LIF expression. The results showed that both LUAD (pooled correlation coefficient = 0.27 ±0.050; n=3963) and LUSC (pooled correlation coefficient = 0.44 ±0.060; n=2076) samples displayed a strong correlation between LIF expression and angiogenesis (representative datasets Fig. 27B).

Additionally, we studied publicly available single cell transcriptomic data from the *Lung endothelial cell atlas* (Schupp *et al*., 2021) to identify the cell types that express LIF receptor (LIFR) within tumoral and non-tumoral tissue samples of lung cancer patients (Fig 28). This revealed that LIFR was almost exclusively expressed in endothelial cells clusters, suggesting that the main role for LIF in lung tumours must be related to the vasculature.

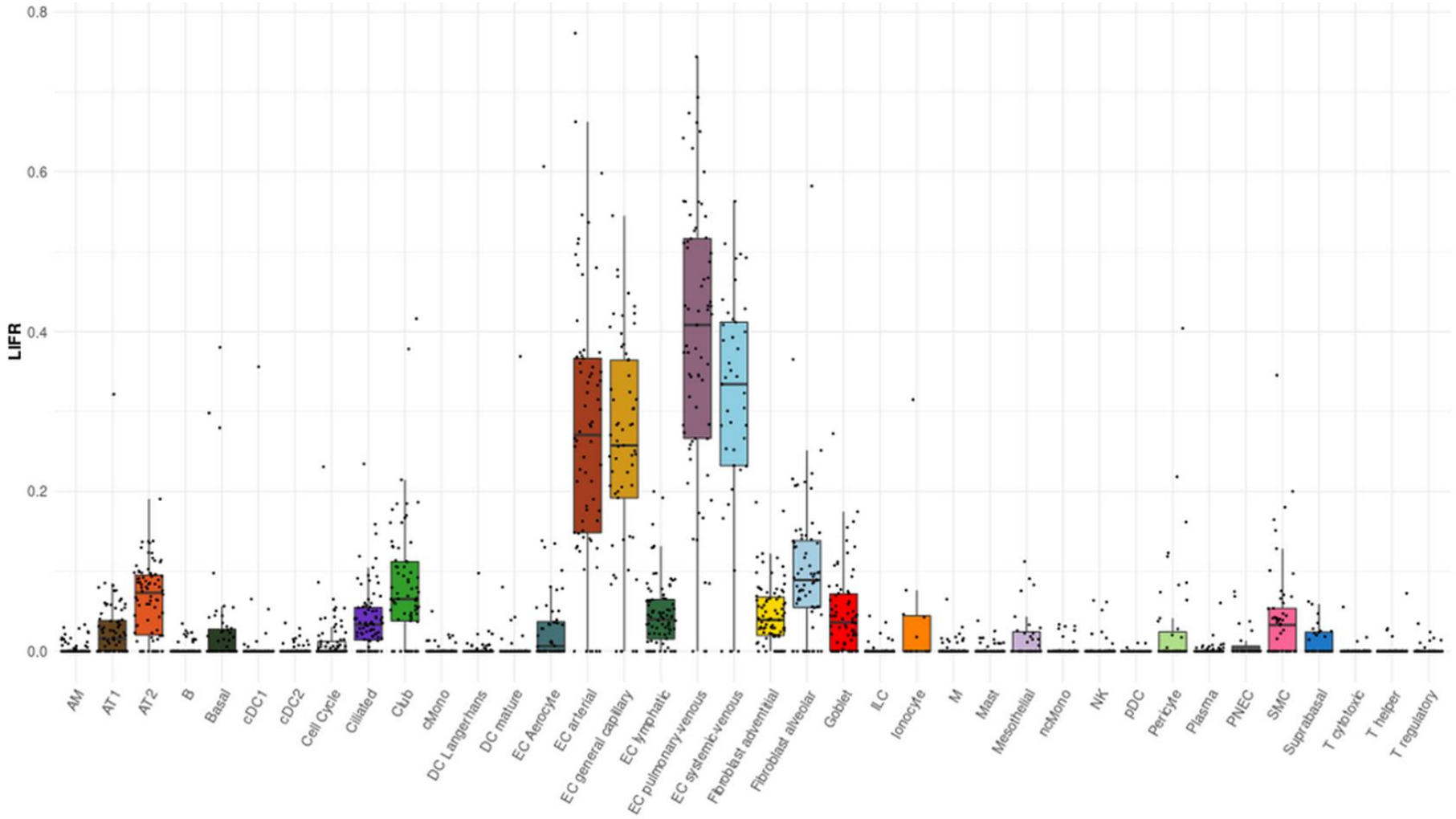

Fig 28. LIFR is mainly expressed by endothelial cells within lungs of lung cancer patients. LIFR expression from six different lung cancer patient single-cell transcriptomic datasets (n = 73) integrated and normalised using the Lung Endothelial Cell Atlas (Schupp *et al*., 2021). Graphs represent the median and IQR and 95% CI.

7.5 LIF and angiogenesis: *in vitro*

To assess the potential pro-angiogenic effects of LIF, we employed human umbilical vein endothelial cells (HUVECs) as a model. As a first approach we used a wound healing assay. Briefly, HUVEC cells were allowed to form a confluent monolayer, then a scratch in the layer was made and culture media was replaced with conditioned media from A549 cells either cultured in presence or absence of glucose, and media supplemented with rhLIF (200pg/mL). A time lapse recording of the cells was used to track individual cell migration using ImageJ TrackMate algorithm (Tinevez *et al*., 2017). Average migration speed was found to be significantly increased in cells treated with rhLIF (Fig 29A), however non-quantifiable observations indicated this method lacked sufficient accuracy to record the qualitative effects observed.

Therefore, we decided to employ transwell migration assays. Briefly, HUVECs were allowed to migrate across a transwell membrane in presence of recombinant human LIF at concentrations in the range of those observed in supernatants of glucose deprived Lung cancer cells, and in conditioned media (CM) from glucose deprived A549 cells with neutralizing antibody against LIF or an isotype control. HUVECs treated with both recombinant LIF or CM displayed a significantly increased migratory ability when compared to untreated cells or those incubated in CM with neutralizing antibody against LIF (Fig 29B). Furthermore, analysis of vessel-like structure formation in matrigel of HUVECs incubated in the aforementioned conditions also revealed a significant increase in vessel formation in LIF and CM treated cells when compared with the corresponding untreated control or CM containing neutralizing anti-LIF antibody (Fig 29C). Changes in proliferation of HUVECs in all these conditions were measured by crystal violet staining. No significant changes in proliferation were observed in response to any treatment (Fig 29D), indicating that changes in migrated cells and vessel formation were not an artifact derived from increased proliferation but an authentic increase in the measured parameters.

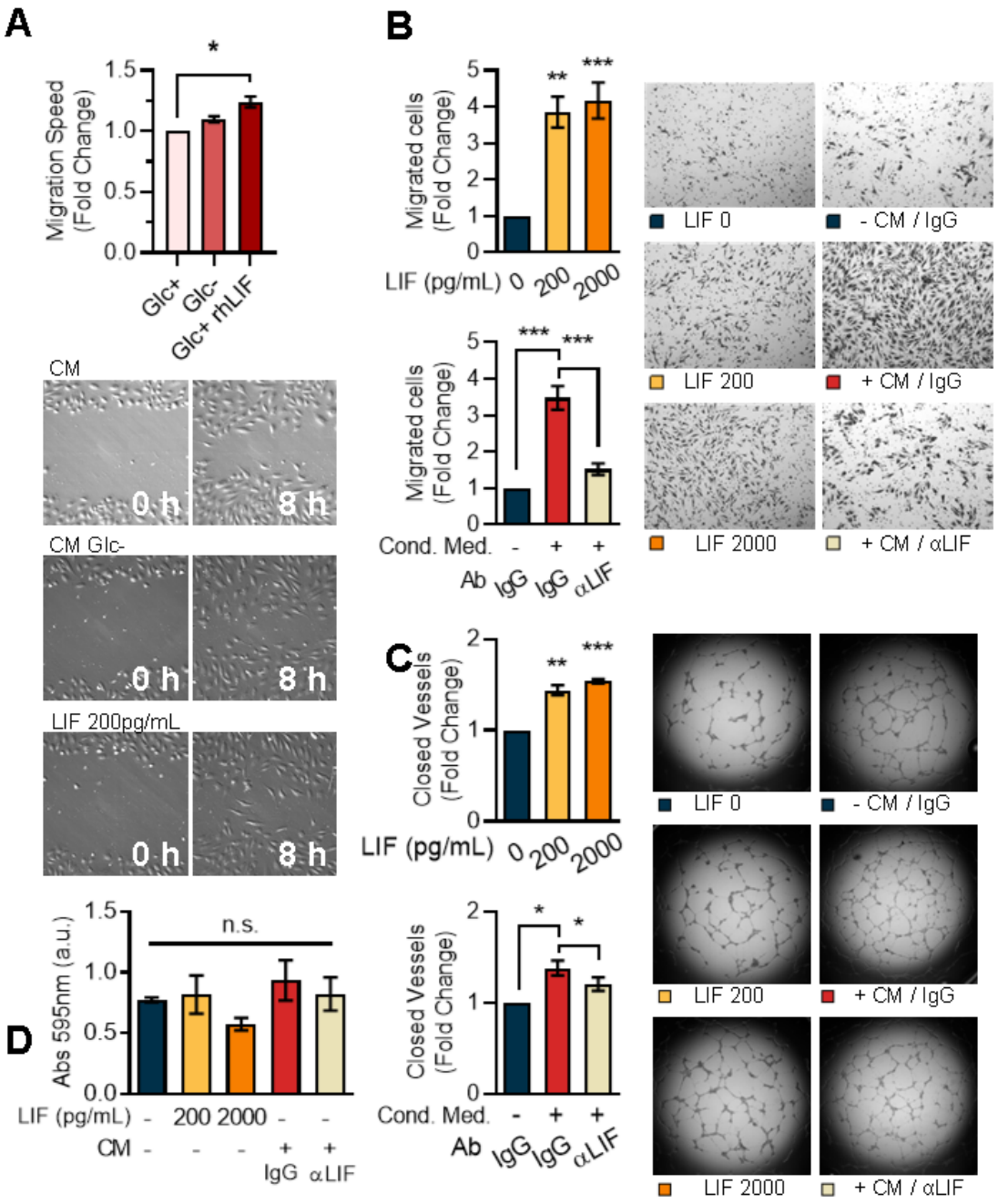

Fig 29. LIF has pro-angiogenic effects *in vitro*. (A) HUVEC migration measured by wound healing assay upon treatment with conditioned media (CM) from A549 cells cultured in presence or absence of glucose, and upon treatment with recombinant human LIF (n=3) Images are representative of two timepoints (0 & 8h) from a 16h timelapse of 0.5h intervals. (B) HUVEC transwell migration towards media containing recombinant human LIF and conditioned media from A549 cells cultured in absence of glucose for 24h with neutralizing antibody against LIF or an isotype control. Images are representative of three biological replicates (n=3) comprising three technical replicates each. (C) HUVEC tube formation assay in the previously detailed conditions. Images are representative of three biological replicates (n=3) comprising three technical replicates each. (D) HUVEC cell proliferation in the previously detailed conditions measured by crystal violet assay. Graphs represent the mean and SEM; *-**** indicates significant differences (p< 0.05 - 0.0001) obtained by paired t-test.

7.6 LIF and angiogenesis: *in vivo*

To explore the pro-angiogenic role of LIF *in vivo,* the aforementioned orthotopic model of lung cancer was used to evaluate the abundance of blood vessels in the tumors. Within the previously determined Ki67-high tumor areas, individual CD31+ structures were counted. The abundance of CD31+ structures was significantly decreased in the LIF-KO tumors (Fig 30), indicating that LIF has a pro-angiogenic role in the tumour.

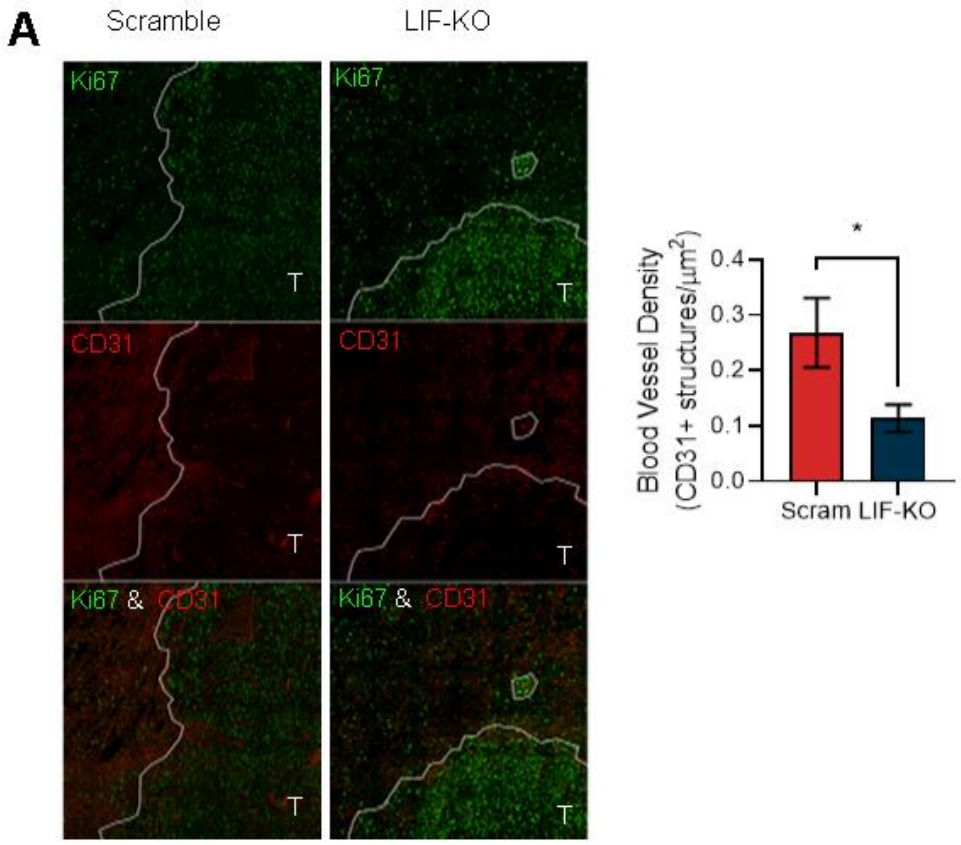

Fig 30. LIF has pro-angiogenic effects *in vivo*. (A) Representative immunofluorescence images depicting the tumour area determination by Ki67 staining (Green channel) and illustrating blood vessel abundance by CD31 staining (Red channel). (B) CD31+ cell quantification in orthotopic tumours from LIF CRISPR KO LLC1 cells and Scramble vector transduced LLC1 cells (n=11) Graphs represent the mean and SEM; *-**** indicates significant differences ($p < 0.05$ - 0.0001) obtained by unpaired t-test.

7.7 Results II: Summary

Through the second part of this PhD study, we have successfully demonstrated that LIF is a pro-tumorigenic cytokine of relevance in lung, as well as in other types of cancer. Furthermore, we have discovered a novel function of LIF as a pro-angiogenic cytokine, which could be linked to its tumour promoting effects.

8. Discussion

8.1 LIF is a novel glycaemic stress signal

LIF is a pleiotropic cytokine, with new roles continuously being discovered and characterised. Moreover, the body of literature dealing with this molecule continues to grow at an increasing pace. Well established research from decades past (Smith *et al*., 1988; Williams *et al*., 1988) has led to it becoming one of the most relevant stemness factors, routinely used to maintain stem cell cultures. Subsequent cumulative research on its role in reproduction (Lass *et al.,* 2001; Kimber, 2005; Salleh & Giribabu, 2014) has led to it being studied as a prognostic marker for fertility (Li *et al*., 2020; Mikolajczyk *et al*., 2003; Margioula-Siarkou *et al*., 2016) and LIF antagonists as non-hormonal contraceptives are progressing towards clinical trials (White *et al*., 2007; Menkhorst *et al*., 2011; Aschenbach *et al*., 2013). Recently, it has become one of the most prominent cytokines in the context of cancer for its role in immunity (Pascual-Garcia *et al*., 2019), EMT and cell differentiation regulation (Shi *et al*., 2019), and cachexia (Arora *et al*., 2018; Kandarian *et al*., 2018).

However, these fields of research remain relatively separate and the possible interconnexion between these seemingly disparate roles in different situations has not been explored. Moreover, although the effects and functions of LIF continue to be increasingly researched, there is a striking lack of scrutiny with regards to how it is regulated and what triggers LIF production.

The present study, based on the novel finding that glucose deprivation induced LIF release in a particular cell line, has aimed to investigate the mechanisms leading to LIF production in the context of cancer, and rather fortunately, we have stumbled into a bigger finding than we ever expected: a novel mechanism for glucose sensing active in both malignant but also non-malignant cells.

Our study of a broad range of cell types (Fig 1) clearly demonstrated that a variety of cells produced LIF when faced with glucose stress. This was independent from the mutational background, the precedence of the cells, their benign or tumoral nature, and even the species of origin. This is suggestive of a well conserved mechanism that could mediate responses to glycaemic stress across a multitude of tissues and physiological situations. Moreover, re-analysis of public data from

Gameiro and Struhl (2018) on translational responses to nutrient stress revealed that this response is also present in non-transformed breast epithelium, as well as in a model of breast cancer (Figs 8, 18).

8.2 LIF acts as a facilitator of glucose for hypoglycaemic tissues

It has been previously reported that LIF induces glucose uptake in myocytes and cardiomyocytes (Brandt *et al*., 2015; Florholmen *et al*., 2004; Florholmen *et al*., 2006), and that bouts of intense exercise, which are known to produce transient local hypoglycaemia, elevate circulating LIF levels and LIFR expression in muscles (Broholm *et al.,* 2011; Jia *et al*., 2018). Moreover, LIF also has been shown to be induced by leptin signalling (Gonzalez *et al*., 2004) and to modulate food intake in a leptin-R independent manner (Arora *et al*., 2018). Lastly, LIF has also been shown to induce lipolysis in adipose tissue, leading to an increase in systemic glucose availability (Arora *et al*., 2018). When we consider these metabolic effects of LIF, it would be a reasonable leap to deduce that the biological reason why LIF is released in hypoglycaemic tissues is to help ameliorate the lack of glucose, at both local and systemic levels depending on the localisation and extension of the glycaemic stress. Therefore, our finding that glucose deprivation is a relevant trigger of LIF release could provide a unifying theory to link the physiological effects of LIF during exercise and reproduction, and the pathological effects on LIF in cancer and cachexia. As previously discussed in the introduction, tumours often hijack normal mechanisms to adapt to the environmental stresses they face, and the adaptation to glycaemic stress should be no exception.

8.3 The glycosylation pathway as a glucose sensor

The process of glycosylation entails a highly specific and resource efficient mechanism. And due to its complexity, much remains to be discovered in this field. What we do know is that eukaryotic cells do not waste their glycans; in fact, up to one third of all protein attached glycans are recycled via the salvage pathway (Varki *et al.,* 1999). Moreover, in order for misfolded proteins to be

completely degraded by the proteasome, total removal of all glycans is needed (Varki *et al.*, 1999). Briefly, nascent glycoproteins are detected and bound by ER lectins calnexin (CNX) and calreticulin (CRT), which perform the quality control function. Hypoglycosylated and malglycosylated proteins are processed by a series of mannosidases that cleave and recycle the mannose residues, and the resulting misfolded protein is targeted for ERAD. If new glycoproteins are correctly glycosylated they get transported into the Golgi for subsequent glycan trimming and subcellular or extracellular distribution (Cherepanova *et al*., 2016). If an excess of malglycosylated proteins overcome the CNX/CRT cycle and accumulate in the ER, UPR kinases activate their stress response pathways. Therefore, although eukaryotic cells are able to recycle a large portion of their glycans, an acute lack of glycosylation substrates can trigger the UPR, thus providing an early glucose stress signal before the damage is irreversible and apoptosis begins.

Beyond our initial finding, we decided to delve deeper and investigate the metabolic trigger downstream of glucose limitation leading to LIF release. This would help better elucidate an actionable intracellular signalling mechanism. The present study has empirically demonstrated that LIF production is triggered by highly-specific sensing of impaired glycosylation (Fig 7), with ample evidence that other metabolic pathways dependent on glucose (Fig 5-6), and that other related types of stresses (Fig 2) do not induce LIF production. In line with this new model for glucose sensing, we proved that inhibition of PERK signalling abrogated the secretion of LIF (Fig 11), further suggesting that the signal originates in the centre for glycosylation control: the ER. Moreover, through re-analysis of public datasets we found a new potential marker for glycaemic stress: GMPPB (Fig 8).

GMPPB gene encodes a subunit of the GMPP, a key enzyme of the MBP that converts mannose-1-P to GDP-mannose, allowing it to bind to dolichol molecules in the ER and be used for protein glycosylation (Ning & Elbein, 2000), thus connecting glucose to glycosylation. We have shown that GMPPB was the most upregulated gene of the MBP and the N-glycosylation pathway both in glucose deprivation and glycosylation inhibition by tunicamycin (Fig 8B-C). Moreover, this enzyme is also key in regulating O-mannosylation, C-mannosylation and glycosylphosphatidylinositol (GPI)-anchor formation (Rodriguez-Cruz *et al*.,

2016). This suggests that GMPPB could potentially be used as a new biomarker for glycaemic stress or a histological marker for tissue hypoglycaemia.

8.4 The Glucose-LIF response yields an extracellular stress signal.

The field of LIF research is currently very active, and thus consensus on sequence annotations, splice variants and isoforms is yet to be reached. Two key studies by the Rathjen group (Haines *et al.,* 1999; Voyle *et al*., 1999), identified three main isoforms of human and murine LIF: LIF-D, -M and -T. Additionally, they identified different subcellular localisation of these isoforms. Subsequent studies have relied on these findings and provided further validity to these sequences (Haines *et al*., 2000; Hill & Vernallis, 2008; Hisaka *et al*., 2004), and some have even found homologous isoforms in other species such as pig (Spötter *et al*., 2001) and elephant (Vazquez *et al*., 2018).

However, major annotated databases such as *ENSEMBL* and *NCBI gene* fail to acknowledge the existence of these isoforms. In fact, the *NCBI* sequence called LIF transcript variant 1 is exactly the same as LIF-D but lacks 90 base-pairs (bp) at the 5' end. Moreover, through the course of this study the exon1 sequence for LIF transcript variant 1 as reported by ENSEMBL and NCBI has been modified several times. The forward primer designed to amplify isoform D is homologous to the part of the 90bp 5' region which is not included in the official annotation of LIF transcript 1. The forward primer designed to amplify isoform M is homologous to the exon 1M, which is not included in the official annotation by *ENSEMBL* and *NCBI gene.* And yet both primers have successfully amplified isoforms -D and -M, providing additional evidence of the existence of these un-official RNA sequences. Additionally, based on the previously described subcellular localisation of these isoforms (Voyle *et al*., 1999), as well as on our own empirical evidence (Fig 3), we have determined that the fate of LIF protein produced upon glucose deprivation is to be secreted, which is coherent with its proposed role as an extracellular stress signal.

8.5 LIF production is regulated at multiple levels

In recent years it has become clear that cellular metabolic homeostasis regulation is a much more complex process than initially thought. A plethora of signalling pathways diverge from different metabolic triggers and converge on multiple transcription factors and translational effectors to achieve specific results by virtue of complex combinations of signals. To add to this network, extensive cross-talk between once thought isolated pathways keeps arising in new studies.

This study has struggled to pin-point key regulators of LIF production triggered by glucose deprivation and impaired glycosylation. Although we have ruled out multiple transcription factors and pathways, a clear picture of the complete regulatory process leading to LIF production remains elusive.

We have, nonetheless, successfully determined that PERK signalling is essential, and that in some cases GCN2 could also be participating in promoting LIF release (Figs 11, 13 & 14). When considering the common target of these kinases, eIF2a, translational regulation is the first thing to come to mind, which is further supported by the complete absence of transcriptional upregulation in some cell lines (Fig 15). Analysis of public ribosome profiling data is suggestive of translational regulation of LIF in the context of glucose deprivation (Fig 18). Moreover, post-transcriptional regulation by modulation of mRNA half-life was also ruled out (Fig 16). And yet the fact that thapsigargin alone did not induce LIF production (Fig 12) and that ActD prevented LIF production (Fig 19) suggests that plain phosphorylation of PERK and its downstream target eIF2a is not sufficient to promote LIF release.

Lastly, we investigated a hypothetical cross talk between PERK and the MAPK signalling pathway, which takes place under glucose deprivation (Shin *et al*., 2015). Bioinformatic data suggested the involvement of MAPK related transcription factors (Fig 21), and preliminary empirical data showed that ERK1/2 inhibition reduced significantly LIF release (Fig 22). These experiments seem to indicate that transcriptional input from the MAPK signalling pathway could be participating in LIF production, however further experiments are needed to provide a definitive answer.

In summary, we have proven the key involvement of PERK in LIF production secondary to impaired glycosylation, which provides a potential therapeutic target for preventing LIF production in the context of cancer. We have also provided evidence suggestive of involvement of MAPK signalling, leading to a hybrid transcriptional and translational regulatory mechanism, which could provide further actionable targets.

8.6 LIF pro-tumorigenic effects: a new mechanism

LIF has been widely regarded as a pro-tumorigenic cytokine for years now. In fact, in the last few years there have been several high-impact studies trying to elucidate the mechanism by which LIF promotes tumour growth.

In 2019, the group of Joan Seoane (Pascual-García *et al*., 2019) found that LIF epigenetically silenced CXCL9 and induced CD206, CD163 and CCL2 in tumour associated macrophages, which in turn affected T-cell recruitment and activation to produce an immunosuppressive microenvironment and help tumours evade the immune response.

Simultaneously, the McCormick lab (Wang *et al*., 2019) published their findings stating that LIF exerts its effects by promoting tumour cell stemness via STAT3-independent Yap/Taz signalling in pancreatic ductal adenocarcinoma (PDAC).

In the same year, the group of Tony Hunter (Shi *et al*., 2019) published that LIF in PDAC did in fact come from the stroma and that it not only promoted cancer cell stemness but was also crucial in their early epithelial-to-mesenchymal transition (EMT). Another recent study (Yue *et al*., 2016) also reported that LIF induced tumorigenesis by aiding EMT transition in a STAT3-dependent manner.

The clear outcome of this avalanche of new research surrounding LIF is that it is indeed pro-tumorigenic, and that it plays as many roles in cancer (immunotolerance, stemness, EMT) as it does in normal human physiology (maternofoetal immunotolerance, developmental stemness). However a unified mechanism leading to LIF production remains elusive.

In light of our preliminary finding that LIF release occurs in response to glucose deprivation, this study also aimed at investigating the functional connexion

between LIF and glucose homeostasis, in the context of cancer. This led to the discovery of a new mechanism through which LIF exerts its pro-tumorigenic actions: promoting angiogenesis.

8.7 LIF is a new pro-angiogenic factor

The initial approach for this part of our study contemplated several potential mechanisms for LIF to impact tumorigenesis. Other group members investigated the effects of the conditioned media of glucose deprived A549 on different PBMC populations (Püschel *et al*.,2020), but results were limited, and attributed to other cytokines. We also personally studied activation and migration of HL60 promyeloblasts (differentiated towards a neutrophil-like lineage) and healthy donor isolated primary neutrophils as well as several metabolic effects on 3T3-L1 cells (differentiated towards a pre-adipocyte lineage) (data not shown). However, the most striking effects were found when looking at the effects of recombinant human LIF or conditioned media from A549 cells in HUVECs (Fig 29).

Once again, we considered the known roles of LIF in healthy physiological conditions as a framework to understand the tools and mechanisms available for cancer cells to hijack in order to survive. In this case, we built our hypothesis based on previous findings that LIF induces expression of pro-invasive factors such as MMPs, inhibits TIMPs, and promotes expression of pro-angiogenic factors in trophoblasts (Poehlmann *et al*, 2005; Suman *et al*., 2013).

Thus, we next demonstrated bioinformatically that expression of LIFR in the lung is almost exclusive to endothelial cells, and that the few cell types that express this receptor do so to a very limited extent when compared to endothelial cells (Fig 28). Furthermore, with the collaboration of bioinformaticians, we validated the findings obtained from the *Lung Endothelial Cell Atlas* on individual scRNA sequencing studies and found that this LIFR expression distribution does not only happen in lung tumour tissue samples, but also in healthy lungs. Additionally, further bioinformatic analysis of several curated lung cancer datasets, performed with the aid of bioinformatician Sara Hijazo, demonstrated strong correlations between LIF and angiogenesis genes (Fig 27).

Lastly, upon consultation with experts in the field of angiogenesis, we decided to use, as they put it, *the gold standard* for demonstrating angiogenic effects in cancer. We generated orthotopic lung tumours in immunocompetent mouse using cells with or without a KO in our gene of interest. And as we show in Fig 30, we found that absence of LIF resulted in a significant decrease in the number of CD31+ cells infiltrating the tumour. This in turn, could be the cause of the smaller size of LIF-KO lesions (Fig 26), since an impaired blood flow should limit the nutrient availability and proliferation of tumour cells.

Although we were unable to investigate in depth the signalling pathway used by LIF to produce its effects on endothelial cells due to the time limitations of the project, we did have some indications that LIF is acting via its receptor, based on the exclusive expression of LIFR by endothelial cells. Moreover, as this project approached completion, two major papers came out on this regard:

Firstly, the group of Carmen Ruiz de Almodovar (Shen *et al*., 2021) published last December their finding that the STAT3-YAP/TAZ signalling axis was a fundamental regulator of tumour angiogenesis. And most importantly, although they showed with great detail the relevance of this pathway in angiogenesis, there was room for speculation with regards to which cytokines were driving this mechanism. We propose that one of the main cytokines producing this signal is LIF, which is known to signal via the LIFR - STAT3 – YAP/TAZ axis.

Secondly, the Ferrara lab (Li *et al*., 2022) published in mid-January a paper demonstrating that LIF induces angiogenesis *in vitro* in bovine choroidal endothelial cells (BCEs) but not in bovine aortic endothelial cells (BAE). They confirmed that signalling took place through the LIFR-STAT3 axis and suggested that LIF targeted small vessel endothelial cells to promote neo-angiogenesis.

Together these two articles serve as supporting pillars for our findings and give further clues as to the mechanism at play in our model.

8.8 Limitations and Further research

Despite the satisfying outcome of this study in fulfilling its main research aims, science never stops, and new questions arise from the answers provided here. Ultimately, this study provided insights on the signalling mechanism behind LIF

production, but the specific MAPK participation in LIF release has not been completely elucidated. Further research could include detection of the main induced MAPK related transcription factors in response to glucose deprivation and under treatment with ERK1/2 inhibitor PD98059 by western blotting. Following this, the most relevant transcription factors found could be knocked down and production of LIF could be explored to potentially determine the specific transcription factor operating under glucose deprivation to induce it.

Moreover, additional experiments could be aimed at elucidating the specific signalling and the mechanism by which LIF promotes angiogenesis. Additional endothelial cell markers could be used in histological sections to determine which specific endothelial cell subtype responds to LIF. Simultaneously, signalling downstream of LIFR could be investigated via western blotting of p-STAT3 and YAP in protein extracts from endothelial cells treated with LIF. Last but not least, a more physiologically relevant endothelial cell line could be used to validate our findings on HUVECs, such as the more popular human microvascular endothelial cells (HMVECs) or animal models such as the BCEs used by Li *et al*. (2022).

9. Conclusions

This study has successfully addressed its two main aims: investigating the mechanisms leading to LIF release in the context of cancer and understanding its potential role in promoting cancer cell survival in a hypoglycaemic microenvironment.

In the first part, we demonstrated that decreased glucose availability triggers LIF production, which would certainly occur in large solid tumours with high glycolytic demands and insufficient nutrient supply due to rapid growth. Moreover, we have proven that defective glycosylation secondary to hypoglycaemia is the main metabolic cue leading to LIF release. Last but not least, we have provided ample evidence that LIF production is mediated by PERK and partially by GCN2 in a complex transcriptional and translational mechanism, and we have provided additional evidence of the participation of MAPK signalling.

In the second part, we have demonstrated that LIF has pro-angiogenic effects *in vitro* and *in vivo*, and we have provided supporting bioinformatic evidence suggesting this mechanism is also at play in human tumours. Thus, we have discovered a new function for LIF in the context of cancer, which links its role as a metabolic sensor with angiogenesis. This implies that LIF-driven angiogenesis could be one of the mechanisms that tumours capitalise on to solve their low nutrient supply issues.

Briefly put, we have shown that:

1. Glucose deprivation, sensed via hypo-glycosylation, induces LIF production in a PERK dependent manner.
2. LIF promotes angiogenesis, potentially ameliorating local hypoglycaemia.

The ramifications of this study could bring about new therapeutic strategies for prevention of LIF production in cancer patients with high expression of this cytokine, and most importantly, provide new insights into the process of glucose sensing both in tumoral and normal tissues. Lastly, our discovery of a new angiogenic regulator could be used for the development of future anti-angiogenic cancer therapies and to better understand resolution of other conditions such as ischemia.

10. References

1. Albrengues, J., Bourget, I., Pons, C., Butet, V., Hofman, P., Tartare-Deckert, S., Feral, C. C., Meneguzzi, G., & Gaggioli, C. (2014). LIF mediates proinvasive activation of stromal fibroblasts in cancer. Cell Reports, 7(5), 1664–1678.
2. Andersen C.L., Ledet-Jensen J., Ørntoft T. (2004) Normalization of real-time quantitative RT-PCR data: a model based variance estimation approach to identify genes suited for normalization - applied to bladder- and colon-cancer data-sets. *Cancer Research*, 64: 5245-5250.
3. Argilés, J. M., Alvarez, B., & López-Soriano, F. J. (1997). The metabolic basis of cancer cachexia. Medicinal Research Reviews, 17(5), 477–498.
4. Arora, G. K., Gupta, A., Narayanan, S., Guo, T., Iyengar, P., & Infante, R. E. (2018). Cachexia-associated adipose loss induced by tumor-secreted leukemia inhibitory factor is counterbalanced by decreased leptin. JCI Insight, 3(14).
5. Aschenbach, L. C., Hester, K. E., McCann, N. C., Zhang, J. G., Dimitriadis, E., & Duffy, D. M. (2013). The LIF receptor antagonist PEGLA is effectively delivered to the uterine endometrium and blocks LIF activity in cynomolgus monkeys. *Contraception*, *87*(6), 813–823.
6. Barton, B. E., & Murphy, T. F. (2001). Cancer cachexia is mediated in part by the induction of IL-6-like cytokines from the spleen. Cytokine, 16(6), 251–257.
7. Baxter, E. W., & Milner, J. (2010). P53 regulates LIF expression in human medulloblastoma cells. *Journal of Neuro-Oncology*, *97*(3), 373–382.
8. Beretta, E., Dhillon, H., Kalra, P. S., & Kalra, S. P. (2002). Central LIF gene therapy suppresses food intake, body weight, serum leptin and insulin for extended periods. Peptides, 23(5), 975–984.
9. Bieberich, E. (2014). Synthesis, Processing, and Function of N-glycans in N-glycoproteins. In Advances in neurobiology (Vol. 9, pp. 47–70). NIH Public Access.
10. Brandt, N., O'Neill, H. M., Kleinert, M., Schjerling, P., Vernet, E., Steinberg, G. R., Richter, E. A., & Jørgensen, S. B. (2015). Leukemia inhibitory factor increases glucose uptake in mouse skeletal muscle. American Journal of Physiology-Endocrinology and Metabolism, 309(2), E142–E153.

11. Broholm, C., Mortensen, O. H., Nielsen, S., Akerstrom, T., Zankari, A., Dahl, B., & Pedersen, B. K. (2008). Exercise induces expression of leukaemia inhibitory factor in human skeletal muscle. The Journal of Physiology, 586(8), 2195–2201.

12. Broholm, C., Laye, M. J., Brandt, C., Vadalasetty, R., Pilegaard, H., Pedersen, B. K., & Scheele, C. (2011). LIF is a contraction-induced myokine stimulating human myocyte proliferation. *Journal of Applied Physiology*, *111*(1), 251–259.

13. Broholm, C., Brandt, C., Schultz, N. S., Nielsen, A. R., Pedersen, B. K., & Scheele, C. (2012). Deficient leukemia inhibitory factor signaling in muscle precursor cells from patients with type 2 diabetes. American Journal of Physiology-Endocrinology and Metabolism, 303(2), E283–E292.

14. Carmeliet, P. (2005). Angiogenesis in life, disease and medicine. In *Nature* (Vol. 438, Issue 7070, pp. 932–936).

15. Carson, J. A., & Baltgalvis, K. A. (2010). Interleukin 6 as a key regulator of muscle mass during cachexia. Exercise and Sport Sciences Reviews, 38(4), 168–176.

16. Chandel, N. (2014). *Navigating metabolism*. Cold Spring Harbor Laboratory Press U.S.

17. Chen, Y., Deng, J., Fujimoto, J., Kadara, H., Men, T., Lotan, D., & Lotan, R. (2010). Gprc5a deletion enhances the transformed phenotype in normal and malignant lung epithelial cells by eliciting persistent Stat3 signaling induced by autocrine leukemia inhibitory factor. Cancer Research.

18. Chen, C. Y. A., Ezzeddine, N., & Shyu, A. Bin. (2008). Chapter 17 Messenger RNA Half-Life Measurements in Mammalian Cells. In *Methods in Enzymology* (Vol. 448, pp. 335–357). Methods Enzymol.

19. Cherepanova, N., Shrimal, S., & Gilmore, R. (2016). N-linked glycosylation and homeostasis of the endoplasmic reticulum. Current opinion in cell biology, 41, 57–65.

20. Coorens, T. H. H., Oliver, T. R. W., Sanghvi, R., Sovio, U., Cook, E., Vento-Tormo, R., Haniffa, M., Young, M. D., Rahbari, R., Sebire, N., Campbell, P. J., Charnock-Jones, D. S., Smith, G. C. S., & Behjati, S. (2021). Inherent mosaicism and extensive mutation of human placentas. *Nature*, *592*(7852), 80–85.

21. Dantz, D., Bewersdorf, J., Fruehwald-Schultes, B., Kern, W., Jelkmann, W., Born, J., Fehm, H. L., & Peters, A. (2002). Vascular endothelial growth factor: A novel endocrine defensive response to hypoglycemia. *Journal of Clinical Endocrinology and Metabolism*, *87*(2), 835–840.

22. DATEMA, R., & SCHWARZ, R. T. (1978). Formation of 2-Deoxyglucose-Containing Lipid-Linked Oligosaccharides. Interference with Glycosylation of Glycoproteins. European Journal of Biochemistry, 90(3), 505–516.

23. Davis, S., Aldrich, T. H., Stahl, N., Pan, L., Taga, T., Kishimoto, T., Ip, N. Y., & Yancopoulos, G. D. (1993). LIFR beta and gp130 as heterodimerizing signal transducers of the tripartite CNTF receptor. Science (New York, N.Y.), 260(5115), 1805–1808.

24. DeChiara, T. M., Vejsada, R., Poueymirou, W. T., Acheson, A., Suri, C., Conover, J. C., Friedman, B., McClain, J., Pan, L., Stahl, N., Ip, N. Y., Kato, A., & Yancopoulos, G. D. (1995). Mice lacking the CNTF receptor, unlike mice lacking CNTF, exhibit profound motor neuron deficits at birth. Cell, 83(2), 313–322.

25. Deng, J., Lu, P. D., Zhang, Y., Scheuner, D., Kaufman, R. J., Sonenberg, N., Harding, H. P., & Ron, D. (2004). Translational Repression Mediates Activation of Nuclear Factor Kappa B by Phosphorylated Translation Initiation Factor 2. Molecular and Cellular Biology, 24(23), 10161–10168.

26. Esper, D. H., & Harb, W. A. (2005). The cancer cachexia syndrome: A review of metabolic and clinical manifestations. Nutrition in Clinical Practice, 20(4), 369–376.

27. Ernst, M., & Jenkins, B. J. (2004). Acquiring signalling specificity from the cytokine receptor gp130. Trends in Genetics, 20(1), 23–32.

28. Evan, G. (2008). The future of cancer therapy: An interview with Gerard Evan. In *DMM Disease Models and Mechanisms* (Vol. 1, Issues 2–3, pp. 90–93). Company of Biologists.

29. Fearon, K. C. H., Glass, D. J., & Guttridge, D. C. (2012). Cancer cachexia: Mediators, signaling, and metabolic pathways. In *Cell Metabolism* (Vol. 16, Issue 2, pp. 153–166). Elsevier.

30. Febbraio, M. A., Hiscock, N., Sacchetti, M., Fischer, C. P., & Pedersen, B. K. (2004). Interleukin-6 is a novel factor mediating glucose homeostasis during skeletal muscle contraction. Diabetes, 53(7), 1643–1648.

31. Ferrara, N., & Kerbel, R. S. (2005). Angiogenesis as a therapeutic target. In *Nature* (Vol. 438, Issue 7070, pp. 967–974). Nature.

32. Ferretti, C., Bruni, L., Dangles-Marie, V., Pecking, A. P., & Bellet, D. (2007). Molecular circuits shared by placental and cancer cells, and their implications in

the proliferative, invasive and migratory capacities of trophoblasts. In *Human Reproduction Update* (Vol. 13, Issue 2, pp. 121–141). Hum Reprod Update.

33. Florholmen, G., Aas, V., Rustan, A. C., Lunde, P. K., Straumann, N., Eid, H., Odegaard, A., Dishington, H., Andersson, K. B., & Christensen, G. (2004). Leukemia inhibitory factor reduces contractile function and induces alterations in energy metabolism in isolated cardiomyocytes. Journal of Molecular and Cellular Cardiology, 37(6), 1183–1193.

34. Florholmen, G., Thoresen, G. H., Rustan, A. C., Jensen, J., Christensen, G., & Aas, V. (2006). Leukaemia inhibitory factor stimulates glucose transport in isolated cardiomyocytes and induces insulin resistance after chronic exposure. Diabetologia, 49(4), 724–731.

35. Forsythe, J. A., Jiang, B. H., Iyer, N. V, Agani, F., Leung, S. W., Koos, R. D., & Semenza, G. L. (1996). Activation of vascular endothelial growth factor gene transcription by hypoxia-inducible factor 1. *Molecular and Cellular Biology*, *16*(9), 4604–4613.

36. Fritz, V., & Fajas, L. (2010). Metabolism and proliferation share common regulatory pathways in cancer cells. In *Oncogene* (Vol. 29, Issue 31, pp. 4369–4377). Oncogene.

37. Gameiro, P. A., & Struhl, K. (2018). Nutrient Deprivation Elicits a Transcriptional and Translational Inflammatory Response Coupled to Decreased Protein Synthesis. *Cell Reports*, *24*(6), 1415–1424.

38. Galan-Cobo, A., Sitthideatphaiboon, P., Qu, X., Poteete, A., Pisegna, M. A., Tong, P., Chen, P. H., Boroughs, L. K., Rodriguez, M. L. M., Zhang, W., Parlati, F., Wang, J., Gandhi, V., Skoulidis, F., DeBerardinis, R. J., Minna, J. D., & Heymach, J. V. (2019). LKB1 and KEAP1/NRF2 pathways cooperatively promote metabolic reprogramming with enhanced glutamine dependence inKRAS-mutant lung adenocarcinoma. Cancer Research, 79(13), 3251–3267.

39. Gloaguen, I., Costa, P., Demartis, A., Lazzaro, D., Di Marco, A., Graziani, R., Paonessa, G., Chen, F., Rosenblum, C. I., Van der Ploeg, L. H., Cortese, R., Ciliberto, G., & Laufer, R. (1997). Ciliary neurotrophic factor corrects obesity and diabetes associated with leptin deficiency and resistance. Proceedings of the National Academy of Sciences of the United States of America, 94(12), 6456–6461.

40. Gonzalez, R. R., Rueda, B. R., Ramos, M. P., Littell, R. D., Glasser, S., & Leavis, P. C. (2004). Leptin-Induced Increase in Leukemia Inhibitory Factor and Its Receptor by Human Endometrium Is Partially Mediated by Interleukin 1 Receptor Signaling. *Endocrinology*, *145*(8), 3850–3857.

41. Gourdin, M., & Dubois, P. (2013). Impact of Ischemia on Cellular Metabolism. In *Artery Bypass*. InTech.

42. Gyorffy, B., Surowiak, P., Budczies, J., & Lánczky, A. (2013). Online survival analysis software to assess the prognostic value of biomarkers using transcriptomic data in non-small-cell lung cancer. PLoS ONE, 8(12).

43. Haines, B. P., Voyle, R. B., Pelton, T. A., Forrest, R., & Rathjen, P. D. (1999). Complex conserved organization of the mammalian leukemia inhibitory factor gene: regulated expression of intracellular and extracellular cytokines. Journal of Immunology (Baltimore, Md. : 1950), 162(8), 4637–4646.

44. Haines, B. P., Voyle, R. B., & Rathjen, P. D. (2000). Intracellular and extracellular leukemia inhibitory factor proteins have different cellular activities that are mediated by distinct protein motifs. *Molecular Biology of the Cell*, *11*(4), 1369–1383.

45. Hanna, J., Goldman-Wohl, D., Hamani, Y., Avraham, I., Greenfield, C., Natanson-Yaron, S., Prus, D., Cohen-Daniel, L., Arnon, T. I., Manaster, I., Gazit, R., Yutkin, V., Benharroch, D., Porgador, A., Keshet, E., Yagel, S., & Mandelboim, O. (2006). Decidual NK cells regulate key developmental processes at the human fetal-maternal interface. *Nature Medicine*, *12*(9), 1065–1074.

46. Hanahan, D., & Weinberg, R. A. (2011). Hallmarks of cancer: The next generation. In Cell (Vol. 144, Issue 5, pp. 646–674). Elsevier.

47. Henderson, J. T., Seniuk, N. A., Richardson, P. M., Gauldie, J., & Roder, J. C. (1994). Systemic administration of ciliary neurotrophic factor induces cachexia in rodents. Journal of Clinical Investigation, 93(6), 2632–2638.

48. Hensley, C. T., Faubert, B., Yuan, Q., Lev-Cohain, N., Jin, E., Kim, J., Jiang, L., Ko, B., Skelton, R., Loudat, L., Wodzak, M., Klimko, C., McMillan, E., Butt, Y., Ni, M., Oliver, D., Torrealba, J., Malloy, C. R., Kernstine, K., … DeBerardinis, R. J. (2016). Metabolic Heterogeneity in Human Lung Tumors. Cell, 164(4), 681–694. https://doi.org/10.1016/j.cell.2015.12.034

49. Hill, E. J., & Vernallis, A. B. (2008). Polarized secretion of leukemia inhibitory factor. *BMC Cell Biology*, *9*.

50. Hisaka, T., Desmoulière, A., Taupin, J. L., Daburon, S., Neaud, V., Senant, N., Blanc, J. F., Moreau, J. F., & Rosenbaum, J. (2004). Expression of leukemia inhibitory factor (LIF) and its receptor gp190 in human liver and in cultured human liver myofibroblasts. Cloning of new isoforms of LIF mRNA. *Comparative Hepatology*, *3*(1).

51. Holash, J., Davis, S., Papadopoulos, N., Croll, S. D., Ho, L., Russell, M., Boland, P., Leidich, R., Hylton, D., Burova, E., Ioffe, E., Huang, T., Radziejewski, C., Bailey, K., Fandl, J. P., Daly, T., Wiegand, S. J., Yancopoulos, G. D., & Rudge, J. S. (2002). VEGF-Trap: A VEGF blocker with potent antitumor effects. *Proceedings of the National Academy of Sciences of the United States of America*, *99*(17), 11393–11398.

52. Holtan, S. G., Creedon, D. J., Haluska, P., & Markovic, S. N. (2009). Cancer and Pregnancy: Parallels in Growth, Invasion, and Immune Modulation and Implications for Cancer Therapeutic Agents. *Mayo Clinic Proceedings*, *84*(11), 985–1000.

53. Hu, W., Feng, Z., Teresky, A. K., & Levine, A. J. (2007). p53 regulates maternal reproduction through LIF. *Nature*, *450*(7170), 721–724.

54. Hunt, L., Anthea Coles, C., Gorman, C. M., Tudor, E. M., Smythe, G. M., & White, J. D. (2011). Alterations in the expression of leukemia inhibitory factor following exercise: Comparisons between wild-type and mdx muscles. *PLoS Currents*, *3*.

55. Hunter, S. A., McIntosh, B. J., Shi, Y., Sperberg, R. A. P., Funatogawa, C., Labanieh, L., Soon, E., Wastyk, H. C., Mehta, N., Carter, C., Hunter, T., & Cochran, J. R. (2021). An engineered ligand trap inhibits leukemia inhibitory factor as pancreatic cancer treatment strategy. *Communications Biology*, *4*(1), 1–13.

56. Hurwitz, H., Fehrenbacher, L., Novotny, W., Cartwright, T., Hainsworth, J., Heim, W., Berlin, J., Baron, A., Griffing, S., Holmgren, E., Ferrara, N., Fyfe, G., Rogers, B., Ross, R., & Kabbinavar, F. (2004). Bevacizumab plus Irinotecan, Fluorouracil, and Leucovorin for Metastatic Colorectal Cancer. *New England Journal of Medicine*, *350*(23), 2335–2342.

57. Iseki, H., Kajimura, N., Ohue, C., Tanaka, R., Akiyama, Y., & Yamaguchi, K. (1995). Cytokine production in five tumor cell lines with activity to induce cancer cachexia syndrome in nude mice. Japanese Journal of Cancer Research : Gann, 86(6), 562–567.

58. Isner, J. M. (1996). The role of angiogenic cytokines in cardiovascular disease. *Clinical Immunology and Immunopathology*, *80*(3 II).

59. Iurlaro, R., León-Annicchiarico, C. L., & Muñoz-Pinedo, C. (2014). Regulation of cancer metabolism by oncogenes and tumor suppressors. In Methods in Enzymology (Vol. 542, pp. 59–80). Academic Press Inc.

60. Iurlaro, R., & Muñoz-Pinedo, C. (2016). Cell death induced by endoplasmic reticulum stress. *The FEBS Journal*, *283*(14), 2640–2652.

61. Jia, D., Cai, M., Xi, Y., Du, S., & ZhenjunTian. (2018). Interval exercise training increases LIF expression and prevents myocardial infarction-induced skeletal muscle atrophy in rats. *Life Sciences*, *193*, 77–86.

62. Kabashima, T., Kawaguchi, T., Wadzinski, B. E., & Uyeda, K. (2003). Xylulose 5-phosphate mediates glucose-induced lipogenesis by xylulose 5-phosphate-activated protein phosphatase in rat liver. Proceedings of the National Academy of Sciences of the United States of America, 100(9), 5107–5112.

63. Kamba, T., Tam, B. Y. Y., Hashizume, H., Haskell, A., Sennino, B., Mancuso, M. R., Norberg, S. M., O'Brien, S. M., Davis, R. B., Gowen, L. C., Anderson, K. D., Thurston, G., Joho, S., Springer, M. L., Kuo, C. J., & McDonald, D. M. (2006). VEGF-dependent plasticity of fenestrated capillaries in the normal adult microvasculature. *American Journal of Physiology - Heart and Circulatory Physiology*, *290*(2).

64. Kandarian, S. C., Nosacka, R. L., Delitto, A. E., Judge, A. R., Judge, S. M., Ganey, J. D., Moreira, J. D., & Jackman, R. W. (2018). Tumour-derived leukaemia inhibitory factor is a major driver of cancer cachexia and morbidity in C26 tumour-bearing mice. *Journal of Cachexia, Sarcopenia and Muscle*, *9*(6), 1109–1120.

65. Kawasaki, T., Akanuma, H., & Yamanouchi, T. (2002). Increased fructose concentrations in blood and urine in patients with diabetes. *Diabetes Care*, *25*(2), 353–357.

66. Kimber, S. J. (2005). Leukaemia inhibitory factor in implantation and uterine biology. In Reproduction (Vol. 130, Issue 2, pp. 131–145). Reproduction.

67. Kurtoglu, M., Maher, J. C., & Lampidis, T. J. (2007). Differential toxic mechanisms of 2-deoxy-D-glucose versus 2-fluorodeoxy-D-glucose in hypoxic and normoxic tumor cells. In Antioxidants and Redox Signaling (Vol. 9, Issue 9, pp. 1383–1390). Antioxid Redox Signal.

68. Lambert, P. D., Anderson, K. D., Sleeman, M. W., Wong, V., Tan, J., Hijarunguru, A., Corcoran, T. L., Murray, J. D., Thabet, K. E., Yancopoulos, G. D., & Wiegand, S. J. (2001). Ciliary neurotrophic factor activates leptin-like pathways and reduces body fat, without cachexia or rebound weight gain, even in leptin-resistant obesity. Proceedings of the National Academy of Sciences, 98(8), 4652–4657.

69. Lambrechts, D., Wauters, E., Boeckx, B., Aibar, S., Nittner, D., Burton, O., Bassez, A., Decaluwé, H., Pircher, A., Van den Eynde, K., Weynand, B., Verbeken, E., De Leyn, P., Liston, A., Vansteenkiste, J., Carmeliet, P., Aerts, S., & Thienpont, B. (2018). Phenotype molding of stromal cells in the lung tumor microenvironment. *Nature Medicine*, *24*(8), 1277–1289.

70. Lass, A., Weiser, W., Munafo, A., & Loumaye, E. (2001). Leukemia inhibitory factor in human reproduction. In Fertility and Sterility (Vol. 76, Issue 6, pp. 1091–1096). Fertil Steril.

71. León-Annicchiarico, C. L., Ramírez-Peinado, S., Domínguez-Villanueva, D., Gonsberg, A., Lampidis, T. J., & Muñoz-Pinedo, C. (2015). ATF4 mediates necrosis induced by glucose deprivation and apoptosis induced by 2-deoxyglucose in the same cells. FEBS Journal, 282(18), 3647–3658.

72. Lee, J., Rhee, M. H., Kim, E., & Cho, J. Y. (2012). BAY 11-7082 is a broad-spectrum inhibitor with anti-inflammatory activity against multiple targets. *Mediators of Inflammation*, *2012*.

73. Lei, Y., Zhou, S., Hu, Q., Chen, X., & Gu, J. (2020). Carbohydrate response element binding protein (ChREBP) correlates with colon cancer progression and contributes to cell proliferation. Scientific Reports, 10(1).

74. Li, Z., Li, R., Li, X., Dai, H., Han, X., Wang, X., & Yang, A. (2020). LIF in embryo culture medium is a predictive marker for clinical pregnancy following IVF-ET of patients with fallopian tube obstruction. Journal of Reproductive Immunology, 141.

75. Li, P., Li, Q., Biswas, N., Xin, H., Diemer, T., Liu, L., Perez Gutierrez, L., Paternostro, G., Piermarocchi, C., Domanskyi, S., Wang, R. K., & Ferrara, N. (2022). LIF, a mitogen for choroidal endothelial cells, protects the choriocapillaris: implications for prevention of geographic atrophy. *EMBO Molecular Medicine*, *14*(1), e14511.

76. Livak K.J. and Schmittgen T.D. (2001) Analysis of relative gene expression data using real-time quantitative PCR and the 2(-Delta C(T)) Method. Methods, 25(4): 402-408.

77. Lopez-Sambrooks, C., Shrimal, S., Khodier, C., Flaherty, D. P., Rinis, N., Charest, J. C., Gao, N., Zhao, P., Wells, L., Lewis, T. A., Lehrman, M. A., Gilmore, R., Golden, J. E., & Contessa, J. N. (2016). Oligosaccharyltransferase inhibition induces senescence in RTK-driven tumor cells. Nature Chemical Biology.

78. Mikolajczyk, M., Wirstlein, P., & Skrzypczak, J. (2007). The impact of leukemia inhibitory factor in uterine flushing on the reproductive potential of infertile women - A prospective study. American Journal of Reproductive Immunology, 58(1), 65–74.

79. McBride, W., Jackman, J. D., & Grayburn, P. A. (1990). Prevalence and clinical characteristics of a high cardiac output state in patients with multiple myeloma. The American Journal of Medicine, 89(1), 21–24.

80. Menkhorst, E., Zhang, J.-G., Sims, N. A., Morgan, P. O., Soo, P., Poulton, I. J., Metcalf, D., Alexandrou, E., Gresle, M., Salamonsen, L. A., Butzkueven, H., Nicola, N. A., & Dimitriadis, E. (2011). Vaginally Administered PEGylated LIF Antagonist Blocked Embryo Implantation and Eliminated Non-Target Effects on Bone in Mice. *PLoS ONE*, *6*(5), e19665.

81. Messeguer, X., Escudero, R., Farré, D., Núñez, O., Martínez, J., & Albà, M. M. (2002). PROMO: Detection of known transcription regulatory elements using species-tailored searches. *Bioinformatics*, *18*(2), 333–334.

82. Miller, K., Wang, M., Gralow, J., Dickler, M., Cobleigh, M., Perez, E. A., Shenkier, T., Cella, D., & Davidson, N. E. (2007). Paclitaxel plus Bevacizumab versus Paclitaxel Alone for Metastatic Breast Cancer. *New England Journal of Medicine*, *357*(26), 2666–2676.

83. Mori, M., Yamaguchi, K., & Abe, K. (1989). Purification of a lipoprotein lipase-inhibiting protein produced by a melanoma cell line associated with cancer cachexia. Biochemical and Biophysical Research Communications.

84. Mori, M., Yamaguchi, K., Honda, S., Nagasaki, K., Ueda, M., Abe, O., & Abe, K. (1991). Cancer Cachexia Syndrome Developed in Nude Mice Bearing Melanoma Cells Producing Leukemia-inhibitory Factor. Cancer Research, 51(24), 6656–6659.

85. Muñoz-Pinedo, C., El Mjiyad, N., & Ricci, J. E. (2012). Cancer metabolism: Current perspectives and future directions. In *Cell Death and Disease* (Vol. 3, Issue 1, pp. e248–e248). Nature Publishing Group.

86. Nelson, D. L., & Cox, M. M. (2017). Lehninger principles of biochemistry (7th ed.). W.H. Freeman.

87. Ning, B., & Elbein, A. D. (2000). Cloning, expression and characterization of the pig liver GDP-mannose pyrophosphorylase. *European Journal of Biochemistry*, *267*(23), 6866–6874.

88. Ohata, Y., Tsuchiya, M., Hirai, H., Yamaguchi, S., Akashi, T., Sakamoto, K., Yamaguchi, A., Ikeda, T., & Kayamori, K. (2018). Leukemia inhibitory factor produced by fibroblasts within tumor stroma participates in invasion of oral squamous cell carcinoma. PLOS ONE, 13(2), e0191865.

89. Pàez-Ribes, M., Allen, E., Hudock, J., Takeda, T., Okuyama, H., Viñals, F., Inoue, M., Bergers, G., Hanahan, D., & Casanovas, O. (2009). Antiangiogenic Therapy Elicits Malignant Progression of Tumors to Increased Local Invasion and Distant Metastasis. Cancer Cell, 15(3), 220–231.

90. Pascual-García, M., Bonfill-Teixidor, E., Planas-Rigol, E., Rubio-Perez, C., Iurlaro, R., Arias, A., Cuartas, I., Sala-Hojman, A., Escudero, L., Martínez-Ricarte, F., Huber-Ruano, I., Nuciforo, P., Pedrosa, L., Marques, C., Braña, I., Garralda, E., Vieito, M., Squatrito, M., Pineda, E., … Seoane, J. (2019). LIF regulates CXCL9 in tumor-associated macrophages and prevents CD8+ T cell tumor-infiltration impairing anti-PD1 therapy. Nature Communications.

91. Patil, V. R. S., Friedrich, E. B., Wolley, A. E., Gerszten, R. E., Allport, J. R., & Weissleder, R. (2005). Bone marrow-derived lin-c-kit+Sca-1+ stem cells do not contribute to vasculogenesis in Lewis lung carcinoma. *Neoplasia*, *7*(3), 234–240.

92. Patra, K. C., & Hay, N. (2014). The pentose phosphate pathway and cancer. In *Trends in Biochemical Sciences* (Vol. 39, Issue 8, pp. 347–354). Elsevier Ltd.

93. Pettersen, K., Andersen, S., Degen, S., Tadini, V., Grosjean, J., Hatakeyama, S., Tesfahun, A. N., Moestue, S., Kim, J., Nonstad, U., Romundstad, P. R., Skorpen, F., Sørhaug, S., Amundsen, T., Grønberg, B. H., Strasser, F., Stephens, N., Hoem, D., Molven, A., … Bjørkøy, G. (2017). Cancer cachexia associates with a systemic autophagy-inducing activity mimicked by cancer cell-derived IL-6 trans-signaling. Scientific Reports, 7(1), 2046.

94. Poehlmann, T. G., Fitzgerald, J. S., Meissner, A., Wengenmayer, T., Schleussner, E., Friedrich, K., & Markert, U. R. (2005). Trophoblast invasion: Tuning through LIF, signalling via Stat3. *Placenta*, *26*(SUPPL.), S37–S41.

95. Puschel, F., Favaro, F., Redondo-Pedraza, J., Lucendo, E., Iurlaro, R., Marchetti, S., Majem, B., Eldering, E., Nadal, E., Ricci, J. E., Chevet, E., & Muñoz-Pinedo, C. (2020). Starvation and antimetabolic therapy promote cytokine release and recruitment of immune cells. Proceedings of the National Academy of Sciences of the United States of America, 117(18), 9932–9941.

96. Qian, L., Xu, F., Wang, X., Jiang, M., Wang, J., Song, W., Wu, D., Shen, Z., Feng, D., Ling, B., Cheng, Y., Xiao, W., Shan, G., & Zhou, Y. (2017). LncRNA expression profile of ΔNp63α in cervical squamous cancers and its suppressive effects on LIF expression. *Cytokine*, *96*, 114–122.

97. Rajput, S., Volk-Draper, L. D., & Ran, S. (2013). TLR4 is a novel determinant of the response to paclitaxel in breast cancer. *Molecular Cancer Therapeutics*, *12*(8), 1676–1687.

98. Ribatti, D. (2016). Tumor refractoriness to anti-VEGF therapy. In *Oncotarget* (Vol. 7, Issue 29, pp. 46668–46677). Impact Journals LLC.

99. Rodríguez-Cruz, P. M., Belaya, K., Basiri, K., Sedghi, M., Farrugia, M. E., Holton, J. L., Liu, W. W., Maxwell, S., Petty, R., Walls, T. J., Kennett, R., Pitt, M., Sarkozy, A., Parton, M., Lochmüller, H., Muntoni, F., Palace, J., & Beeson, D. (2016). Clinical features of the myasthenic syndrome arising from mutations in GMPPB. *Journal of Neurology, Neurosurgery and Psychiatry*, *87*(8), 802–809.

100. Rojas-Rivera, D., Delvaeye, T., Roelandt, R., Nerinckx, W., Augustyns, K., Vandenabeele, P., & Bertrand, M. J. M. (2017). When PERK inhibitors turn out to be new potent RIPK1 inhibitors: Critical issues on the specificity and use of GSK2606414 and GSK2656157. Cell Death and Differentiation.

101. Salleh, N., & Giribabu, N. (2014). Leukemia inhibitory factor: Roles in embryo implantation and in nonhormonal contraception. In *Scientific World Journal* (Vol. 2014). Hindawi Publishing Corporation.

102. Sandler, A., Gray, R., Perry, M. C., Brahmer, J., Schiller, J. H., Dowlati, A., Lilenbaum, R., & Johnson, D. H. (2006). Paclitaxel–Carboplatin Alone or with Bevacizumab for Non–Small-Cell Lung Cancer. *New England Journal of Medicine*, *355*(24), 2542–2550.

103. Satake, S., Kuzuya, M., Miura, H., Asai, T., Ramos, M. A., Muraguchi, M., Ohmoto, Y., & Iguchi, A. (1998). Up-regulation of vascular endothelial growth factor in response to glucose deprivation. *Biology of the Cell*, *90*(2), 161–168.

104. Schindelin, J., Arganda-Carreras, I., Frise, E., Kaynig, V., Longair, M., Pietzsch, T., … Cardona, A. (2012). Fiji: an open-source platform for biological-image analysis. Nature Methods, 9(7), 676–682.

105. Schofield, G., & Kimber, S. J. (2005). Leukocyte Subpopulations in the Uteri of Leukemia Inhibitory Factor Knockout Mice During Early Pregnancy1. *Biology of Reproduction*, *72*(4), 872–878.

106. Schupp, J. C., Adams, T. S., Cosme, C., Raredon, M. S. B., Yuan, Y., Omote, N., Poli, S., Chioccioli, M., Rose, K. A., Manning, E. P., Sauler, M., Deiuliis, G., Ahangari, F., Neumark, N., Habermann, A. C., Gutierrez, A. J., Bui, L. T., Lafyatis, R., Pierce, R. W., … Kaminski, N. (2021). Integrated Single-Cell Atlas of Endothelial Cells of the Human Lung. *Circulation*, 286–302.

107. Seaman, S., Stevens, J., Yang, M. Y., Logsdon, D., Graff-Cherry, C., & St. Croix, B. (2007). Genes that Distinguish Physiological and Pathological Angiogenesis. Cancer Cell, 11(6), 539–554.

108. Shen, Y., Wang, X., Liu, Y., Singhal, M., Gürkaşlar, C., Valls, A. F., Lei, Y., Hu, W., Schermann, G., Adler, H., Yu, F. X., Fischer, T., Zhu, Y., Augustin, H. G., Schmidt, T., & De Almodóvar, C. R. (2021). STAT3-YAP/TAZ signaling in endothelial cells promotes tumor angiogenesis. *Science Signaling*, *14*(712).

109. Shi, Y., Gao, W., Lytle, N. K., Huang, P., Yuan, X., Dann, A. M., Ridinger-Saison, M., DelGiorno, K. E., Antal, C. E., Liang, G., Atkins, A. R., Erikson, G., Sun, H., Meisenhelder, J., Terenziani, E., Woo, G., Fang, L., Santisakultarm, T. P., Manor, U., … Hunter, T. (2019). Targeting LIF-mediated paracrine interaction for pancreatic cancer therapy and monitoring. In Nature (Vol. 569, Issue 7754, pp. 131–135). Nature Publishing Group.

110. Shin, S., Buel, G. R., Wolgamott, L., Plas, D. R., Asara, J. M., Blenis, J., & Yoon, S. O. (2015). ERK2 Mediates Metabolic Stress Response to Regulate Cell Fate. Molecular Cell, 59(3), 382–398.

111. Shojaei, F., & Ferrara, N. (2008). Role of the microenvironment in tumor growth and in refractoriness/resistance to anti-angiogenic therapies. *Drug Resistance Updates*, *11*(6), 219–230.

112. Smith, A. G., Heath, J. K., Donaldson, D. D., Wong, G. G., Moreau, J., Stahl, M., & Rogers, D. (1988). Inhibition of pluripotential embryonic stem cell differentiation by purified polypeptides. *Nature*, *336*(6200), 688–690.

113. Sone, H., Deo, B. K., & Kumagai, A. K. (2000). Enhancement of glucose transport by vascular endothelial growth factor in retinal endothelial cells - PubMed. Invest Ophthalmol Vis Sci, 41(7), 1876–1884.

114. Spötter, A., Drögemüller, C., Kuiper, H., Brenig, B., Leeb, T., & Distl, O. (2001). Molecular characterization and chromosome assignment of the porcine gene for leukemia inhibitory factor LIF. *Cytogenetics and Cell Genetics*, *93*(1–2), 87–90.

115. Stefater, M. A., MacLennan, A. J., Lee, N., Patterson, C. M., Haller, A., Sorrell, J., Myers, M., Woods, S. C., & Seeley, R. J. (2012). The Anorectic Effect of CNTF Does Not Require Action in Leptin-Responsive Neurons. Endocrinology, 153(6), 2647–2654.

116. Stephens, J. M., & Elks, C. M. (2017). Oncostatin M: Potential Implications for Malignancy and Metabolism. Current Pharmaceutical Design, 23(25), 3645–3657.

117. Stouthard, J. M., Romijn, J. A., Van der Poll, T., Endert, E., Klein, S., Bakker, P. J., Veenhof, C. H., & Sauerwein, H. P. (1995). Endocrinologic and metabolic effects of interleukin-6 in humans. The American Journal of Physiology, 268(5 Pt 1), E813-9.

118. Sullivan, M. R., Danai, L. V., Lewis, C. A., Chan, S. H., Gui, D. Y., Kunchok, T., Dennstedt, E. A., Heiden, M. G. V., & Muir, A. (2019). Quantification of microenvironmental metabolites in murine cancers reveals determinants of tumor nutrient availability. ELife, 8.

119. Suman, P., Shembekar, N., & Gupta, S. K. (2013). Leukemia inhibitory factor increases the invasiveness of trophoblastic cells through integrated increase in the expression of adhesion molecules and pappalysin 1 with a concomitant decrease in the expression of tissue inhibitor of matrix metalloproteinases. *Fertility and Sterility*, *99*(2), 533-542.e2.

120. Sun, B., Zhang, D., Zhao, N., & Zhao, X. (2017). Epithelial-to-endothelial transition and cancer stem cells: Two cornerstones of vasculogenic mimicry in malignant tumors. In *Oncotarget* (Vol. 8, Issue 18, pp. 30502–30510). Impact Journals LLC.

121. Tate, J. G., Bamford, S., Jubb, H. C., Sondka, Z., Beare, D. M., Bindal, N., Boutselakis, H., Cole, C. G., Creatore, C., Dawson, E., Fish, P., Harsha, B., Hathaway, C., Jupe, S. C., Kok, C. Y., Noble, K., Ponting, L., Ramshaw, C. C., Rye, C. E., … Forbes, S. A. (2019). COSMIC: The Catalogue Of Somatic Mutations In Cancer. Nucleic Acids Research, 47(D1), D941–D947.

122. Tinevez, J. Y., Perry, N., Schindelin, J., Hoopes, G. M., Reynolds, G. D., Laplantine, E., Bednarek, S. Y., Shorte, S. L., & Eliceiri, K. W. (2017). TrackMate: An open and extensible platform for single-particle tracking. *Methods*, *115*, 80–90.

123. Van der Veldt, A. A. M., Lubberink, M., Bahce, I., Walraven, M., deBoer, M. P., Greuter, H. N. J. M., Hendrikse, N. H., Eriksson, J., Windhorst, A. D., Postmus, P. E., Verheul, H. M., Serné, E. H., Lammertsma, A. A., & Smit, E. F. (2012). Rapid decrease in delivery of chemotherapy to tumors after anti-vegf therapy: Implications for scheduling of anti-angiogenic drugs. Cancer Cell, 21(1), 82–91.

124. Varki, A., Prestegard, J., Schnaar, R., Seeberger, P., Cummings, R., & Esko, J. *et al*. (1999). Essentials of Glycobiology: Chapter 18 Degradation and Turnover of Glycans (1st ed.). Cold Spring Harbor Laboratory Press.

125. Vazquez, J. M., Sulak, M., Chigurupati, S., & Lynch, V. J. (2018). A Zombie LIF Gene in Elephants Is Upregulated by TP53 to Induce Apoptosis in Response to DNA Damage. Cell Reports, 24(7), 1765–1776.

126. Voyle, R. B., Haines, B. P., Pera, M. F., Forrest, R., & Rathjen, P. D. (1999). Human germ cell tumor cell lines express novel leukemia inhibitory factor transcripts encoding differentially localized proteins. *Experimental Cell Research*, *249*(2), 199–211.

127. Wang, M. T., Fer, N., Galeas, J., Collisson, E. A., Kim, S. E., Sharib, J., & McCormick, F. (2019). Blockade of leukemia inhibitory factor as a therapeutic approach to KRAS driven pancreatic cancer. Nature Communications.

128. Warburg, O. (1956). On the origin of cancer cells. *Science*, *123*(3191), 309–314.

129. White, C. A., Zhang, J. G., Salamonsen, L. A., Baca, M., Fairlie, W. D., Metcalf, D., Nicola, N. A., Robb, L., & Dimitriadis, E. (2007). Blocking LIF action in the uterus by using a PEGylated antagonist prevents implantation: A nonhormonal contraceptive strategy. *Proceedings of the National Academy of Sciences of the United States of America*, *104*(49), 19357–19362.

130. Williams, R. L., Hilton, D. J., Pease, S., Willson, T. A., Stewart, C. L., Gearing, D. P., Wagner, E. F., Metcalf, D., Nicola, N. A., & Gough, N. M. (1988). Myeloid leukaemia inhibitory factor maintains the developmental potential of embryonic stem cells. *Nature*, *336*(6200), 684–687.

131. Winship, A., Correia, J., Zhang, J. G., Nicola, N. A., & Dimitriadis, E. (2015). Leukemia inhibitory factor (LIF) inhibition during mid-gestation impairs trophoblast invasion and spiral artery remodelling during pregnancy in mice. *PLoS ONE*, *10*(10).

132. Yamashita, H., Takenoshita, M., Sakurai, M., Bruick, R. K., Henzel, W. J., Shillinglaw, W., Arnot, D., & Uyeda, K. (2001). A glucose-responsive transcription factor that regulates carbohydrate metabolism in the liver. Proceedings of the National Academy of Sciences of the United States of America, 98(16), 9116–9121.

133. Yang, Y., Zhang, Y., Cao, Z., Ji, H., Yang, X., Iwamoto, H., Wahlberg, E., Länne, T., Sun, B., & Cao, Y. (2013). Anti-VEGF- and anti-VEGF receptor-induced vascular alteration in mouse healthy tissues. *Proceedings of the National Academy of Sciences of the United States of America*, *110*(29), 12018–12023.

134. Ye, H., Adane, B., Khan, N., Alexeev, E., Nusbacher, N., Minhajuddin, M., Stevens, B. M., Winters, A. C., Lin, X., Ashton, J. M., Purev, E., Xing, L., Pollyea, D. A., Lozupone, C. A., Serkova, N. J., Colgan, S. P., & Jordan, C. T. (2018). Subversion of Systemic Glucose Metabolism as a Mechanism to Support the Growth of Leukemia Cells. Cancer Cell, 34(4), 659-673.e6.

135. Ye, J., Kumanova, M., Hart, L. S., Sloane, K., Zhang, H., De Panis, D. N., Bobrovnikova-Marjon, E., Diehl, J. A., Ron, D., & Koumenis, C. (2010). The GCN2-ATF4 pathway is critical for tumour cell survival and proliferation in response to nutrient deprivation. *The EMBO Journal*, *29*(12), 2082–2096.

136. Yoo, J., Mashalidis, E. H., Kuk, A. C. Y., Yamamoto, K., Kaeser, B., Ichikawa, S., & Lee, S. Y. (2018). GlcNAc-1-P-transferase-tunicamycin complex structure reveals basis for inhibition of N-glycosylation. *Nature Structural and Molecular Biology*, 25(3), 217–224.

137. Yue, X., Zhao, Y., Zhang, C., Li, J., Liu, Z., Liu, J., & Hu, W. (2016). Leukemia inhibitory factor promotes EMT through STAT3- dependent miR-21 induction. *Oncotarget*, *7*(4), 3777–3790.

Annex I. Contributions

Sara Hijazo-Perchero performed the bioinformatic correlation analyses discussed in section 6.4 and 7.4. Francesca Favaro, Franciska Püschel and Jaime Redondo-Pedraza contributed some supernatants and western blot validations from experiments they previously performed for their research, as detailed in figures 2, 6, 11, 20 and 23. Fedra Luciano-Mateo and Felipe Jimenez-Hernandez optimized and performed the *in vivo* LLC1 cell injections, animal monitoring and tissue collection. Cristina Muñoz-Pinedo directed and supervised the experimental design and drafting of this thesis.

Annex II. Abbreviations

2DG – 2-deoxyglucose

3PO – 3-(3-Pyridinyl)-1-(4-pyridinyl)-2-propen-1-one

A76 – A769662

Ab – Antibody

ActD – Actinomycin D

AMP – Adenosine monophosphate

ANOVA – Analysis of variance

ATP – Adenosine triphosphate

B-Act – β-Actin

BAE – Bovine Aortic Endothelial cells

BCA - Bicinchoninic acid assay

BCE – Bovine Choroidal Endothelial cells

BSA – Bovine Serum Albumin

CM – Conditioned Media

CNX – Calnexin

ComC – Compound C

ConA – Concanavalin A

CRT – Calreticulin

DAPI – 4,6-diamidino-2-phenylindole, dihydrochloride

DHEA – Dehydroepiandrosterone

DMEM – Dulbecco's Modified Eagle Medium

DMSO – Dimethylsulfoxyde

DNA – Deoxyribonucleic Acid

Dol-P – Dolichyl phosphate

DPAGT1 – Acetylglucosaminephosphotransferase 1

ECL – Electrochemiluminescence

EDTA – Ethylenediaminetetraacetic acid

EGA – European Genome-Phenome Archive

ELISA – Enzyme-Linked Immunosorbent Assay

EMT – Epithelial to Mesenchymal Transition

ER – Endoplasmic Reticulum

EtOH – Ethanol (referred to a non-transformed breast epithelial cell line)

FBS – Foetal Bovine Serum

Fru – Fructose

FSC – Forward Scatter

Gal – Galactose

GDP – Guanosine diphosphate

GEO – Gene Expression Omnibus

Glc – Glucose

GlcNAc – N-acetylglucosamine

GMPP – GDP-Mannose Pyrophosphorylase

gRNA – guide RNA

GSVA – Gene Set Variation Analysis

HBEC – Human Bronchial Epithelial Cells

HBSS – Hanks' Balanced Salt Solution

HEPES – 4-(2-hydroxyethyl)-1-piperazineethanesulfonic acid

HMVEC – Human Microvascular Endothelial Cells

HRP – Horse Radish Peroxidase

HUVEC – Human Umbilical Vein Endothelial Cells

IgG – Immunoglobulin G

IQR – Interquartile Range

KO – Knock-Out

Lac – Lactate

LIF – Leukemia Inhibitory Factor

LIF-KO – Leukemia Inhibitory Factor Knock-Out (Referred to CRISPR-Cas9 LIF-KO LLC1 cells or the cohort of mice bearing LLC1 tumours with this modification)

LIFR – LIF Receptor

LLC1 – Lewis Lung Carcinoma 1

LUAD – Lung Adenocarcinoma

LUSC – Lung Squamous cell Carcinoma

M-1-P / M-6-P – Mannose-1-Phosphate / Mannose-6-Phosphate

Man – Mannose

MBP – Mannose Biosynthesis Pathway

Metf – Metformin

Mit – MitoTempo®

MMP – Matrix Metalloproteinase

mRNA – messenger RNA

MW – Molecular Weight

NAC – N-Acetylcysteine

NEAA – Non-Essential Amino Acids

NT – Non-targeting (referred to a siRNA oligonucleotide sequence)

OM – Oligomycin

OS – Overall Survival

OST – Oligosaccharyltransferase

PBS – Phosphate Buffered Saline

PCR – Polymerase Chain Reaction

PDAC – Pancreatic Ductal Adenocarcinoma

PI – Propidium Iodide

PMM – Phosphomannomutase

PPP – Pentose Phosphate Pathway

Pyr – Pyruvate

qPCR – real time PCR

Rapa – Rapamycin

rcf – relative centrifugal force

rhLIF – recombinant human LIF

RNA – Ribonucleic Acid

ROS – Reactive Oxygen Species

Scram – Scramble (Referred to CRISPR-Cas9 LLC1 cells with scramble gRNA or the cohort of mice bearing LLC1 tumours with this modification)

SDS – Sodium Dodecyl Sulphate

SDS-PAGE – SDS Polyacrylamide Gel Electrophoresis

SEM – Standard Error of the Mean

siRNA – small interference RNA

SSC – Side Scatter

TAM – Tamoxifen (Refers to a transformed malignant breast epithelial cell line)

TBS-T – Tris Buffered Saline – Tween

TCA – Tricarboxylic Acid

TCGA – The Cancer Genome Atlas

Tem – Tempol®

TFBS – Transcription Factor Binding Site

Thg – Thapsigargin

TIMP – Tissue Inhibitor of Metalloproteinases

Tun – Tunicamycin

UDP – Uridine diphosphate

UPR – Unfolded Protein Response

WT – Wild Type